Publications

Paper 1: **Measurement of Chromosomal Arms and FISH Reveal Complex Genome Architecture and Standardized Karyotype of Model Fish, Genus Carassius**

cells

MDPI

Article

Measurement of Chromosomal Arms and FISH Reveal Complex Genome Architecture and Standardized Karyotype of Model Fish, Genus *Carassius*

Martin Knytl * and Nicola Reinaldo Fornaini

Department of Cell Biology, Faculty of Science, Charles University, 12843 Prague, Czech Republic; fornainni@natur.cuni.cz;
* Correspondence: martin.knytl@natur.cuni.cz

Abstract: The widely distributed ray-finned fish genus *Carassius* is very well known due to its unique biological characteristics such as polyploidy, clonality, and/or interspecies hybridization. These biological characteristics have enabled *Carassius* species to be successfully widespread over relatively short period of evolutionary time. Therefore, this fish model deserves to be the center of attention in the research field. Some studies have already described the *Carassius* karyotype, but results are inconsistent in the number of morphological categories for individual chromosomes. We investigated three focal species: *Carassius auratus*, *C. carassius* and *C. gibelio* with the aim to describe their standardized diploid karyotypes, and to study their evolutionary relationships using cytogenetic tools. We measured length ($q + p$ *length*) of each chromosome and calculated centromeric index (i value). We found: (i) The relationship between $q + p$ *length* and i value showed higher similarity of *C. auratus* and *C. carassius*. (ii) The variability of i value within each chromosome expressed by means of the first quartile (Q_1) up to the third quartile (Q_3) showed higher similarity of *C. carassius* and *C. gibelio*. (iii) The fluorescent in situ hybridization (FISH) analysis revealed higher similarity of *C. auratus* and *C. gibelio*. (iv) Standardized karyotype formula described using *median* value (Q_2) showed differentiation among all investigated species: *C. auratus* had 24 metacentric (m), 40 submetacentric (sm), 2 subtelocentric (st), 2 acrocentric (a) and 32 telocentric (T) chromosomes ($24m + 40sm + 2st + 2a + 32T$) ; *C. carassius*: $16m + 34sm + 8st + 42T$; and *C. gibelio*: $16m + 22sm + 10st + 2a + 50T$. (v) We developed R scripts applicable for the description of standardized karyotype for any other species. The diverse results indicated unprecedented complex genomic and chromosomal architecture in the genus *Carassius* probably influenced by its unique biological characteristics which make the study of evolutionary relationships more difficult than it has been originally postulated.

Keywords: chromosome; karyogram; in situ hybridization; i value; q/p arm ratio; *Carassius auratus*; *Carassius carassius*; *Carassius gibelio*

Citation: Knytl, M.; Fornaini, N.R. Measurement of Chromosomal Arms and FISH Reveal Complex Genome Architecture and Standardized Karyotype of Model Fish, Genus *Carassius*. *Cells* **2021**, *10*, 2343. https://doi.org/10.3390/cells10092343

Academic Editor: Smina Mukhtar

Received: 1 August 2021
Accepted: 29 August 2021
Published: 7 September 2021

1. Introduction

Karyotype analysis is a fundamental approach by which chromosomes are arranged into homologous pairs with a respect to certain morphological categories. In the broader sense, the term karyotype is also referred to as a complete number of chromosomes describing typical taxon, species, biotype or individual [1]. Homologous chromosome pairs and morphological categories are determined based on the ratio of the long (q) and short (p) arm and the position of the centromere (centromeric index, i value). If the centromere is situated in median, submedian, subterminal or terminal region of the chromosome, the morphological category might be designated as metacentric (M, m), submetacentric (sm), subtelocentric (st) or acrocentric (a)/telocentric (t, T), respectively [2]. Two edge points that are located on median and terminal position sensu stricto have centromeric index 50 (assigned as M) and 0 (assigned as T chromosomes), respectively [2]. In order to maximize the diagnostic information obtainable from a chromosome preparation, the

precise arrangement of individual chromosomes within a single image might be used as a standardized format. The term karyogram can be also used for a graphical depiction of chromosome complements [3,4].

Knowledge of the karyotype is necessary in (cyto)genetics, or related fields, in order to study chromosomal rearrangements and abnormalities [5,6], the identification of sex chromosomes [7,8], and/or chromosome-specific genes [9]. Although chromosomal changes, (i.e., chromosomal losses, duplications, rearrangements), are strictly linked to a certain locus, without the knowledge of detailed karyotype, it is not possible to precisely identify chromosomal aberration, mutation or syndrome [10,11]. Heteromorphic sex chromosomes (morphologically distinct in male or female individuals) can be distinguished by classic cytogenetic procedures based on Giemsa-staining karyogram of both sexes and/or by chromosome painting and fluorescent in situ hybridization (FISH) [12,13]. Cytogenetic mapping and localization of single-copy gene regions in the genome generally reveal both intra- and interchromosomal rearrangements (i.e., inversions, insertions, deletions or duplications) determined using karyograms [9]. Moreover, gene loci, which have not yet been mapped within a genome, can be assigned to a specific chromosome within a standardized karyogram [14].

In some model vertebrate species, a low/moderate number of chromosomes, meaning up to approximately 50 chromosomes, of relatively large-size allows for easy identification of each chromosome according to q/p arm ratio and centromeric index [15]. Each chromosome is usually assigned a numeric code, necessary in evolutionary studies pertaining to patterns of orthologous chromosomes between species. Orthologous chromosomes are inferred to be descended from the same ancestral chromosome separated by a speciation event. This concept is also referred to as shared synteny. In a non-model organism with a high number of relatively small chromosomes, identification of chromosomes into categories are inconsistent (e.g., Knytl et al. [16] vs. Kobayasi et al. [17] vs. Ojima and Takai [18]), as is that case with cyprinid fish from the genus *Carassius*. Although a large number of studies describing *Carassius* karyotype, there is no study proposing a standardized karyogram based on exact measurements of the difference between q and p chromosome arm, arm ratio and centromeric index in any *Carassius* species.

The genus *Carassius* belongs to the monophyletic paleotetraploid tribe, Cyprinini sensu stricto [19], within the family Cyprinidae (ray-finned fishes, Teleostei). Several species have been described within the genus *Carassius* and three of them are widely used in cytogenetic research: (i) *Carassius carassius* (Crucian carp), native and threaten in many European countries [20,21], is diploid with chromosome number $2n = 4x = 100$ [17], where n refers to the number of chromosomes in each gamete of extant species, and x refers to the number of chromosomes in a gamete of the most recent diploid ancestor of the extant species. Most members of the family Cyprinidae contain 25 chromosomes in each gamete, considered as the most recent diploid ancestral state of extant *Carassius* [22]. (ii) *Carassius auratus* (goldfish), well known for its colourful varieties, bizarre shapes of body and formation of domesticated and feral populations [23]. (iii) *Carassius gibelio* (Silver Prussian carp) has recently spread throughout most continental waters, as a result of relocation from native habitats most likely by humans [24–27]. In addition, *Carassius auratus* and *C. gibelio* form diploid ($2n = 4x = 100$), triploid ($3n = 6x \approx 150$), and tetraploid biotypes ($4n = 8x \approx 200$) [28–30].

Here we described standardized karyotype of diploid *Carassius* species with 100 chromosomes (*C. auratus*, *C. carassius* and *C. gibelio*) based on measuring of chromosomal $q + p$ arm *length*, q/p arm ratio, and i value. We performed FISH experiments with ribosomal probes, and analysed values of $q + p$ *length* and i in order to characterize the inter-species differences between three *Carassius* species, which commonly co-occur in European waters (*C. carassius* and *C. gibelio*), and bred/distributed worldwide as part of the pet trade (*C. auratus*).

2. Materials and Methods

2.1. Fish Sampling and Origin

Carassius auratus were obtained via the aquarium trade (transported to Czech Republic from Israel). *Carassius carassius* was captured in the Elbe River basin closed to the city Lysá nad Labem, Czech Republic [16,31] and in small pond in Helsinki, Finland [32]. *Carassius gibelio* originated from the Dyje Rive basin, South Moravia, Czech Republic [28].

2.2. Chromosome Analysis

Both males and females of each species (*C. auratus*, *C. carassius*, *C. gibelio*) were used for karyotype analysis. In *C. auratus*, mitotic activity was stimulated by intraperitoneal injection of 0.1% $CoCl_2$ [32]. Somatic chromosomal complements were synchronized in metaphase of cell mitotic division using 0.1% colchicine (Sigma, St. Louis, MO, USA). Chromosome suspension was generated from the cephalic kidney [33] and stored in fixative solution (methanol: acetic acid, 3:1) at −20 °C, before being observed on a glass slide and stained with 5% Giemsa solution in 1x PBS. The chromosome suspensions used in this study have been used in prior analyses of *C. carassius* and *C. gibelio* [16,28,31,32] meaning that chromosomal suspensions were stored 3–7 years in −20 °C. Chromosomal suspensions were spun in a centrifuge, and fresh methanol and acetic acid were added every three months to maintain the constant ratio of methanol and acetic acid in fixative solution.

2.3. Measurements of q + p Chromosomal Arm Length

Photos of mitotic metaphase were taken using a Leica DFC 7000T camera and Leica DM6 microscope equipped with a EL6000 (metal halide) fluorescence illumination. A total of ten high-quality photos were taken for each species, five male and five female metaphases, from which measurements of the length of q and p chromosomal arms were taken. The centromere of each chromosome was identified as the narrowest part of a chromosome (Figure S2). Both arms of each chromatid (i.e., long arm 1 ($q1$), long arm 2 ($q2$), short arm 1 ($p1$), short arm 2 ($p2$)) were measured using `ImageJ` (V 1.53i) [34]. Chromosomal length (*length*), difference between q and p arm (d), q/p arm ratio (r) and centromeric index (i) were calculated according following formulas adopted from Levan et al. [2]:

$$p = \frac{p1 + p2}{2} \qquad q = \frac{q1 + q2}{2} \tag{1}$$

$$length = p + q \qquad d = q - p \qquad r = \frac{q}{p} \qquad i = \frac{100}{r + 1} \tag{2}$$

Measurements of p, q, *length*, d, r, and i were calculated as values in pixels from each image/metaphase and were further analyzed using `R` software for statistical computing (V 4.1.0) [35] and `RStudio` environment (V 1.4.1717) [36]. The i value was selected as a crucial characteristics for karyotypic analysis because it generally ranges from 0 to 50 [2]. The r value generally ranges from 1 to ∞ and thus this value is not suitable for graphical expression of results. The *length* and i value were used for calculation of an arithmetic mean of *length* (*mean_length*) and an arithmetic mean of i (*mean_i*) separately for each *Carassius* species. The *mean_length* and *mean_i* of each species were plotted (`plot` function in `R`).

2.4. Standardized Carassius Karyotype

Two highest i values (one chromosomal pair) were dissected from each of the metaphases (ten metaphases in total) and put into additional data frame as a numeric vector. This group of i values were identified as chromosome 1 (hereafter chr1). The third and fourth highest i values were dissected from each metaphase and identified as chr2 and so on up to two chromosomes with the lowest i values identified as chr50. This `function(){}` is named `Select_chrome` and shown in the supplemental results. All i values of each identified chromosome were plotted (`boxplot` function in `R`) separately in

each species. The default interquartile range 1.5 was used for elimination of extreme values (errors). Output value ($*stats*) was called in R. The *i* values within the the minimum (Q_0), first quartile (Q_1), median (Q_2), third quartile (Q_3) and maximum (Q_4) were investigated in detail, especially if some *i* values of each individual chromosome were shared among focal *Carassius* species. Chromosomal categories (*M*, *m*, *sm*, *st*, *a* and *T*) were determined according Q_2 of *i* values in each *Carassius* species. A morphological category of each chromosome was determined according chromosomal nomenclature Levan et al [2]. The following Table 1 shows boundaries between each morphological category:

Table 1. Chromosomal nomenclature used for determination of chromosomal categories according to Levan et al. [2].

Centromeric Position	Arm Ratio	Centromeric Index	Chromosome Category
median sensu stricto	1.00	50	M (metacentric sensu stricto)
median	1.01–1.70	49.9–37.51	m (metacentric)
submedian	1.71–3.00	37.50–25.01	sm (submetacentric)
subterminal	3.01–7.00	25.00–12.51	st (subtelocentric)
terminal	>7.01	12.50–0.01	a/t (acro-/telocentric)
terminal sensu stricto	∞	0	T (telocentric sensu stricto)

2.5. Preparation of 5S and 28S Ribosomal Probes

New 5S PCR primers 5S_F (5′-CAGGGTGGTATGGCCGTAGG-3′) and 5S_R (5′-AGCGCCCGATCTCGTCTGAT-3′) were designed according to the 5S gene of the western clawed frog, *Xenopus tropicalis*. The *X. tropicalis* genomic sequence is available on Xenbase, accessed on 11 June 2020 (http://www.xenbase.org). The 28S primers 28S_A (5′-AAACTCTG GTGGAGGTCCGT-3′) and 28S_B (5′-CTTACCAAAAGTGGCCCACTA-3′) used in this study were designed by Naito et al. [37]. Total genomic DNA (gDNA) was extracted from pectoral fin tissue using the DNeasy Blood & Tissue Kit (Qiagen, Hilden, Germany) according to manufacturer's instructions. *Carassius gibelio* and *X. tropicalis* gDNA were used as a template for 5S and 28S PCR amplification, respectively. Primers were made by Integrated DNA Technologies (Coralville, IA, USA). The PPP Master Mix (Top-Bio, Prague, Czech Republic) was used for efficient amplification of ribosomal gene fragments. The temperature profile for the non-labelling amplification of the 5S and 28S loci followed Top-Bio instructions: initial denaturation step for 1 min at 94 °C, followed by 35 cycles (94 °C for 15 s, 53 °C for 15 s and 72 °C for 40 s) and a final extension step at 72 °C for 7 min. The obtained PCR products were separated on a 1.25% agarose gel with TA buffer and extracted from the gel using MicroElute Gel Extraction Kit (Omega Bio-tek, Norcross, GA, USA) according to manufacturer's instructions. The PCR amplicons were sequenced and mapped using `blastn` algorithm for finding out of the locus- and species-specificity of amplification. Subsequently, the 5S and 28S ribosomal DNA (rDNA) loci were indirectly labelled by Digoxigenin-11-dUTP (Roche, Mannheim, Germany) and Biotin-16-dUTP (Jena Bioscience, Jena, Germany), respectively, by PCR reaction again. Taq DNA polymerase (Top-Bio) was used for labelling instead of The PPP Master Mix which was used for non-labelling amplification. Conditions for labelling PCR of the 5S and 28S loci were adopted from Sember et al. [38] and slightly modified as follows: initial denaturation step for 3 min at 94 °C, followed by 30 cycles (94 °C for 30 s, 53 °C for 30 s and 72 °C for 40 s) with final extension step at 72 °C for 10 min. The PCR product was separated on an 1% agarose gel with TBE buffer and purified using E.Z.N.A. Cycle Pure Kit (Omega Bio-tek) according to manufacturer's instructions.

2.6. Fluorescent In Situ Hybridization

Cell suspensions prepared from each *Carassius* species were spread onto clean microscopic slides, which were subsequently used for FISH on the same day. The 5S probe from *C. gibelio* was used for chromosomal spreads of *C. auratus*, *C. carassius* and *C. gibelio*.

The 28S probe from *X. tropicalis* was used for *C. auratus*, *C. carassius* and *C. gibelio* chromosomal spreads. In total 44 μl of the hybridization mixture containing 100 ng of either 5S or 28S rDNA probe, 50% deionized formamide, 2x SSC, 10% dextran sulphate and water was placed on a slide and covered with a 24 × 50 mm coverslip. Both probe and chromosomal DNA were denatured in a PCR machine with special block for slides at 70 °C for 5 min [9]. Hybridization, post-hybridization washing, blocking reaction and visualization of 5S and 28S rDNA signals were carried out as described in Knytl et al. [39]. The Digoxigenin-11-dUTP/Biotin-16-dUTP labelled probe was detected by Anti-Digoxigenin-Fluorescein (Roche)/ CY^{TM}3-Streptavidin (Invitrogen, Camarillo, CA, USA), respectively, diluted according to manufacturer's instructions. Chromosomes were counterstained with ProLong^{TM} Diamond Antifade Mountant with DAPI (Invitrogen by Thermo Fisher Scientific, Waltham, MA, USA). At least 20 metaphase spreads in total were analysed per individual.

3. Results

3.1. Karyotype Analysis

Number of chomosomes in all studied species (*C. auratus*, *C. carassius* and *C. gibelio*) was uniform ($2n = 4x = 100$). We did not find any differences in chromosomal morphology between male and female individuals. This finding confirmed homomorphic sex chromosomes at least in diploid biotypes of the genus *Carassius*.

3.2. Interspecies Variability Based on Chromosomal Length

Detailed description of `R` analysis including `R` scripts are given in Supplementary Results. All steps outlining how the measured values were calculated and processed into tables and plots are shown on the *C. auratus* dataset. The *mean_i* and *mean_length* of each individual chromosome were plotted onto x axis and y axis, respectively, (Figure 1). Morphological chromosomal categories *m*, *sm*, *st*, *a* and *T* are present in each species. Extreme category, such as *T*, is represented by 19, 26, and 25 chromosomes of *C. auratus*, *C. carassius* and *C. gibelio*, respectively (i.e., 19, 26, and 25 points lie on gray dashed vertical lines of interval 0). The *T* chromosomes have small *mean_length*, approaching 0. Other chromosomal categories, such as *M*, are not represented in any species—no *i* value reached 50, with the highest *i* of 48.778 found in chromosome 1 of *C. gibelio*. Chromosomal length of *C. auratus*, *C. carassius*, and *C. gibelio* range from 23.340–40.614, 26.799–44.092, and 15.205–29.496, respectively. It is evident that chromosomes of *C. gibelio* are generally smaller (mean of $q + p$ length was 21.36) than those of both *C. auratus* (31.53) and *C. carassius* (35.05). For the minimum of errors we calculated *mean_length* and *mean_i* from a group of ten measured $q + p$ values, i.e., each dot on Figure 1 is arithmetic mean resulted from ten measured $q + p$ values. Potential influences on chromosomal length are discussed (Section 4).

3.3. Interspecies Variability Based on Centromeric Index Linked to Individual Chromosomes of the Whole Chromosomal Complement, and Standardized Carassius Karyotype

The *i* values were assigned to each individual chromosome by dissection of chr1–50 from each metaphase (also Section 2.4, `R` protocol is described in the section of `R` analysis of Supplementary Results) and plotted onto x and y axis (Figure 2). Each box depicts a group of chromosomes dependent on *i* values ordered from most metacentric chromosomes on the left side of plots (chr1) to most telocentric chromosomes on the right side of plots (chr50). In general, each species has six to seven chromosomes that were highly variable in *i*, i.e., chr31–37 in *C. auratus*, chr27–33 in *C. carassius* and chr23–29 in *C. gibelio*. The Q_1 and Q_3 cover *i* values from 0 to 29.342 in *C. auratus*, from 0 to 23.9 in *C. carassius* and from 0 to 25.747 in *C. gibelio*. *Carassius auratus* has the highest variability of *i* value.

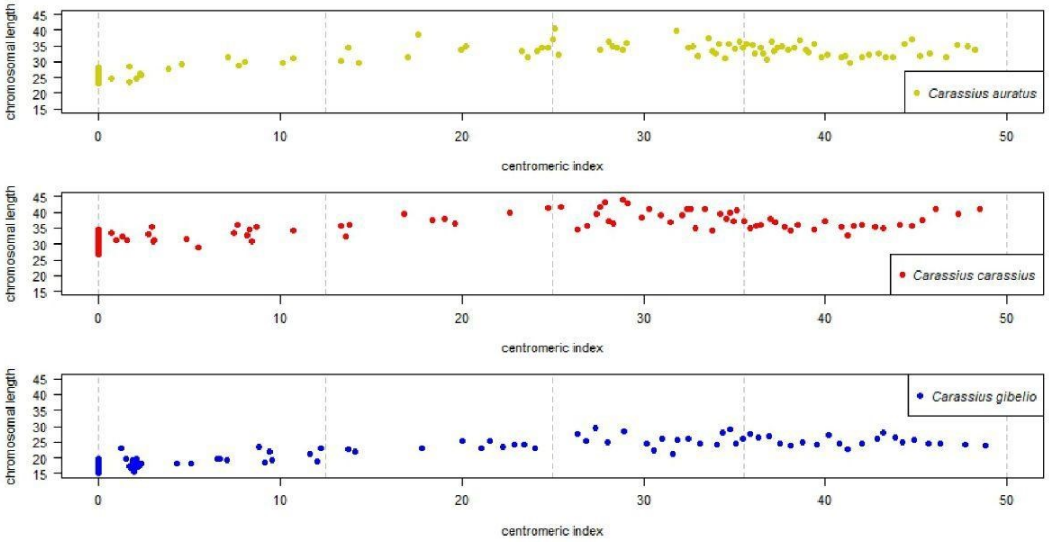

Figure 1. Relationship between centromeric index (*i*) and chromosomal length (*length*). Top plot shows chromosomes of *Carassius auratus* in yellow, middle plot shows chromosomes of *C. carassius* in red and bottom plot shows chromosomes of *C. gibelio* in blue. Chromosomal categories are bounded by gray dashed vertical lines which define intervals 0–12.5, 12.5–25, 25–37.5 and 37.5–50 corresponding to acrocentric (*a*), subtelocentric (*st*), submetacentric (*sm*) and metacentric (*m*) chromosomes, respectively. Both plotted *i* value and *length* are presented as an arithmetic mean of each chromosome.

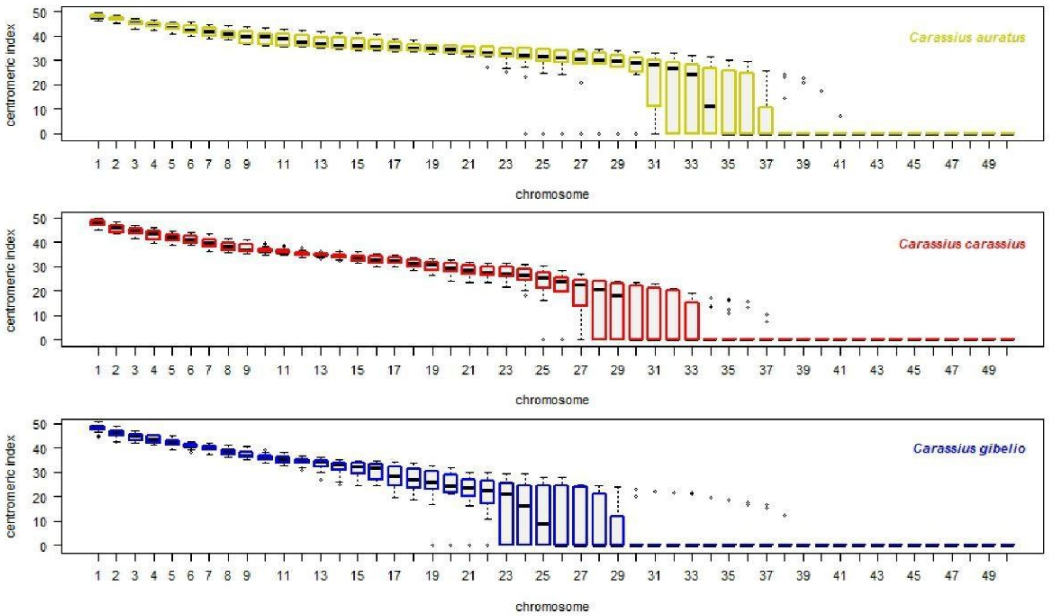

Figure 2. Intrachromosomal variability of *i* displayed on a whole chromosomal complement. Top plot shows haploid chromosomal complement (50 chromosomes) of *C. auratus* in yellow, middle plot shows 50 chromosomes of *C. carassius* in red and bottom plot shows 50 chromosomes of *C. gibelio* in blue. Each chromosome is linked to *i* value (y axis). Upper and lower whiskers show extreme values, the minimum (Q_0) and maximum (Q_4), respectively, boxes involve the first quartile (Q_1) and the third quartile (Q_3) group of values. Black line within box indicates *median* value of the dataset (Q_2). Outliers (errors) are drawn as black points.

If some i values are shared among *C. auratus*, *C. carassius* and *C. gibelio*, the range of i values of each individual chromosome (chr1–50) from ten metaphases were compared with the range of i values of other two orthologs of each of other two species (ten metaphases from each species). The Q_1–Q_3 range of i value within chr1 of *C. auratus* was compared with the Q_1–Q_3 range of i value within chr1 of *C. carassius* and *C. gibelio*, similarly the Q_1–Q_3 range of i value within chr2 of *C. auratus* was compared with the Q_1–Q_3 range of i value of *C. carassius* and *C. gibelio* etc. up to the Q_1–Q_3 range of i value within chr50 of *C. auratus*, *C. carassius* and *C. gibelio*. As an additional analysis, multi-plot with 50 separate box plots (chr1–50) was generated, each box plot was composed of orthologous chromosomes of all three species (Figure 3).

Based on i value (Figure 1 and 3), we concluded that:

1. Each orthologous chromosome of *C. carassius* and *C. gibelio* shared i values within Q_1–Q_3 range and therefore we consider that karyotypes of *C. carassius* and *C. gibelio* to be more similar based on i value.
2. Chromosomes 12–30 of *C. auratus* were represented by different i values within Q_1–Q_3 range those of *C. carassius* and *C. gibelio*. Therefore, we consider the karyotypes of *C. auratus* to be most variable for this parameter.
3. Chromosomes 8, 11 and 31 of *C. auratus* were represented by different i values within Q_1–Q_3 range those of *C. gibelio* but *C. carassius* shared i values in these chromosomes with both *C. auratus* and *C. gibelio*.

The Q_2 range (*median*) of i value was used for determination of a standardized karyotype formula. Chromosome1 of *C. auratus*, *C. carassius* and *C. gibelio* with *median* of i value 47.87 (CAU_median_i column of Table 2), 48.28 (CCA_median_i) and 48.55 (CGI_median_i), respectively, were identified as m chromosomes in all three *Carassius* species ($CAU\_category$, $CCA\_category$, $CGI\_category$ columns of Table 2). Karyotypes all three *Carassius* species were different in the number of chromosomal categories sensu Levan et al. [2]. The number of chromosomes in categories found out by arithmetic mean (Figure 1) slightly differed from the number of chromosomes in categories determined by Q_2 range (Figure 2). The Q_2 range eliminated errors and thus we inferred standardized karyotype formula according to the Q_2 range.

$$\textit{Carassius auratus} : 24m + 40sm + 2st + 2a + 32T \quad (3)$$

$$\textit{Carassius carassius} : 16m + 34sm + 8st + 42T \quad (4)$$

$$\textit{Carassius gibelio} : 16m + 22sm + 10st + 2a + 50T \quad (5)$$

3.4. Fluorescent In Situ Hybridization with 5S and 28S Ribosomal Probes

The PCR amplification of 28S and 5S rDNA locus resulted consistently in approximately 300 bp long fragments. Searches, using the `blastn` algorithm, confirmed the locus- and species-specificity of each amplicon: 100% identity with 28S rRNA of *X. tropicalis* (accession numbers XR_004223792–XR_004223798), 95% identity with sequence of 5S rRNA of *C. gibelio* (accession number DQ659261). The amplified 5S rDNA sequence was deposited to the NCBI/GenBank database (accession number BankIt2492026 5s, MZ927820). Mapping of the 5S and 28S loci showed different patterns in the number and position within each investigated *Carassius* species (Figure 4). No differences between males and females were detected. The $q + p$ arms of the FISH images were measured on chromosomes that bear positive rDNA loci because the FISH protocol involves denaturation step after which chromosomal structure is disrupted due to high temperature. The rDNA positive loci are mostly accumulated at the pericentromeric chromosomal region in Carassius and another cyprinid fishes [32,40,41] and thus the identification of the centromere and measurement of the $q + p$ arms are precise on rDNA positive chromosomes. The i value of rDNA positive chromosomes (arrows on Figure 4) were assigned to the closest i value of the standardized karyotype from Table 2.

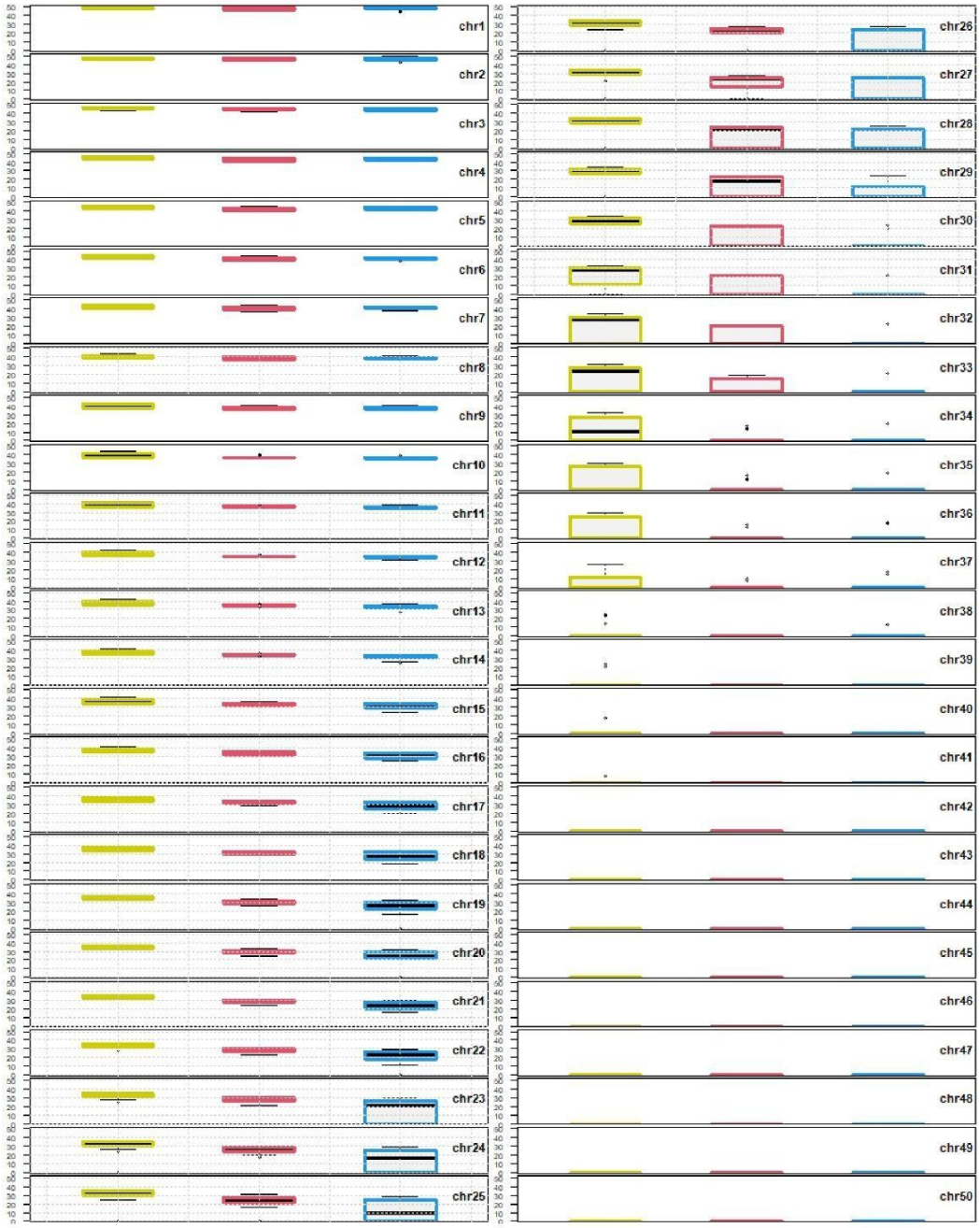

Figure 3. Box plots composed of orthologous chromosomes of each species. Chromosomes are ordered decreasingly according to the *i* value. Chromosomes on the top left of the figure are the most metacentric, chromosome 1 (chr1), chromosomes on the bottom right of the figure are the most telocentric (chr50). Yellow, red and blue boxes represents *C. auratus*, *C. carassius* and *C. gibelio*, respectively. Each chromosome is linked to *i* value (y axis). Upper (Q_0) and lower (Q_4) whiskers show extreme values, boxes involve Q_1 and Q_3 group of values. The black line within boxes indicates *median* value of the dataset (Q_2). Outliers (errors) are drawn as black points. The grid in some box plots represents significantly different *i* values within the Q_1–Q_3 range. Box plots without the grid share some *i* values within the Q_1–Q_3 range.

Table 2. Table of values used for determination of standardized karyotype. Each *median* (Q_2) of *i* values corresponds to certain chromosomal category of chr1–50. The *medians* of *i* value are sorted decreasingly. CAU = *C. auratus*, CCA = *C. carassius*, CGI = *C. gibelio*, m = metacentric, sm = submetacentric, st = subtelocentric, a = acrocentric, T = telocentric sensu stricto.

	CAU_median_i	CCA_median_i	CGI_median_i	CAU_category	CCA_category	CGI_category
chromosome1	47.87	48.28	48.55	m	m	m
chromosome2	47.07	45.68	46.12	m	m	m
chromosome3	45.74	44.74	44.99	m	m	m
chromosome4	44.81	43.52	43.47	m	m	m
chromosome5	43.46	42.11	42.53	m	m	m
chromosome6	42.43	41.08	40.89	m	m	m
chromosome7	41.63	39.58	39.89	m	m	m
chromosome8	40.84	37.90	38.42	m	m	m
chromosome9	40.13	36.81	36.91	m	sm	sm
chromosome10	39.67	36.17	35.84	m	sm	sm
chromosome11	38.75	35.79	35.41	m	sm	sm
chromosome12	37.65	35.19	34.73	m	sm	sm
chromosome13	36.77	34.86	34.25	sm	sm	sm
chromosome14	36.19	34.36	33.36	sm	sm	sm
chromosome15	35.88	33.66	32.61	sm	sm	sm
chromosome16	35.71	32.70	31.90	sm	sm	sm
chromosome17	35.48	32.22	28.62	sm	sm	sm
chromosome18	35.21	31.23	26.86	sm	sm	sm
chromosome19	34.87	30.54	26.07	sm	sm	sm
chromosome20	34.33	29.11	24.42	sm	sm	st
chromosome21	33.45	28.54	23.45	sm	sm	st
chromosome22	33.03	27.41	22.83	sm	sm	st
chromosome23	32.78	26.86	21.37	sm	sm	st
chromosome24	31.95	26.25	16.52	sm	sm	st
chromosome25	31.41	25.22	9.19	sm	sm	a
chromosome26	31.08	24.00	0.00	sm	st	T
chromosome27	30.70	22.57	0.00	sm	st	T
chromosome28	30.11	20.62	0.00	sm	st	T
chromosome29	29.75	18.13	0.00	sm	st	T
chromosome30	28.96	0.00	0.00	sm	T	T
chromosome31	28.17	0.00	0.00	sm	T	T
chromosome32	26.87	0.00	0.00	sm	T	T
chromosome33	24.41	0.00	0.00	st	T	T
chromosome34	11.19	0.00	0.00	a	T	T
chromosome35	0.00	0.00	0.00	T	T	T
chromosome36	0.00	0.00	0.00	T	T	T
chromosome37	0.00	0.00	0.00	T	T	T
chromosome38	0.00	0.00	0.00	T	T	T
chromosome39	0.00	0.00	0.00	T	T	T
chromosome40	0.00	0.00	0.00	T	T	T
chromosome41	0.00	0.00	0.00	T	T	T
chromosome42	0.00	0.00	0.00	T	T	T
chromosome43	0.00	0.00	0.00	T	T	T
chromosome44	0.00	0.00	0.00	T	T	T
chromosome45	0.00	0.00	0.00	T	T	T
chromosome46	0.00	0.00	0.00	T	T	T
chromosome47	0.00	0.00	0.00	T	T	T
chromosome48	0.00	0.00	0.00	T	T	T
chromosome49	0.00	0.00	0.00	T	T	T
chromosome50	0.00	0.00	0.00	T	T	T

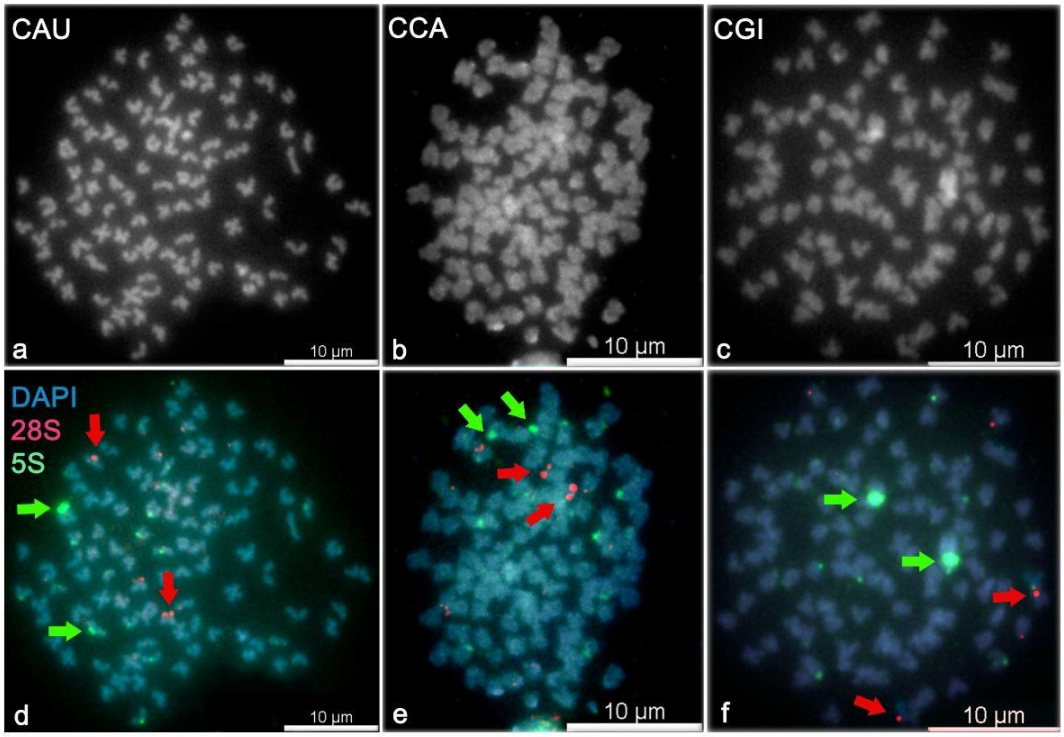

Figure 4. Double-colour fluorescent *in situ* hybridization with 5S and 28S ribosomal probes. DAPI-counterstained metaphase spreads show 100 chromosomes (B&W) in (**a**) *C. auratus* (CAU), (**b**) *C. carassius* (CCA) and (**c**) *C. gibelio* (CGI). The 5S (green) probe shows two more intensive (strong) signals and eight, six and eight less intensive (weak) signals in (**d**) *C. auratus*, (**e**) *C. carassius* and (**f**) *C. gibelio*, respectively. The 28S rDNA probe (red) reveals two strong signals and two, four and two weak signals in (**d**) *C. auratus*, (**e**) *C. carassius* and (**f**) *C. gibelio*, respectively. Green and red arrows correspond to 5S and 28S ribosomal loci, respectively.

Summary of 5S rDNA (corresponding to non-nucleolar region). We found:

- Two more intensive (strong) 5S rDNA signals at the *p* arm of *sm* chromosomes (chr28, *i* value = 30.06) and eight weak signals in *C. auratus*.
- Two strong 5S rDNA signals at the *p* arm of *sm* chromosomes (chr19, *i* value = 30.60) and six weak signals in *C. carassius*.
- Two strong 5S rDNA signals at the *p* arm of *sm* chromosomes (chr17, *i* value = 30.00) and eight weak signals in *C. gibelio*.

Summary of 28S rDNA (corresponding to nucleolar organizer region). We found:

- two strong 28S rDNA signals at the *p* arm of two *sm* chromosomes (chr16, *i* value = 35.69) and two weak signals in *C. auratus*.
- two strong 28S rDNA signals at the *p* arm of two *sm* chromosomes (chr13, *i* value = 34.72) and four weak signals in *C. carassius*.
- two strong 28S rDNA signals at the pericentromeric region of two *T* chromosomes (in the range of chr26–50, *i* value = 0) and two weak 28S rDNA signals in *C. gibelio*.

4. Discussion

Diploid vs. polyploid biotypes—sexual vs. asexual reproduction—genetic vs. environmental sex determination: All these natural phenomena make *Carassius* a valuable experimental model for evolutionary studies. The study of these aforementioned unique characteristics of *Carassius* require basic cytogenetic techniques such as chromosome prepa-

rations and/or karyotype. Diploid biotypes of the genus *Carassius* have a karyotype consisting of 100 chromosomes (e.g., [28], this study), with some exceptions, i.e., 50, 94, 98, 102 or 104 chromosomes [22,42–46] . Karyotype formula of diploid *Carassius* is inconsistently defined by several authors (Table 3) and $q + p$ arms have not been measured. An application of a technique of measurement, and the following determination of standardized karyotype is needed in order to clear up genome architecture and its evolution.

Table 3. Previously published karyotypes of diploid *C. auratus*, *C. carassius* and *C. gibelio* including information about sex and locality of the investigated individuals. NA = information not available, F = female, M = male.

Karyotype	Sex	Locality	References
C. auratus			
$2n = 94$	NA	Japan	[42,47]
$2n = 96$–104	F, M	NA	[48]
$2n = 100(12m + 36sm + 52st–a)$	F, M	Japan	[49,50]
$2n = 104(46m + 16sm + 42a)$	F, M	NA	[22]
$2n = 104(20m + 72sm–st + 12a)$	NA	NA	[44]
$2n = 100(20m + 40sm + 40a)$	F, M	NA	[17]
$2n = 100(16m + 84sm–a)$	NA	NA	[51]
$2n = 100(12m + 36sm + 52st–a)$	F, M	China	[18,52,53]
$2n = 100(22m + 30sm + 48st–a)$	F, M	China	[54–56]
C. carassius			
$2n = 104(20m + 72sm–st + 12a)$	NA	NA	[44]
$2n = 100(20m + 40sm + 40a)$	F, M	Netherlands	[17,57–59]
$2n = 100(20m + 44sm + 36a)$	NA	France	[60]
$2n = 100$	F, M	Bosnia	[61]
$2n = 50(20m + 12sm + 18st–a)$	NA	Romania	[45]
$2n = 100$	F, M	Czech Republic	[62]
$2n = 100(20m + 36sm + 44st–a)$	F, M	Czech Republic	[16,31]
$2n = 100(20m + 36sm + 44st–a)$	F, M	Poland	[40]
$2n = 100(20m + 36sm + 44st–a)$	M	Finland	[32]
C. gibelio			
$2n = 94$	F, M	Belarus	[43]
$2n = 100(20m + 40sm + 40a)$	NA	River Amur	[63]
$2n = 98(48m–st + 50a)$	NA	Romania	[45]
$2n = 102(24m + 36sm–st + 42a)$	F	Yugoslavia	[46]
$2n = 104(24m + 36sm–st + 44a)$	M	Yugoslavia	[46]
$2n = 100(14m + 24sm + 62st–a)$	F, M	Poland	[64]
$2n = 100(26m + 38sm + 36st–a)$	F, M	Poland	[65]

We generated a revised karyotype as a result of novel measurement and using statistical programming we described standardized karyotype of three species (*C. auratus*, *C. carassius* and *C. gibelio*). We measured the length of each individual chromosome of each species and identified each chromosome using i value. Groups of i values were divided into quartiles Q_0–Q_4. Our results based on *median* (Q_2) of i value for each chromosome revealed three different karyotypes; not one of these three karyotypes corresponded to any of the previously published karyotypes from Table 3. The karyotype of *C. auratus* had $24m$, $40sm$, $2st$, $2a$ and $32T$ chromosomes (shortened formula $24m + 40sm + 36st–T$). The karyotype of *C. carassius* had $16m$, $34sm$, $8st$ and $42T$ chromosomes (shortened formula $16m + 34sm + 50st–T$). The karyotype of *C. gibelio* possessed $16m$, $22sm$, $10st$, $2a$ and $50T$ chromosomes (shortened formula $16m + 22sm + 62st–T$). These standardized karyotypes are likely highly reproducible and could be applied to the reconstruction of cytogenetic maps, comparative cytogenetics and genomics, or cytotaxonomy and karyosystematics. The designed `R` scripts (Supplementary Results) could be applied to the description of

standardized karyotype for another species with relatively high number of chromosomes similar to that of *Carassius*.

In the wider range of *i* values (Q_1–Q_3) for each chromosome, we found karyotypes of *C. carassius* and *C. gibelio* more similar, as both *C. carassius* and *C. gibelio* shared some *i* values within Q_1–Q_3 range of corresponding orthologous counterparts. The *i* values in Q_1–Q_3 of chr8 and chr11–31 in *C. auratus* were significantly different those of *i* values in Q_1–Q_3 of *C. carassius* and *C. gibelio* (Figures 2 and 3). This finding indicates higher divergence of *C. auratus* karyotype based on *i* value. The *i* value divergence might be supported by distinct origin of the samples used in this investigation—*C. auratus* used in this study was imported from Israel and was domesticated in ancient China [23]. Both *C. carassius* and *C. gibelio* used in this study originated from Europe and mostly from the Czech Republic (only four individuals of *C. carassius* were caught in Finland). A phylogenetic study of Asian–European *Carassius* suggests a closer evolutionary relationship exists between diploid *C. auratus* and diploid *C. gibelio* compared to *C. carassius* and diploid *C. auratus/gibelio* [66]. Thus, phylogenetic distance does not reflect *i* value divergence in *C. carassius*, as demonstrated in this study. The higher similarity between *C. carassius* and *C. gibelio i* values could be caused by hybridization, as previously confirmed by molecular genetic and cytogenetic tools in several European *Carassius* populations [16,67,68]. Although, we can not exclude a hybrid origin for diploid *Carassius* individuals.

In addition, female meiotic drive might also affect *i* values [69]. Chromosomes of particular morphology might be preferentially transmitted to the egg during meiosis and the chromosomal complement of new offspring can be rapidly changed. Interestingly, polyploid *Carassius* biotypes have variable numbers of microchromosomes [16] which results in odd or variable chromosome numbers within polyploid *Carassius* [28]. The uniform chromosome numbers, we have described in diploid *Carassius*, are in accordance with expectations that female meiotic drive has never been shown in diploid *Carassius*.

We also showed a relationship between the mean of *i* value and the mean of $q + p$ chromosomal length. Chromosomes of *C. gibelio* had smaller size (mean of chromosomal length was 21.36) those of *C. auratus* (31.53) and *C. carassius* (35.05, Figure 1). This difference in chromosomal length in *Carassius* might be promoted by altered chromatin spiralisation and condensation during cell cycle, especially during interphase and mitosis [70–72]. In this study, chromosomes were synchronized in metaphase by colchicine but some chromosomes can be fixed in prometaphase, early metaphase or late metaphase and we assume that slight differences in chromosomal length can be present in different *Carassius* species. The length of chromosomes might theoretically be influenced by storage time if the ratio or concentration of acetic acid and methanol is slightly changed [72]. To avoid these inaccuracies and preserving the chromosome suspension, we used a fixative solution with an acetic acid : methanol ratio of 1:3. This ratio was restored through the addition of fresh acetic acid and methanol. In addition, we statistically processed metaphases with different storage times, for which we found no difference in chromosome length. For the case of standardized karyotype, all previous negative effects that influence $q + p$ arm length can be discounted because even if the length of chromosome had changed, the position of the centromere remains identical, thus *i* values never change [2]. In addition, the *i* value errors were eliminated through analysis of the median Q_2 range.

The correct order of chromosomes in *Carassius* karyograms remains difficult to determine. For our purposes, we arranged chromosomes according to decreasing *i* values. As such, chr1 has the highest *i* value and chr50 has the lowest *i* value. Using this approach describes a shared synteny of *i* value among *C. auratus*, *C. carassius* and *C. gibelio* (Figure 3). This method of numbering of chromosomes according *i* value in *Carassius* can be modified in future studies such as the numbering in human decreasingly according to $q + p$ chromosomal length [73].

FISH analysis revealed two large non-nucleolar 5S loci and two large nucleolar 28S ribosomal loci in each of the *Carassius* species that were investigated; this indicates functional diploidy in evolutionary tetraploid biotype. Two strong rDNA signals were found

in other studies which described *Carassius* karyotype [32,40,74]. The number of 5S rDNA loci (strong and weak signals in total) ranged from eight to ten, and 28S rDNA loci ranged from four to six, with a single chromosome-bearing rDNA locus differing in each *Carassius* species. We found higher similarity in a number of rDNA loci in *C. auratus* and *C. gibelio*, i.e., ten 5S and four 28S rDNA signals in these two species. *Carassius carassius* possessed eight 5s and six 28S rDNA signals. Knytl et al. [32] identified 18 5S and four 28S rDNA loci in diploid *C. carassius* originating from Finland waters. Spoz et al. [40] pointed out ten 5S and four 28S rDNA loci in *C. carassius* from Poland. Chinese *C. auratus* has 2–8 5S rDNA signals [74]. This study brought the first report of the FISH analysis used on diploid European *C. gibelio*, which belongs to phylogentically very diverse taxonomic group [66]. Our results showed variability in the number and position of ribosomal tandem repeats in *Carassius* which is in accordance with other rDNA studies [32,40,74]. This variability in rDNA loci has been shown between species of the same genus [38] and even between individuals of the same species for 18S and 28S loci [75,76]. The present variability of rDNA loci can be attributed to degree in heterochromatin condensation and nucleolar activity during mitosis [77].

Overall, we have described a standardized karyotype of three species of *Carassius* genus: *C. auratus*, *C. carassius* and *C. gibelio*. We compared these three species using cytogenetic tools: The arithmetic mean of the length of $q + p$ chromosomal arm showed higher similarity of *C. auratus* and *C. carassius*, and a difference of *C. gibelio* (Figure 1). Analysis of median of the i value showed higher similarity of *C. carassius* and *C. gibelio*, and higher difference of *C. auratus* (Figures 2 and 3). FISH confirmed a higher similarity of *C. auratus* to *C. gibelio*, compared to *C. carassius* (Figure 4). Thus, we can conclude that the genus *Carassius* has a very complex cytogenetic background, which can be distinguished using cytogenetic tools, with some inconsistencies in measuring propinquity and congeniality. The findings presented here are consistent with the presence of great genome variability and plasticity. Such geneome variability could be attributed to the occurance of rare natural phenomena such as interspecies hybridization, polyploidization, and/or alternation of reproduction modes within the genus *Carassius* [16,43,78,79].

Supplementary Materials: The following are available online at https://www.mdpi.com/article/10.3390/cells10092343/s1, Figure S1: Giemsa-stained chromosome metaphases (B&W) used for long (q) and short (p) chromosome arms measurement. The Figure shows one representative metaphase for each sex of each species. Each chromosome has a working numeric code 1–100. Metaphases show 100 chromosomes in (**a**) *Carassius auratus* (CAU) male, (**b**) *C. auratus* female, (**c**) *C. carassius* (CCA) male, (**d**) *C. carassius* female, (**e**) *C. gibelio* (CGI) male and (**f**) *C. gibelio* female, white circles in (**f**) indicate centromeric regions assigned as the narrowest part of chromosome. Figure S2: Giemsa-stained chromosome dissected from metaphase. Graphical example of the measurement of metacentric chromosome with four chromosomal arms (two chromatids). Two thin lines which lead through all four arms cross in the centromeric region—the narrowest part of chromosome. Long arm 1 ($q1$), long arm 2 ($q2$), short arm 1 ($p1$), short arm 2 ($p2$) have 14.8, 13.6, 12.6 and 12.4 pixels, respectively. Calculation of the $q + p$ arm length is shown at the top right of the figure. Table S1: *Carassius auratus* $q + p$ lengths were dissected from each metaphase and added into separate table. The last column (*mean_length*) shows arithmetic mean of length used for dot plot (Figure 1). Table S2: *Carassius auratus* i values were dissected from each metaphase and added into separate table. The last column (*mean_i*) shows arithmetic mean of the i value used for dot plot (Figure 1).

Author Contributions: Conceptualization, M.K.; methodology, M.K. and N.R.F.; software, M.K.; validation, M.K.; formal analysis, M.K.; investigation, M.K. and N.R.F.; data curation, M.K.; writing—original draft preparation, M.K.; writing—review and editing, M.K., N.R.F.; visualization, M.K.; supervision, M.K.; project administration, M.K. All authors have read and agreed to the published version of the manuscript.

Funding: This research received no external funding.

Institutional Review Board Statement: All experimental procedures involving fish were approved by the Institutional Animal Care and Use Committee of the Czech Academy of Sciences, Institute of

Animal Physiology and Genetics, according to the directives from the State Veterinary Administration of the Czech Republic, permit number 124/2009, and by the permit number CZ 00221 issued by the Ministry of Agriculture of the Czech Republic. M.K. is a holder of the Certificate of professional competence to design experiments according to §15d(3) of the Czech Republic Act No. 246/1992 coll. on the Protection of Animals against Cruelty (Registration number CZ 03973), provided by the Ministry of Agriculture of the Czech Republic.

Informed Consent Statement: Not applicable.

Data Availability Statement: Sanger sequencing data are available on-line at the NCBI database, accessed on 26 August 2021 (https://www.ncbi.nlm.nih.gov/). All data generated by `R Studio` are not presented in this study and they may be available on request from the corresponding author. All steps generating data frames and plots in `R` were summarized on-line on GitHub, accessed on 26 August 2021 (https://www.github.com/) available on request. Basic $q + p$ arm measurements can be provided in the form of `RData` file as `R` workspace, also upon request.

Acknowledgments: We are very grateful to Evans lab (Department od Biology, McMaster University, Canada) which helped us with the basis of computational programming in `R` (namely Ben J. Evans, Caroline M.S. Cauret and Xue-Ying Song). We thank very much Adrian Forsythe (Department of Zoology, Evolutionary Biology Center, Uppsala University, Sweden) for English correction. We thank Abhishek Koladiya (Department of Immunomonitoring and Flow Cytometry, Institute of Hematology and Blood Transfusion, Czech Republic) for improvement `R` scripts. Furthermore, we thank MDPI Production Team (especially Liu and Jing) for figuring out LaTeX issues, and Editorial Board of Cells for quick and positive feedback.

Conflicts of Interest: The authors declare no conflict of interest.

References

1. Delaunay, L. Comparative karyological study of species Muscari Mill. and Bellevalia Lapeyr [in Russian]. *Bull. Tiflis Bot. Gard.* **1922**, *2*, 1–32.
2. Levan, A.; Fredga, K.; Sandberg, A.A. Nomenclature for centromeric position on chromosomes. *Hereditas* **1964**, *52*, 201–220, doi:10.1111/j.1601-5223.1964.tb01953.x.
3. White, M.J.D. *Animal Cytology and Evolution*, 3rd ed.; Cambridge University Press: Cambridge, UK, 1973; p. 468.
4. White, M.J.D. *The Chromosomes*, 6th ed.; Chapman Hall: London, UK, 1973; p. 188.
5. Kretschmer, R.; Gunski, R.J.; Garnero, A.D.V.; de Freitas, T.R.O.; Toma, G.A.; Cioffi, M.D.B.; de Oliveira, E.H.C.; O'Connor, R.E.; Griffin, D.K. Chromosomal Analysis in Crotophaga ani (Aves, Cuculiformes) Reveals Extensive Genomic Reorganization and an Unusual Z-Autosome Robertsonian Translocation. *Cells* **2020**, *10*, 4, doi:10.3390/cells10010004.
6. O'Connor, R.E.; Kiazim, L.G.; Rathje, C.C.; Jennings, R.L.; Griffin, D.K. Rapid Multi-Hybridisation FISH Screening for Balanced Porcine Reciprocal Translocations Suggests a Much Higher Abnormality Rate Than Previously Appreciated. *Cells* **2021**, *10*, 250, doi:10.3390/cells10020250.
7. Cauret, C.M.; Gansauge, M.T.; Tupper, A.S.; Furman, B.L.; Knytl, M.; Song, X.Y.; Greenbaum, E.; Meyer, M.; Evans, B.J.; Wilson, M. Developmental Systems Drift and the Drivers of Sex Chromosome Evolution. *Mol. Biol. Evol.* **2020**, *37*, 799–810, doi:10.1093/molbev/msz268.
8. Augstenová, B.; Pensabene, E.; Kratochvíl, L.; Rovatsos, M. Cytogenetic Evidence for Sex Chromosomes and Karyotype Evolution in Anguimorphan Lizards. *Cells* **2021**, *10*, 1612, doi:10.3390/cells10071612.
9. Knytl, M.; Tlapakova, T.; Vankova, T.; Krylov, V. Silurana Chromosomal Evolution: A New Piece to the Puzzle. *Cytogenet. Genome Res.* **2018**, *156*, 223–228, doi:10.1159/000494708.
10. Gillberg, C. Chromosomal disorders and autism. *J. Autism Dev. Disord.* **1998**, *28*, 415–25, doi:10.1023/a:1026004505764.
11. Erkilic, N.; Gatinois, V.; Torriano, S.; Bouret, P.; Sanjurjo-Soriano, C.; Luca, V.D.; Damodar, K.; Cereso, N.; Puechberty, J.; Sanchez-Alcudia, R.; Hamel, C.P.; Ayuso, C.; Meunier, I.; Pellestor, F.; Kalatzis, V. A Novel Chromosomal Translocation Identified due to Complex Genetic Instability in iPSC Generated for Choroideremia. *Cells* **2019**, *8*, 1068, doi:10.3390/cells8091068.
12. Sember, A.; Bertollo, L.A.C.; Ráb, P.; Yano, C.F.; Hatanaka, T.; de Oliveira, E.A.; Cioffi, M.d.B. Sex Chromosome Evolution and Genomic Divergence in the Fish Hoplias malabaricus (Characiformes, Erythrinidae). *Front. Genet.* **2018**, *9*, 71, doi:10.3389/fgene.2018.00071.
13. Miura, I.; Shams, F.; Lin, S.M.; Cioffi, M.d.B.; Liehr, T.; Al-Rikabi, A.; Kuwana, C.; Srikulnath, K; Higaki, Y.; Ezaz, T. Evolution of a Multiple Sex-Chromosome System by Three-Sequential Translocations among Potential Sex-Chromosomes in the Taiwanese Frog Odorrana swinhoana. *Cells* **2021**, *10*, 661, doi:10.3390/cells10030661.
14. Seroussi, E.; Knytl, M.; Pitel, F.; Elleder, D.; Krylov, V.; Leroux, S.; Morisson, M.; Yosefi, S.; Miyara, S.; Ganesan, S.; Ruzal, M.; Andersson, L.; Friedman-Einat, M. Avian Expression Patterns and Genomic Mapping Implicate Leptin in Digestion and TNF in Immunity, Suggesting That Their Interacting Adipokine Role Has Been Acquired Only in Mammals. *Int. J. Mol. Sci.* **2019**, *20*, 4489, doi:10.3390/ijms20184489.

15. Tymowska, J. Polyploidy and cytogenetic variation in frogs of the genus Xenopus. In *Amphibian Cytogenetics and Evolution*; Green, D.M.; Sessions, S.K., Eds.; Academic Press: San Diego, CA, USA, 1991; pp. 259–297.
16. Knytl, M.; Kalous, L.; Symonová, R.; Rylková, K.; Ráb, P. Chromosome studies of European cyprinid fishes: Cross-species painting reveals natural allotetraploid origin of a Carassius female with 206 chromosomes. *Cytogenet. Genome Res.* **2013**, *139*, 276–283, doi:10.1159/000350689.
17. Kobayasi, H.; Kawashima, Y.; Takeuchi, N. Comparative Chromosome Studies in the Genus Carassius, Especially with a Finding of Polyploidy in the Ginbuna (C.auratus langsdorfii). *Jpn. J. Ichthyol.* **1970**, *17*, 153–160, doi:10.11369/JJI1950.17.153.
18. Ojima, Y.; Takai, A. Further cytogenetical studies on the origin of the gold-fish. *Proc. Jpn. Academy. Ser. B: Phys. Biol. Sci.* **1979**, *55*, 346–350, doi:10.2183/pjab.55.346.
19. Yang, L.; Sado, T.; Vincent Hirt, M.; Pasco-Viel, E.; Arunachalam, M.; Li, J.; Wang, X.; Freyhof, J.; Saitoh, K.; Simons, A.M.; Miya, M.; He, S.; Mayden, R.L. Phylogeny and polyploidy: Resolving the classification of cyprinine fishes (Teleostei: Cypriniformes). *Mol. Phylogenetics Evol.* **2015**, *85*, 97–116, doi:10.1016/j.ympev.2015.01.014.
20. Lusk, S.; Hanel, L.; Lojkásek, B.; Lusková, V.; Muška, M. The Red List of Lampreys and Fishes of the Czech Republic. In *Red List of threatened species of the Czech Republic, Vertebrates*; Němec, M.; Chobot, K., Eds.; Příroda: Prague, Czech Republic, 2017; chapter 34, pp. 51–82.
21. Sayer, C.D.; Copp, G.H.; Emson, D.; Godard, M.J.; Zięba, G.; Wesley, K.J. Towards the conservation of crucian carp Carassius carassius: understanding the extent and causes of decline within part of its native English range. *J. Fish Biol.* **2011**, *79*, 1608–1624, doi:10.1111/j.1095-8649.2011.03059.x.
22. Ohno, S.; Muramoto, J.; Christian, L.; Atkin, N.B. Diploid-tetraploid relationship among old-world members of the fish family Cyprinidae. *Chromosoma* **1967**, *23*, 1–9, doi:10.1007/BF00293307.
23. Balon, E.K. About the oldest domesticates among fishes. *J. Fish Biol.* **2004**, *65*, 1–27, doi:10.1111/j.0022-1112.2004.00563.x.
24. Lusková, V.; Lusk, S.; Halačka, K.; Vetešník, L. Carassius auratus gibelio—The most successful invasive fish in waters of the Czech Republic. *Russ. J. Biol. Invasions* **2010**, *1*, 176–180, doi:10.1134/S2075111710030069.
25. Tarkan, A.S.; Güler Ekmekçi, F.; Vilizzi, L.; Copp, G.H. Risk screening of non-native freshwater fishes at the frontier between Asia and Europe: First application in Turkey of the fish invasiveness screening kit. *J. Appl. Ichthyol.* **2014**, *30*, 392–398, doi:10.1111/jai.12389.
26. Card, J.T.; Hasler, C.T.; Ruppert, J.L.; Donadt, C.; Poesch, M.S. A Three-pass electrofishing removal strategy is not effective for eradication of prussian Carp in a North American stream network. *J. Fish Wildl. Manag.* **2020**, *11*, 485–493, doi:10.3996/JFWM-20-031.
27. Haynes, G.D.; Gongora, J.; Gilligan, D.M.; Grewe, P.; Moran, C.; Nicholas, F.W. Cryptic hybridization and introgression between invasive Cyprinid species Cyprinus carpio and Carassius auratus in Australia: Implications for invasive species management. *Anim. Conserv.* **2012**, *15*, 83–94, doi:10.1111/j.1469-1795.2011.00490.x.
28. Kalous, L.; Knytl, M. Karyotype diversity of the offspring resulting from reproduction experiment between diploid male and triploid female of silver Prussian carp, Carassius gibelio (Cyprinidae, Actinopterygii). *Folia Zool.* **2011**, *60*, 115–121.
29. Xiao, J.; Zou, T.; Chen, Y.; Chen, L.; Liu, S.; Tao, M.; Zhang, C.; Zhao, R.; Zhou, Y.; Long, Y.; You, C.; Yan, J.; Liu, Y. Coexistence of diploid, triploid and tetraploid crucian carp (Carassius auratus) in natural waters. *BMC Genet.* **2011**, *12*, 20, doi:10.1186/1471-2156-12-20.
30. Jiang, F.F.; Wang, Z.W.; Zhou, L.; Jiang, L.; Zhang, X.J.; Apalikova, O.V.; Brykov, V.A.; Gui, J.F. High male incidence and evolutionary implications of triploid form in northeast Asia Carassius auratus complex. *Mol. Phylogenetics Evol.* **2013**, *66*, 350–359, doi:10.1016/j.ympev.2012.10.006.
31. Knytl, M.; Kalous, L.; Rab, P. Karyotype and chromosome banding of endangered crucian carp, Carassius carassius (Linnaeus, 1758) (Teleostei, Cyprinidae). *Comp. Cytogenet.* **2013**, *7*, 205–213, doi:10.3897/compcytogen.v7i3.5411.
32. Knytl, M.; Kalous, L.; Rylková, K.; Choleva, L.; Merilä, J.; Ráb, P. Morphologically indistinguishable hybrid Carassius female with 156 chromosomes: A threat for the threatened crucian carp, C. carassius, L. *PLoS ONE* **2018**, *13*, e0190924, doi:10.1371/journal.pone.0190924.
33. Bertollo, L.; Cioffi, M. Direct chromosome preparation from freshwater teleost fishes. In *Fish Cytogenetic Techniques: Ray-Fin Fishes and Chondrichthyans*; Ozouf-Costaz, C.; Pisano, E.; Foresti, F.; Foresti, L.d.A.T., Eds.; CRC Press: Enfield, CT, USA, 2015; pp. 21–26.
34. Schneider, C.A.; Rasband, W.S.; Eliceiri, K.W. NIH Image to ImageJ: 25 years of image analysis. *Nat. Methods* **2012**, *9*, 671–675, doi:10.1038/nmeth.2089.
35. R Core Team. R: A Language and Environment for Statistical Computing; Vienna, Austria, 2020., https://www.R-project.org
36. RStudio Team. RStudio: Integrated Development Environment for R; RStudio, PBC., Boston, MA, **2019.**, http://www.rstudio.com
37. Naito, E.; Dewa, K.; Ymanouchi, H.; Kominami, R. Ribosomal ribonucleic acid (rRNA) gene typing for species identification. *J. Forensic Sci.* **1992**, *37*, 396–403, doi:10.1520/JFS13249J.
38. Sember, A.; Bohlen, J.; Šlechtová, V.; Altmanová, M.; Symonová, R.; Ráb, P. Karyotype differentiation in 19 species of river loach fishes (Nemacheilidae, Teleostei): Extensive variability associated with rDNA and heterochromatin distribution and its phylogenetic and ecological interpretation. *BMC Evol. Biol.* **2015**, *15*, 1–22, doi:10.1186/s12862-015-0532-9.
39. Knytl, M.; Smolík, O.; Kubíčková, S.; Tlapáková, T.; Evans, B.J.; Krylov, V. Chromosome divergence during evolution of the tetraploid clawed frogs, Xenopus mellotropicalis and Xenopus epitropicalis as revealed by Zoo-FISH. *PLoS ONE* **2017**, *12*, e0177087, doi:10.1371/journal.pone.0177087.

40. Spoz, A.; Boron, A.; Porycka, K.; Karolewska, M.; Ito, D.; Abe, S.; Kirtiklis, L.; Juchno, D. Molecular cytogenetic analysis of the crucian carp, Carassius carassius (Linnaeus, 1758) (Teleostei, Cyprinidae), using chromosome staining and fluorescence in situ hybridisation with rDNA probes. *Comp. Cytogenet.* **2014**, *8*, 233–248, doi:10.3897/compcytogen.v8i3.7718.
41. Sember, A.; Pelikánová, Š.; de Bello Cioffi, M.; Šlechtová, V.; Hatanaka, T.; Do Doan, H.; Knytl, M.; Ráb, P. Taxonomic Diversity Not Associated with Gross Karyotype Differentiation: The Case of Bighead Carps, Genus Hypophthalmichthys (Teleostei, Cypriniformes, Xenocyprididae). *Genes* **2020**, *11*, 479, doi:10.3390/genes11050479.
42. Makino, S. Notes on the chromosomes of some fresh-water Teleosts. *Jpn. J. Genet.* **1934**, *9*, 100–103.
43. Cherfas, N.B. Natural triploidy in females of the unisexual form of silver crucian carp (Carassius auratus gibelio Bloch). *Genetika* **1966**, *2*, 16–24.
44. Chiarelli, B.; Ferrantelli, O.; Cucchi, C. The caryotype of some teleostea fish obtained by tissue culture in vitro. *Experientia* **1969**, *25*, 426–427, doi:10.1007/BF01899963.
45. Raicu, P.; Taisescu, E.; Banarescu, P. Carassius carassius and Carassius auratus , a pair of diploid and tetraploid representative species (Pices, Cyprinidae). *Cytologia* **1981**, *46*, 233–240.
46. Fister, S.; Soldatovic, B. Karyotype analysis of male and diploid female Carassius auratus gibelio, Bloch (Pisces, Cyprinidae) caught in the Danube at Belgrade, evidence for the existence of a bisexual population. *Acta Vet. Beogr.* **1991**, *41*, 81–90.
47. Makino, S. A Karyological Study of Gold-fish of Japan. *Cytologia* **1941**, *12*, 96–111.
48. Ohno, S.; Atkin, N.B. Comparative DNA values and chromosome complements of eight species of fishes. *Chromosoma* **1966**, *18*, 455–466, doi:10.1007/BF00332549.
49. Ojima, Y.; Hitotsumachi, S.; Makino, S. Cytogenetic Studies in Lower Vertebrates. I A Preliminary Report on the Chromosomes of the Funa (Carassius auratus) and Gold-fish (A Revised Study). *Proc. Jpn. Acad.* **1966**, *42*, 62–66, doi:10.2183/pjab1945.42.62.
50. Ojima, Y.; Hitotsumachi, S. Cytogenetic studies in lower vertebrates. IV. a note on the chromosomes of the carp (cyprinus carpio) in comparison with those of the funa and the goldfish (Carassius Auratus). *Jpn. J. Genet.* **1967**, *42*, 163–167, doi:10.1266/jjg.42.163.
51. Arai, R.; Fujiki, A. Chromosomes of three races of Goldfish, Kuro-demekin, Sanshiki- demekin and Ranchu. *Bull. Natl. Sci. Museum, Ser. A, Zool.* **1977**, *3*, 187–192.
52. Ojima, Y.; Ueda, T.; Narikawa, T. A Cytogenetic Assessment on the Origin of the Gold-fish. *Proc. Jpn. Acad. Ser. B* **1979**, *55*, 58–63, doi:10.2183/pjab.55.58.
53. Ojima, Y.; Yamano, T. The assignment of the nucleolar organizer in the chromosomes of the funa (Carassius, cyprinidae, pisces). *Proc. Jpn. Acad. Ser. B* **1980**, *56*, 551–556, doi:10.2183/pjab.56.551.
54. Zan, R.G.; Song, Z. Analysis and comparison between the karyotypes of Cyprinus carpio and Carassius auratus as well as Aristichthys nobilis and Hypophthalmichthys molitrix. *Acta Genet. Sin.* **1980**, *7*, 72–77.
55. Zan, R.G. Studies of sex chromosomes and C-banding karyotypes of two forms of Carassius auratus in Kunming Lake. *Acta Genet. Sin.* **1982**, *9*, 32–39.
56. Wang, R.F.; Shi, L.M.; He, W.S. A Comparative Study of the Ag-NORS of Carassius auratus from Different Geographic Districts. *Zool. Res.* **1988**, *9*, 165–169.
57. Kasama, M.; Kobayasi, H. Hybridization Experiment Between Female Crucian Carp and Male Grass Carp. *Nippon. Suisan Gakkaishi Jpn. Ed.* **1989**, *55*, 1001–1006, doi:10.2331/suisan.55.1001.
58. Kasama, M.; Kobayasi, H. Hybridization experiment between Carassius carassius female and Gnathopogon elongatus elongatus male. *Jpn. J. Ichthyol.* **1990**, *36*, 419–426, doi:10.1007/BF02905461.
59. Kasama, M.; Kobayashi, H. Hybridization experiment between Gnathopogon elongatus elongatus female and Carassius carassius male. *Jpn. J. Ichthyol.* **1991**, *38*, 295–300, doi:10.1007/bf02905575.
60. Hafez, R.; Labat, R.; Quillier, R. Cytogenetic study of some species of Cyprinidae from the Midi-Pyrenees region. *Bull. De La Soc. D'Histoire Nat. De Toulouse* **1978**, *114*, 122–159.
61. Sofradžija, A.; Berberović, L.; Hadžiselimović, R. Hromosomske garniture karaša (Carassius carassius) i babuške (Carassius auratus gibelio). *Ichthyologia* **1978**, *10*, 135–148.
62. Mayr, B.; Ráb, P.; Kalat, M. NORs and counterstain-enhanced fluorescence studies in Cyprinidae of different ploidy level. *Genetica* **1986**, *69*, 111–118, doi:10.1007/BF00115130.
63. Kobayasi, H.; Ochi, H.; Takeuchi, N. Chromosome studies in the genus Carassius: Comparison of C. auratus grandoculis, C. auratus buergeri, and C. auratus langsdorfii. *Jpn. J. Ichthyol.* **1973**, *20*, 6, doi:10.11369/jji1950.20.7.
64. Boron, A. Karyotypes of diploid and triploid silver crucian carp Carassius auratus gibelio (Bloch). *Cytobios* **1994**, *80*, 117–124.
65. Boron, A.; Szlachciak, J.; Juchno, D.; Grabowska, A.; Jagusztyn, B.; Porycka, K. Karyotype, morphology, and reproduction ability of the Prussian carp, Carassius gibelio (Actinopterygii: Cypriniformes: Cyprinidae), from unisexual and bisexual populations in Poland. *Acta Ichthyol. Et Piscat.* **2011**, *41*, 19–28, doi:10.3750/AIP2011.41.1.04.
66. Kalous, L.; Bohlen, J.; Rylková, K.; Petrtýl, M. Hidden diversity within the Prussian carp and designation of a neotype for Carassius gibelio (Teleostei: Cyprinidae). *Ichthyol. Explor. Freshwaters* **2012**, *23*, 11–18.
67. Papoušek, I.; Vetešník, L.; Halačka, K.; Lusková, V.; Humpl, M.; Mendel, J. Identification of natural hybrids of gibel carp Carassius auratus gibelio (Bloch) and crucian carp Carassius carassius (L.) from lower Dyje River floodplain (Czech Republic). *J. Fish Biol.* **2008**, *72*, 1230–1235, doi:10.1111/j.1095-8649.2007.01783.x.

68. Wouters, J.; Janson, S.; Lusková, V.; Olsén, K.H. Molecular identification of hybrids of the invasive gibel carp Carassius auratus gibelio and crucian carp Carassius carassius in Swedish waters. *J. Fish Biol.* **2012**, *80*, 2595–2604, doi:10.1111/j.1095-8649.2012.03312.x.
69. King, M. *Species Evolution: The Role of Chromosome Change*; Cambridge University Press: Cambridge, UK, 1993; p. 336.
70. Cremer, T.; Cremer, C. Chromosome territories, nuclear architecture and gene regulation in mammalian cells. *Nat. Rev. Genet.* **2001**, *2*, 292–301, doi:10.1038/35066075.
71. Chevret, E.; Volpi, E.; Sheer, D. Mini review: Form and function in the human interphase chromosome. *Cytogenet. Genome Res.* **2000**, *90*, 13–21, doi:10.1159/000015654.
72. Claussen, U.; Michel, S.; Mhlig, P.; Westermann, M.; Grummt, U.W.; Kromeyer-Hauschild, K.; Liehr, T. Demystifying chromosome preparation and the implications for the concept of chromosome condensation during mitosis. *Cytogenet. Genome Res.* **2002**, *98*, 136–146, doi:10.1159/000069817.
73. Tjio, J.H.; Levan, A. The chromosome number of man. *Hereditas* **1956**, *42*, 1–6, doi:10.1111/j.1601-5223.1956.tb03010.x.
74. Zhu, H.P.; Ma, D.M.; Gui, J.F. Triploid origin of the gibel carp as revealed by 5S rDNA localization and chromosome painting. *Chromosome Res.* **2006**, *14*, 767–776, doi:10.1007/s10577-006-1083-0.
75. Mantovani, M.; Abel, L.D.d.S.; Moreira-Filho, O. Conserved 5S and variable 45S rDNA chromosomal localisation revealed by FISH in Astyanax scabripinnis (Pisces, Characidae). *Genetica* **2005**, *123*, 211–6, doi:10.1007/s10709-004-2281-3.
76. Gromicho, M.; Coutanceau, J.P.; Ozouf-Costaz, C.; Collares-Pereira, M.J. Contrast between extensive variation of 28S rDNA and stability of 5S rDNA and telomeric repeats in the diploid-polyploid Squalius alburnoides complex and in its maternal ancestor Squalius pyrenaicus (Teleostei, Cyprinidae). *Chromosome Res.* **2006**, *14*, 297–306, doi:10.1007/s10577-006-1047-4.
77. Schmid, M.; Vitelli, L.; Batistoni, R. Chromosome banding in amphibia. XI. Constitutive heterochromatin, nucleolus organizers, 18S + 28S and 5S ribosomal RNA genes in Ascaphidae, Pipidae, Discoglossidae and Pelobatidae. *Chromosoma* **1987**, *95*, 271–84.
78. Zhou, L.; Wang, Y.; Gui, J.F. Genetic Evidence for Gonochoristic Reproduction in Gynogenetic Silver Crucian Carp (Carassius auratus gibelio Bloch) as Revealed by RAPD Assays. *J. Mol. Evol.* **2000**, *51*, 498–506, doi:10.1007/s002390010113.
79. Daněk, T.; Kalous, L.; Veselý, T.; Krásová, E.; Reschová, S.; Rylková, K.; Kulich, P.; Petrtýl, M.; Pokorová, D.; Knytl, M. Massive mortality of Prussian carp Carassius gibelio in the upper Elbe basin associated with herpesviral hematopoietic necrosis (CyHV-2). *Dis. Aquat. Org.* **2012**, *102*, 87–95, doi:10.3354/dao02535.

Paper 2: **Divergent subgenome evolution in the allotetraploid frog *Xenopus calcaratus***

Gene 851 (2023) 146974

Contents lists available at ScienceDirect

Gene

journal homepage: www.elsevier.com/locate/gene

Research paper

Divergent subgenome evolution in the allotetraploid frog *Xenopus calcaratus*

Martin Knytl [a,*], Nicola R. Fornaini [a], Barbora Bergelová [a], Václav Gvoždík [b], Halina Černohorská [c], Svatava Kubíčková [c], Eric B. Fokam [d], Ben J. Evans [e,1], Vladimír Krylov [a,1]

[a] Department of Cell Biology, Faculty of Science, Charles University, Viničná 7, Prague 12843, Czech Republic
[b] Institute of Vertebrate Biology of the Czech Academy of Sciences, Brno, Czech Republic
[c] Department of Genetics and Reproduction, CEITEC - Veterinary Research Institute, Hudcova 296/70, Brno 62100, Czech Republic
[d] Department of Animal Biology and Conservation, University of Buea, PO Box 63, Buea 00237, Cameroon
[e] Department of Biology, McMaster University, 1280 Main Street West, Hamilton L8S4K1, Ontario, Canada

ARTICLE INFO

Edited by Andre van Wijnen

Keywords:
Genome
Chromosome
Cytogenetics
FISH
Chromosome length
Allopolyploidization

ABSTRACT

Allopolyploid genomes are divided into compartments called subgenomes that are derived from lower ploidy ancestors. In African clawed frogs of the subgenus *Xenopus* (genus *Xenopus*), allotetraploid species have two subgenomes (L and S) with morphologically distinct homoeologous chromosomes. In allotetraploid species of the sister subgenus *Silurana*, independently evolved subgenomes also exist, but their cytogenetics has not been investigated in detail. We used a diverse suite of cytogenetic and molecular FISH techniques on an allotetraploid species in *Silurana*—*Xenopus calcaratus*—to explore evolutionary dynamics of chromosome morphology and rearrangements. We find that the subgenomes of *X. calcaratus* have distinctive characteristics, with a more conserved a-subgenome resembling the closely related genome of the diploid species *X. tropicalis*, and a more rapidly evolving b-subgenome having more pronounced changes in chromosome structure, including diverged heterochromatic blocks, repetitive sequences, and deletion of a nucleolar secondary constriction. Based on these cytogenetic differences, we propose a chromosome nomenclature for *X. calcaratus* that may apply to other allotetraploids in subgenus *Silurana*, depending on as yet unresolved details of their evolutionary origins. These findings highlight the potential for large-scale asymmetry in subgenome evolution following allopolyploidization.

1. Introduction

Whole genome duplication (polyploidization) and large-scale chromosomal rearrangements are important evolutionary driving forces that contribute to genome variability, for example by creating duplicate genes and affecting patterns of recombination (Wolfe, 2001). Polyploidization is a potential mode of sympatric speciation wherein reproductive isolation from progenitor species is achieved via inviability or sterility of offspring of a cross between parents of differing ploidy levels (Janko et al., 2018). Polyploidization occurs via genome duplication within a single species (autopolyploidization) or in association with hybridization between two or more distinct species (allopolyploidization). Divergence between homoeologous chromosomes could expedite rediploidization of a polyploid genome, wherein chromosomes acquire disomic inheritance, with each having only one homologous partner during meiosis. This has the effect of creating separate genomic compartments called "subgenomes"; in allopolyploid genomes, each subgenome is derived mostly or entirely from a different ancestral species (Schiavinato et al., 2021).

Chromosomal changes such as translocations, inversions, insertions, and deletions are divided into small- and large-scale rearrangements. Small-scale rearrangements involve regions smaller than one megabase. Large-scale rearrangements affect regions larger than one megabase, may include fusions and fissions of different chromosomes, and may alter karyotype organization and gene expression. In any genome, the frequency of chromosomal rearrangements is governed by several factors including presence of retrotransposons in genome (Biémont and Vieira, 2006), spatial variation in DNA stability and fragility, and external factors such as radiation or environmental conditions (Feder et al., 2011). Within a polyploid genome, the frequency of rearrangements may differ between subgenomes (Brunet et al., 2006; Session et al., 2016; Li et al., 2021).

* Corresponding author.
E-mail address: martin.knytl@natur.cuni.cz (M. Knytl).
[1] B.J. Evans and V. Krylov are joint last authors.

https://doi.org/10.1016/j.gene.2022.146974
Received 23 July 2022; Received in revised form 30 September 2022; Accepted 11 October 2022
Available online 27 October 2022

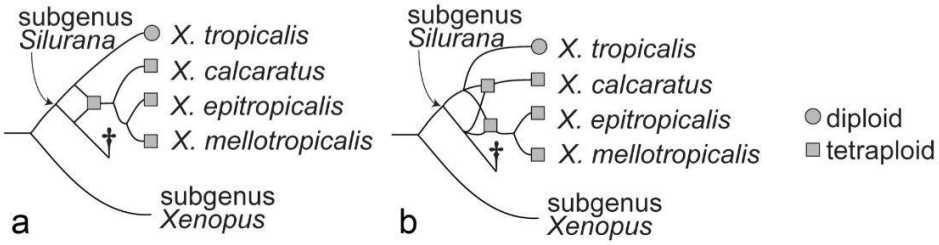

Fig. 1. Phylogenetic scenarios of the subgenus *Silurana*. A sister clade, subgenus *Xenopus*, is depicted as an outgroup. **(a)** A scenario involving one allotetraploidization via the fusion of two diploid ancestors, one of which was closely related to *X. tropicalis* and the other of which went extinct (dagger), to give rise to the most recent common ancestor of all three allotetraploid species in subgenus *Silurana*. **(b)** An alternative scenario involving two independent allotetraploidization events; one gave rise to the ancestor of *X. calcaratus* and the other to the most recent common ancestor of *X. epitropicalis* and *X. mellotropicalis*.

1.1. Allopolyploid genomes of African clawed frogs (Xenopus)

African clawed frogs, genus *Xenopus* (family Pipidae), are divided into subgenera *Xenopus* and *Silurana*, that include diploid and tetraploid species in *Silurana*, and tetraploid, octoploid, and dodecaploid species in *Xenopus* (Tymowska, 1991; Evans, 2008; Evans et al., 2015). This high species diversity (29 species in total) with a range of ploidy levels makes *Xenopus* a compelling focal group for studying cytogenetics and chromosomal rearrangements in the wake of polyploidization, with the potential to provide insights into whether and how genomic rearrangements are linked to speciation and adaptation.

Available information from extant tetraploids, octoploids, and dodecaploids indicates that they are allopolyploids rather than autopolyploids (Evans et al., 2005; Evans et al., 2015; Session et al., 2016). For example, in *X. laevis* (subgenus *Xenopus*), each subgenome contains different transposable element complements that originate from distinct ancestors (Session et al., 2016).

In subgenus *Xenopus*, several large-scale rearrangements have been identified. The largest involves a fusion between chromosomes 9 and 10 in a diploid ancestor of allopolyploids in subgenus *Xenopus* (Session et al., 2016). Comparison to a high-quality genome assembly of the diploid species *X. tropicalis* evidences several other rearrangements within the *X. laevis* S-subgenome and comparative genomic stability of the *X. laevis* L-subgenome (Session et al., 2016).

In *Silurana* tetraploids, divergence between the homoeologous a- and b-subgenomes is higher than between the a-subgenome and the genome of diploid *X. tropicalis* (Evans, 2008; Evans et al., 2015), as expected by allotetraploidy. In *Silurana*, one large-scale rearrangement has been identified—a nonreciprocal interchromosomal translocation of pericentromeric region between chromosomes 9b and 2a of the tetraploid species *X. mellotropicalis* (sensu Knytl et al., 2017; Knytl et al., 2018b). This rearrangement was identified using fluorescent in situ hybridization (FISH) in which whole chromosome painting (WCP) probes from *X. tropicalis* were hybridized to chromosomes of *X. mellotropicalis* (Zoo-FISH).

It remains unknown whether this rearrangement occurred in the ancestor of all three allotetraploid species in *Silurana* (*X. mellotropicalis*, *X. epitropicalis*, *X. calcaratus*) or more recently after the ancestor of *X. mellotropicalis* diverged from the ancestor(s) of the other species (Fig. 1). This is because evolutionary relationships among species in subgenus *Silurana* remain poorly resolved; very little genomic data has been collected from *X. calcaratus* and *X. epitropicalis* that could be leveraged for phylogenetic estimation along with genomic data from other *Silurana* species (Hellsten et al., 2010; Cauret et al., 2020). Available information from two tightly linked genes (*RAG1* and *RAG2*) suggest that two separate allotetraploidization events occurred in *Silurana*: one generated *X. calcaratus* and the other resulted in the ancestor of *X. mellotropicalis* and *X. epitropicalis* (Evans et al., 2005; Evans, 2007) (Fig. 1b). However, a simplier scenario is also possible where allotetraploidization occurred only once in *Silurana* (Fig. 1a). Also lacking are cytogenetic characters that can clearly distinguish homoeologous chromosomes of the *Silurana* subgenomes.

Large-scale genomic rearrangements occurred multiple times in genus *Xenopus* and may have been influential in the evolution of *Xenopus*. In this study, we examined cytogenetic evolution of *X. calaratus* with an aim of better understanding genome evolution in this species and also to further contextualize evolution of the interchromosomal translocation in *X. mellotropicalis* (Knytl et al., 2017). We used a suite of chromosome banding and FISH techniques and statistically processed chromosomal measurement information to provide unprecedented resolution of the karyotype of the allotetraploid Biafran clawed frog, *X. calcaratus*.

2. Methods

2.1. Establishment of primary cell cultures

Primary cell cultures were derived from the hind limb of tadpoles at stage NF55(±1) (Sinzelle et al., 2012) of *X. calcaratus* originated from Bakingili, Cameroon, and *X. tropicalis*, derived from an Ivory Coast laboratory strain. Both species were bred at Charles University, Faculty of Science, Prague, Czech Republic. Briefly, tadpoles were anesthetized by 0.4% MS-222 (Sigma–Aldrich, St. Louis, MO, USA) and then washed with sterile MilliQ water following euthanasia. The hind limbs were removed and homogenized in cultivation medium which was prepared from components as described in Knytl et al. (2017) and modified by addition of Gibco™ Antibiotic–Antimycotic (100X) and 0.1 mM Gibco™ 2-mercaptoethanol (both Thermo Fisher Scientific, Waltham, MA, USA). The explants were then cultivated at 29.5°C with 5.5% CO_2 for five days without disturbance. The medium was then changed every second day. The first and next passages were performed with trypsin-ethylenediaminetetraacetic acid according to Knytl et al. (2017). For cryopreservation, cell aliquots were stored at −80°C in the cultivation medium with the addition of 10% Dimethyl sulfoxid (Sigma–Aldrich).

2.2. Preparation of chromosomal suspension and metaphase spreads

Both *X. tropicalis* and *X. calcaratus* chromosomal suspensions were prepared according to Krylov et al. (2010) and stored in fixative solution (methanol:acetic acid, 3:1, v/v) at −20°C. For laser microdissection, a fresh metaphase suspension was dropped onto a polyethylene-naphthalene membrane. For cytogenetic analysis, a chromosome suspension was dropped onto a microscope slide according to Courtet et al. (2001). Chromosome preparations were aged at −20°C for at least one week with the exception of that for FISH with tyramide signal amplification, FISH-TSA, in which the chromosome suspension was dropped and directly followed by further experimental procedures.

For each experiment, mitotic metaphase spreads were

counterstained with ProLong™ Diamond Antifade Mountant with the fluorescent 4',6-diamidino-2-phenylindole, DAPI stain (Invitrogen by Thermo Fisher Scientific). Ten to 20 metaphase spreads were analyzed per each banding technique and probe. Microscopy and processing of metaphase images using Leica Microsystem (Wetzlar, Germany) were conducted as detailed in Seroussi et al. (2019).

2.3. Laser microdissection and whole chromosome painting

All ten individual chromosomes from *X. tropicalis* (20 copies of each chromosome) were separately isolated by laser microdissection as previously described in Kubickova et al. (2002) using a PALM Microlaser system (Carl Zeiss MicroImaging GmbH, Munich, Germany). The WCP probes were prepared according to Krylov et al. (2010) with the following modifications in labeling. During whole genome amplification, digoxigenin-11-dUTP and biotin-16-dUTP (both Jena Bioscience, Jena, Germany) were incorporated into the probes (the nucleotide ratio for digoxigenated probes: 10 mM dATP, dGTP, dCTP: 6.5 mM dTTP, biotinylated probes: 10 mM dATP, dGTP, dCTP: 5 mM dTTP). Control double-colour intraspecies painting FISH on *X. tropicalis* and single-colour cross-species Zoo-FISH on *X. calcaratus* chromosomes were carried out as described by Krylov et al. (2010) with minor modifications as detailed in Knytl et al. (2017). Autoclaved *X. tropicalis* genomic DNA was used as a competitor (blocking DNA) according to Bi and Bogart (2006). In the control double-colour painting FISH, the digoxigenin and biotin labeled probe was detected by anti-digoxigenin-fluorescein (Roche, Basel, Switzerland) and CY™3-streptavidin (Invitrogen, Camarillo, CA, USA), respectively, diluted with blocking reagents as used in double-colour FISH with ribosomal probes in Knytl et al. (2017). In single-colour Zoo-FISH, fluorescent signal of digoxigenin labeled probes was visualized by anti-digoxigenin-rhodamine (Roche).

2.4. Whole genome painting

Xenopus tropicalis genomic DNA (gDNA) was used as a probe for genomic in situ hybridization (GISH) experiments. Whole genome painting (WGP) probes were prepared using the GenomePlex Single Cell Whole Genome Amplification Kit (WGA4), Sigma–Aldrich, according to the manufacturer's whole genome amplification protocol with extracted gDNA. GenomePlex WGA Reamplification Kit (WGA3), Sigma–Aldrich, and labeling with digoxigenin-11-dUTP (Jena Bioscience) was carried out as described in Krylov et al. (2010). A combination of salmon sperm (Knytl et al., 2013b) and autoclaved *X. tropicalis* gDNA (Bi and Bogart, 2006) was used as a competitor DNA. Control GISH was performed on *X. tropicalis* chromosomes as detailed in painting FISH in Krylov et al. (2010), and cross-species GISH was carried out on *X. calcaratus* chromosomes as detailed in Zoo-FISH in Krylov et al. (2010) with minor changes described in Knytl et al. (2017).

2.5. Ribosomal gene mapping and chromosome banding

Double-colour FISH was performed with *5S* and *28S* ribosomal DNA probes (rDNA FISH), followed by two chromosome banding techniques that were conducted sequentially on the same metaphase spread: C-banding, and then Chromomycin A_3, CMA_3 (Sigma–Aldrich).

Xenopus calcaratus gDNA was used as a template for amplification of both *5S* and *28S* loci. Total gDNA was extracted from the tail tissue of a tadpole using the DNeasy Blood & Tissue Kit (Qiagen, Hilden, Germany) according to manufacturer's instructions. *5S* and *28S* primer sequences (Integrated DNA Technologies, Coralville, IA, USA) are listed in Table S1. Preparation of *5S* and *28S* probes including modified PCR conditions (Sember et al., 2015) and labelling with digoxigenin-11-dUTP and biotin-16-dUTP (both Jena Bioscience) is detailed in Knytl and Fornaini (2021). The *5S* and *28S* probes were hybridized with chromosomal spreads of *X. calcaratus*. In total 22 μL of the hybridization mixture containing 100 ng of either *5S* or *28S* rDNA probe, and 14 μL master mix (10% dextran sulfate) was placed on a slide and covered with a 22 × 22 mm coverslip. Both probe and chromosomal DNA were denatured at 72°C for 5 min with subsequent overnight hybridization in a dark wet chamber. Post-hybridization washing and blocking reactions were performed as described for painting FISH in Krylov et al. (2010). Probe signal was visualized as described in Knytl et al. (2017).

The sequential chromosome banding protocol (C-banding, CMA_3) followed Rábová et al. (2015), with the modifications described in Knytl et al. (2017).

2.6. Single-copy gene mapping

We set out to assess whether the *X. mellotropicalis* translocation between chromosomes 9b and 2a (sensu Knytl et al., 2017), with the nomenclature of 2a revised to be chromosome 2b as detailed below in Section 4.2, also was present in *X. calcaratus*. To accomplish this, mapping analysis was performed in *X. calcaratus* for five single-copy genes that flank the translocated region (rearrangement-associated genes) in *X. mellotropicalis* as revealed by Zoo-FISH and FISH-TSA (Knytl et al., 2017; Knytl et al., 2018b). Two of these genes are situated on the short (*p*) arm of the *X. tropicalis* chromosome 2 (XTR 2) (glycogenin 2, *gyg2* and choline/ethanolamine phosphotransferase1, *cept1*) and three are on the long (*q*) arm of XTR 9 (splicing factor 3b subunit 1, *sf3b1*, NADH: ubiquinone oxidoreductase core subunit S1, *ndufs1*, and fibronectin 1, *fn1*) (Uno et al., 2012; Seifertova et al., 2013; Knytl et al., 2018b). The same probes from Knytl et al. (2018b) (*gyg2*, *cept1*, *sf3b1*, *ndufs1*, and *fn1* genes prepared from *X. mellotropicalis* RNA) were used and labelled with digoxigenin-11-dUTP (Roche). The FISH-TSA protocol was adapted from Krylov et al. (2007) with minor modifications described in Knytl et al. (2018b). Sequences for alpha and beta single-copy gene loci (*gyg2*, *cept1*, *sf3b1*, *ndufs1*, and *fn1*) that were used as probes for FISH-TSA are deposited in the NCBI GenBank database (Knytl et al., 2018b). Primer sequences are listed in Table S1.

2.7. Measurement and identification of X. calcaratus chromosomes

A total of 35 *X. calcaratus* individual metaphase figures were analyzed. Half of the metaphases selected for the identification of individual chromosomes was stained with 5% Giemsa/PBS solution (v/v). The rest were stained with DAPI during FISH experiments. Both arms of each chromatid were measured in pixels using `ImageJ`, V 1.53i (Schneider et al., 2012). The *p* and *q* arm lengths were quantified as described in Knytl and Fornaini (2021). To identify each chromosome, we analyzed chromosomal length (*l*), *p*/*q* arm ratio (r_1) (Tymowska, 1973), centromeric index (*i*), and *q*/*p* arm ratio (r_2) (Levan et al., 1964).

$$l = p + q \qquad r_1 = \frac{p}{q} \qquad r_2 = \frac{q}{p} \qquad i = \frac{100}{r_2 + 1} \tag{1}$$

Chromosomal numbering was adopted from Knytl et al. (2017) with proposed revisions detailed below. Data were analyzed in `R` software for statistical computing, V 4.1.0 (R Core Team, 2020). One-way analysis of variance (one-way ANOVA) was performed to compare *l* and *i* values between each homoeologous pair of chromosomes using `R` scripts modified from Knytl and Fornaini (2021). All steps outlining how the measured values were calculated and processed into tables and plots are available on https://github.com/martinknytl/R.

3. Results

3.1. Species identification

Species of *Xenopus* frogs are notoriously difficult to diagnose based on external anatomy. We therefore used Sanger sequencing of our experimental individual for species diagnosis. PCR amplifications of portions of the *5S* and *28S* nuclear rRNA genes, and the *16S*

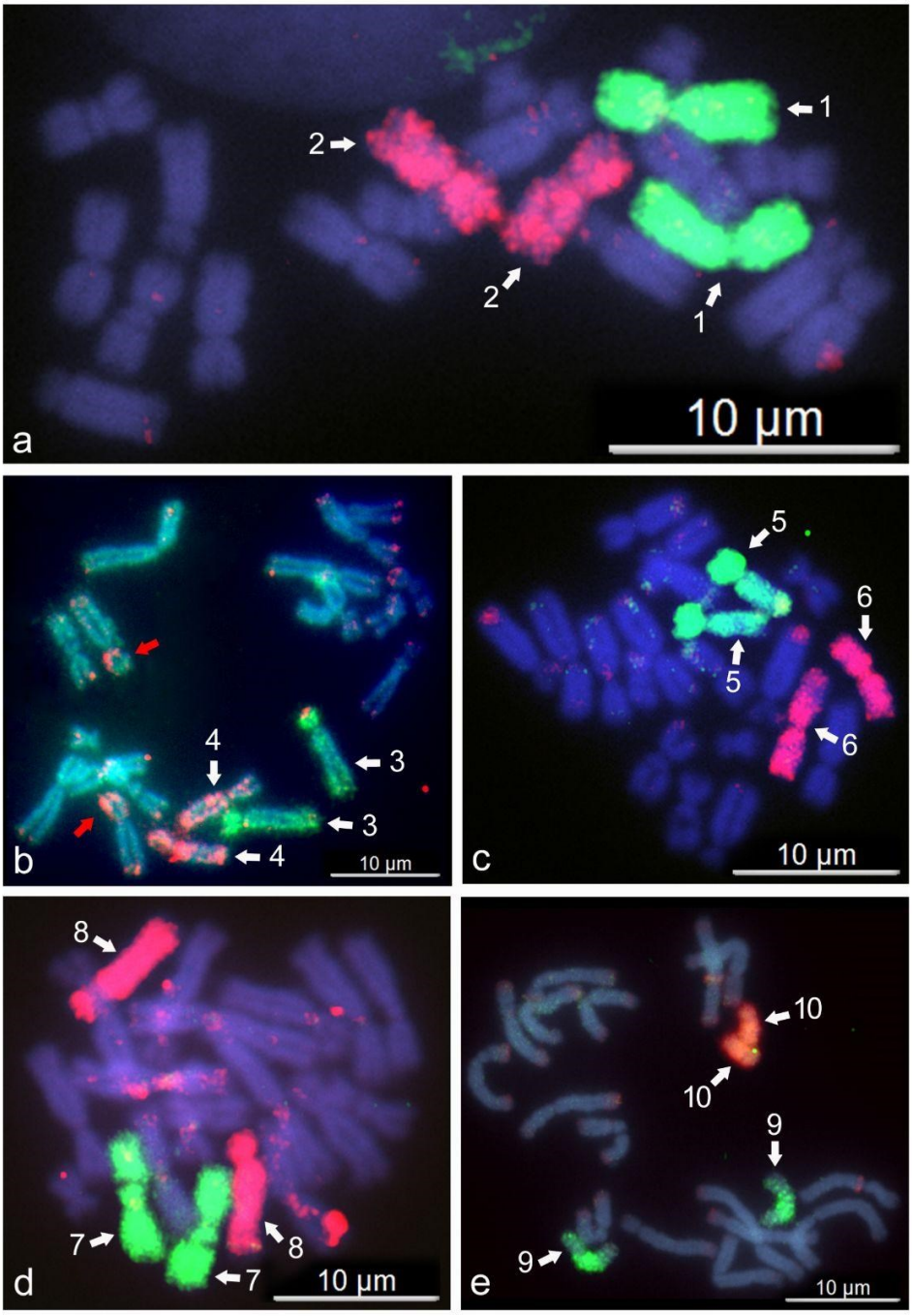

Fig. 2. Double-colour painting fluorescent in situ hybridization on 20 *X. tropicalis* chromosomes (XTR) with *X. tropicalis* whole chromosome painting (WCP) probes (intraspecies painting FISH). White arrowheads indicate painting of whole chromosome pairs using WCP probes derived from **(a)** XTR 1 (green) and XTR 2 (red), **(b)** XTR 3 (green) and XTR 4 (red), **(c)** XTR 5 (green) and XTR 6 (red), **(d)** XTR 7 (green) and XTR 8 (red), and **(e)** XTR 9 (green) and XTR 10 (red). Chromosomes were counterstained with 4',6-diamidino-2-phenylindole, DAPI (blue). In addition to stained homologous chromosome pairs, (b) some WCP probes had an additional signal on pericentromeric and telomeric regions, which presumably is caused by repetitive sequences (red arrowheads). Each scale bar represents 10 μm.

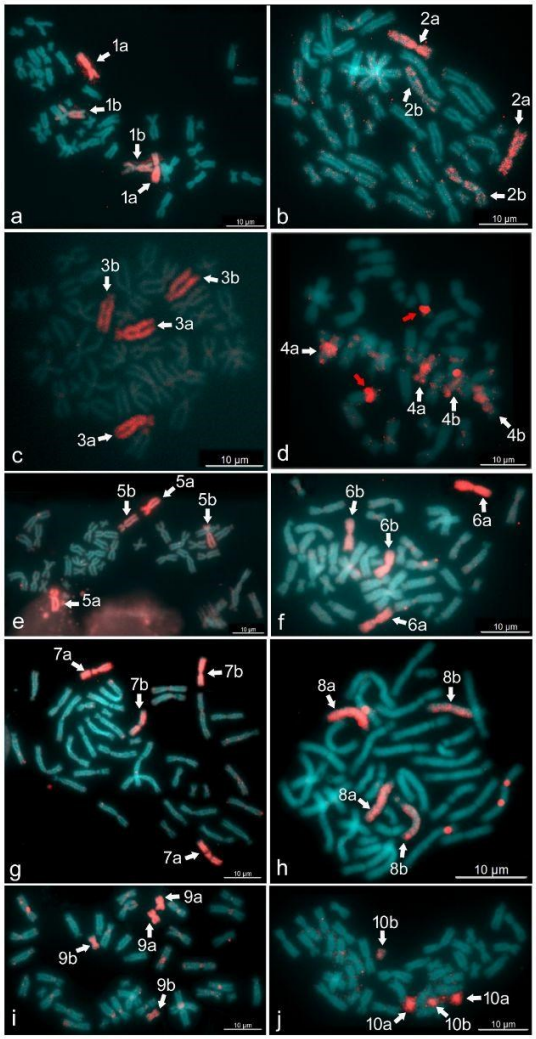

Fig. 3. Cross-species painting FISH (Zoo-FISH) on 40 *X. calcaratus* chromosomes (XCA) using *X. tropicalis* WCP probes. The WCP probes stain the appropriate chromosomal quartets in red. **(a)** XTR 1–XCA 1a and 1b, **(b)** XTR 2–XCA 2a and 2b, **(c)** XTR 3–XCA 3a and 3b, **(d)** XTR 4–XCA 4a and 4b, **(e)** XTR 5–XCA 5a and 5b, **(f)** XTR 6–XCA 6a and 6b, **(g)** XTR 7–XCA 7a and 7b, **(h)** XTR 8–XCA 8a and 8b, **(i)** XTR 9–XCA 9a and 9b and **(j)** XTR 10–XCA 10a and 10b. White arrowheads show labeled chromosomal quartets. Chromosomes were counterstained with DAPI (blue-green). In addition to red-stained homoeologous chromosomes, some WCP probes also had an additional signal on pericentromeric and telomeric regions, which presumably is caused by repetitive sequences (red arrowheads). Each scale bar represents 10 μm.

mitochondrial rRNA gene resulted in approximately 200 and 300, and 900 bp long amplicons.

Based on `blastn` results, the *5S* amplicon had 96% identity with the sequence of *5S* rDNA of *X. tropicalis* (accession number X12624.1), and *28S* amplicon had 100% identity with *28S* rRNA of *X. tropicalis* (accession number XR_004223802.1), which is consistent with membership in subgenus *Silurana* (at the time of this study, sequences of these genes for *X. calcaratus* are not present in the GenBank database). The *16S* amplicon showed 100% identity with *16S* rRNA of *X. calcaratus* (accession number KT728037.1) from the same locality in Cameroon but 2.8–3.0% divergence from *X. tropicalis* (accession numbers KT728027.1 and KT728029.1), which is not known to occur in this locality. Together these results confirmed the species identity of the *X. calcaratus* cells. As detailed below, this species diagnosis is also consistent with chromosome counts that also distinguish these two species. Sequences are deposited to the NCBI GenBank database (*5S* accession number ON908197, *28S* accession number OM910742, *16S* accession number OM912675).

3.2. Fluorescent in situ hybridization with whole chromosome painting probes

Ten WCP probes were prepared from each separately microdissected chromosome of *X. tropicalis*. As expected, each probe hybridized specifically and stained a whole *X. tropicalis* homologous chromosome pair 1–10 (Fig. 2a-e, with pairs of probes labeled in green and red). This control in *X. tropicalis* demonstrates high specificity of the WCP probes derived from this diploid species.

Having confirmed specificity of the *X. tropicalis* WCP probes, we went on to perform Zoo-FISH experiments on *X. calcaratus* metaphase spreads using each *X. tropicalis* WCP probe. The WCP probes derived from XTR 1–10 hybridized to whole chromosomal quartets (the homoeologous chromosome groups) without evidence of large-scale translocations as follows: XTR 1 to *X. calcaratus* chromosome 1a (XCA 1a) + 1b (Fig. 3a); XTR 2 to XCA 2a + 2b (Fig. 3b); XTR 3 to XCA 3a + 3b (Fig. 3c); XTR 4 to XCA 4a + 4b (Fig. 3d); XTR 5 to XCA 5a + 5b (Fig. 3e); XTR 6 to XCA6a + 6b (Fig. 3f); XTR 7 to XCA 7a + 7b (Fig. 3g); XTR 8 to XCA 8a + 8b (Fig. 3h); XTR 9 to XCA 9a + 9b (Fig. 3i); and XTR 10 to XCA 10a + 10b (Fig. 3j).

A key finding that emerged from the *X. calcaratus* Zoo-FISH experiments is that one homologous chromosome pair had consistently higher fluorescent intensity than the other. Based on this, we defined *X. calcaratus* "a" homoeologs (or α, sensu Evans et al. (2005)) to be the more intensely painted chromosomes and "b" homoeologs (or β, sensu Evans et al. (2005)) to be the less intensely painted ones. The observation of differential painting intensity is consistent with an allotetraploid origin of *X. calcaratus* from a diploid common ancestor of *X. tropicalis* and another divergent diploid ancestor whose diploid descendants are either extinct or have not yet been discovered (Fig. 1). That these experiments found no evidence of a chromosomal translocation between chromosomes homologous to XTR 9 and 2 in *X. calcaratus* suggests this translocation occurred in an ancestor of *X. mellotropicalis* after divergence from an ancestor of *X. calcaratus*.

Using the WCP probe from *X. tropicalis* chromosome 4, we found an additional signal on XTR 5 (Fig. 2b, red arrowheads) and XCA 5a (Fig. 3d, red arrowheads) which is possibly caused by accumulation of repetitive sequences on a portion of the *p* arm.

3.3. Genomic in situ hybridization with whole genome painting probes

Two GISH experiments were performed with *X. tropicalis* WGP probe. The first one was a control to evaluate the efficacy of the WGP probe against *X. tropicalis* chromosomes (Fig. 4a). All 20 chromosomes were consistently painted, indicating high efficacy. The second GISH experiment hybridized the WGP probe to *X. calcaratus* chromosomes with an aim of providing verification of a distinctive cytogenetic signature of each subgenome. Similar to the WCP experiments shown in Section 3.2, this technique recovered differences in the intensity of fluorescence between several homoeologous pairs (Fig. 4b). In particular, chromosomes XCA 7a, 9a, and 10a were notably more intensely painted than XCA 7b, 9b, and 10b (labeled with arrowheads). These results are consistent with the analysis of p/q arm ratio and Zoo-FISH data discussed below, and with a closer evolutionary relationship between the XCA homoeologs "a" and XTR orthologs than between the XCA

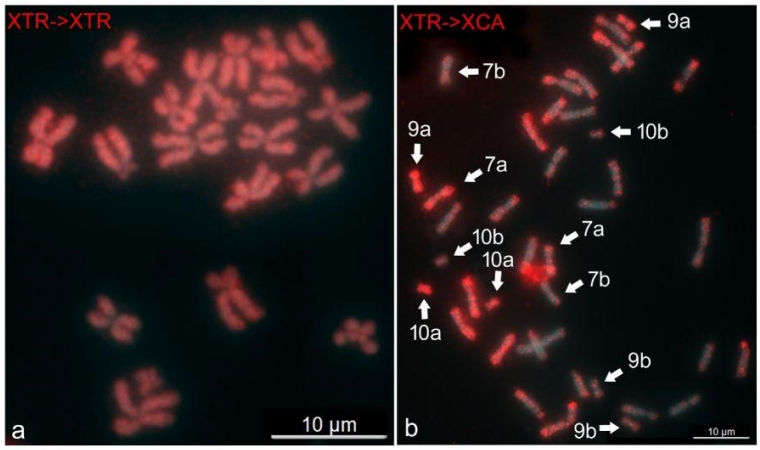

Fig. 4. Genomic in situ hybridization (GISH) using *X. tropicalis* whole genome painting (WGP) probes (in red) against **(a)** *X. tropicalis* and **(b)** *X. calcaratus* chromosomes. In **(a)**, the *X. tropicalis* WGP probes hybridized to all 20 *X. tropicalis* chromosomes (XTR→XTR) with a consistent fluorescent signal. In **(b)**, the *X. tropicalis* WGP probes hybridized to all 40 *X. calcaratus* chromosomes but with different intensities between homoeologs—especially between homoeologs XCA 7, 9, and 10 (white arrowheads). Each scale bar represents 10 μm.

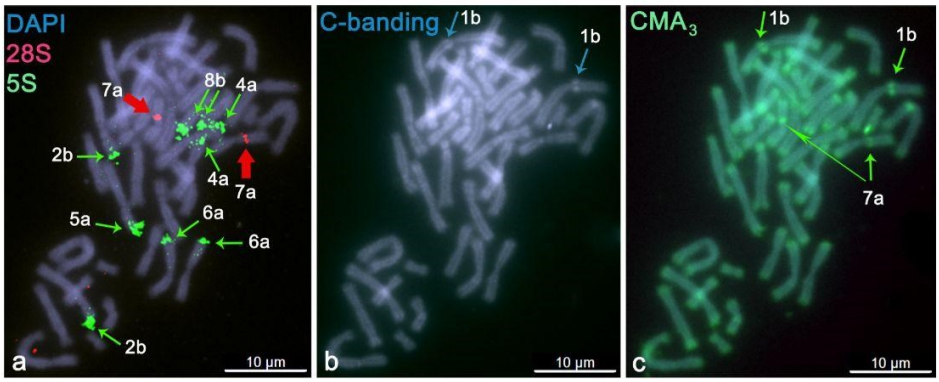

Fig. 5. Sequential fluorescent chromosome mapping (ribosomal DNA FISH/C-banding/Chromomycin A_3, CMA_3) on metaphase spread of *X. calcaratus*. DAPI (blue-green) counter-stained metaphase spreads show all 40 chromosomes. **(a)** FISH with *5S* (green) and *28S* (red) ribosomal probes identifies XCA 2b, 4a, 5a, 6a, and 8b (green arrows) and the nucleolar secondary constriction on the *q* arm of XCA 7a (red arrowheads), respectively. **(b)** C-banding (brighter staining) highlights heterochromatic blocks on the *p* arm of XCA 1b (blue arrows). **(c)** CMA_3 banding in green (green arrows) shows heterochromatic blocks on the *p* arm of XCA 1b that co-localize with C-bands, and additional CMA_3 positive band on the *q* arm of XCA 7a (nucleolar secondary constriction) that co-localize with *28S* rDNA loci. Scale bars represent 10 μm.

homoeologs "b" and XTR orthologs. Other homoeologous chromosomes within the *X. calcaratus* karyotype apart from XCA 7, 9, and 10 also were painted with slightly different but less distinguishable intensities.

3.4. Ribosomal gene mapping and chromosome banding

Nucleolar organizer regions (NORs) are regions in eukaryotic genomes that contain tandem arrays of three ribosomal genes (*18S*, *5.8S*, *28S*). In eukaryotes the ribosome includes small and large subunits; the *18S* rRNA gene is part of the small subunit and the *5.8S*, *28S* and *5S* rRNAs are part of the large subunit, though the *5S* rRNA gene is not contained within the NOR (Vierna et al., 2013). In diploid genomes there is generally only one pair of NORs (Schmid et al., 1987). Building on the findings from Zoo-FISH (Section 3.2), we expected a NOR pair to have been inherited from each of the diploid ancestral species of *X. calcaratus*. However, the FISH experiment with *28S* rDNA probes identified only one pair of NORs situated on the nucleolar secondary constriction of XCA 7*aq* (Fig. 5a, in red). The FISH with *5S* probes revealed 8–10 positive loci located on telomeric regions of the XCA 2b, 4a, 5a, 6a, and 8b as evidenced in Fig. 5a in green.

Xenopus calcaratus is closely related to *X. mellotropicalis* and for this reason we expected similar patterns and localization of the heterochromatic blocks in these two species. To test this expectation, we used C- and CMA_3-banding, which are staining techniques that highlight GC rich chromosomal loci and blocks of constitutive heterochromatin. These staining methods can be helpful for distinguishing and assigning chromosomes based on banding patterns. C- and CMA_3-banding showed positive signals on XCA 1b*p* (Figs. 5b and 5c). C-banding also exhibited a faint signal in portions of stained regions on XCA 2b, 6b, 7b, and 8b (not shown by arrows). CMA_3-banding also identified nucleolar secondary constriction of XCA 7*aq* (Fig. 5c). All *X. calcaratus* chromosomes bore weak CMA_3-bands on telomeres that presumably are caused by repetitive sequences.

3.5. Single-copy gene mapping

To test whether *X. calcaratus* shared a large scale translocation with *X. mellotropicalis*, we mapped the alpha and beta homoeologs of *gyg2*,

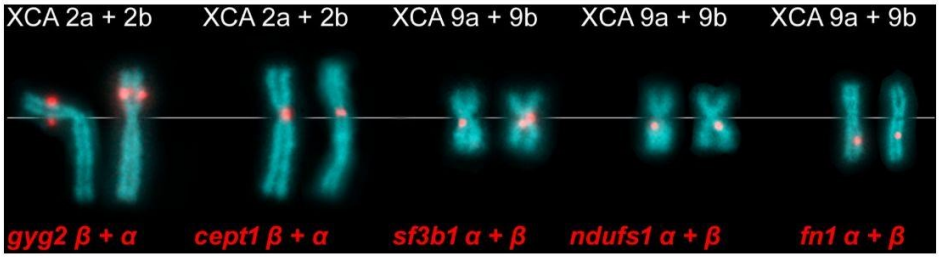

Fig. 6. FISH coupled with tyramide signal amplification (FISH-TSA) with positive red signals on *X. calcaratus* chromosomes. The *gyg2β* and *α*, *cept1β* and *α* loci were localized on the *p* arm of XCA 2a and 2b, respectively. The *sf3b1α* and *β*, *ndufs1α* and *β*, and *fn1α* and *β* loci were mapped on the *q* arm of XCA 9a and 9b, respectively. A white line indicates the centromere position.

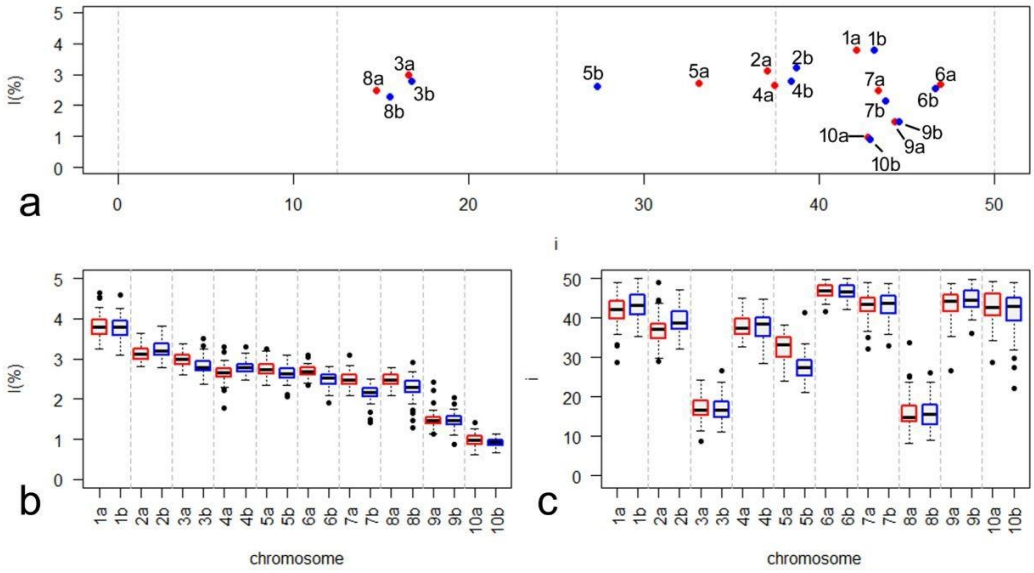

Fig. 7. Analysis of *X. calcaratus* short and long arm chromosome length measurements. The a-subgenome is shown in red and the b-subgenome is in blue. **(a)** the relationship between centromeric index (*i*), x-axis, and chromosomal length (*l*), y-axis. Gray dashed vertical lines define intervals 0–12.5, 12.5–25, 25–37.5, and 37.5–50 that correspond to acrocentric, subtelocentric, submetacentric, and metacentric chromosomes, respectively. Plotted values of *i* and *l* are medians for each chromosome. **(b)** shows intrachromosomal variability of *l* value (y axis) for the haploid complement of 20 *X. calcaratus* chromosomes (x axis). **(c)** intrachromosomal variability of *i* value (y axis) on the haploid complement of 20 *X. calcaratus* chromosomes (x axis). b and c: gray dashed vertical lines delimit homoeologous pairs. The upper and lower whiskers show the minimum and maximum values, respectively, the boxes involve the lower (Q_1) and upper (Q_3) quartiles, the black lines inside the boxes indicate the median values (Q_2); outliers are indicated by black points.

cept1, *sf3b1*, *ndufs1*, and *fn1* in *X. calcaratus*. In *X. mellotropicalis gyg2α* and *β*, and *cept1α* and *β* map to chromosomes 2a*p* and 2b*p*, respectively. The *ndufs1α* and *β*, and *fn1α* and *β* map to chromosomes 9a and 9b, respectively. The *sf3b1α* and *β* genes map to *X. mellotropicalis* chromosomes 2b*p* and 9a*q*, respectively (Knytl et al., 2018b).

In *X. calcaratus* the *gyg2α* and *cept1α* mapped to 2b*p*, and *gyg2β* and *cept1β* mapped to 2a*p*. *fn1α*, *ndufs1α*, and *sf3b1α* mapped to XCA 9a*q*, and *fn1β*, *ndufs1β*, and *sf3b1β* mapped to XCA 9b*q*, respectively (Fig. 6). The metaphases with 40 chromosomes and FISH-TSA signals are shown in Supplementary material (Figs. S1–S5). Thus, similar to the findings from the WCP probes discussed above, mapping of single-copy genes in *X. calcaratus* recovered no evidence of the translocation involving chromosomes 9b and 2b that was observed in *X. mellotropicalis* (Knytl et al., 2017; Knytl et al., 2018b).

3.6. Mensural analysis of *X. calcaratus* chromosomes

As expected, across all *X. calcaratus* spreads ($n = 35$) we consistently counted 40 chromosomes, indicating that $2n = 4x = 40$, where *n* refers to the haploid number of chromosomes of the extant species, and *x* refers to the haploid number of chromosomes in the most recent diploid ancestor of the extant species.

Each chromosome was measured from 35 metaphases spreads, with each chromosome identified based on comparison to the FISH results, and the median values of l, r_1, and *i* were calculated. *l* was quantified as a percentage of the sum of *l* across all chromosomes in order to account for variation in resolution and pixel size of our images. Each individual chromosome was also assigned a chromosomal category based on the *i* value. If the *i* value was equal to or greater than 37.5, the chromosome was categorized to be metacentric. If the *i* value was equal to or higher than 25 and lower than 37.5, the chromosome was categorized to be

Table 1
Measurements of *X. calcaratus* chromosomes formulated in medians of l (%), p/q arm ratio (r_1), and i. Chromosomal categories correspond to m = metacentric, sm = submetacentric, and st = subtelocentric chromosomes. Significance codes following l and i values define whether pairs of homoeologous chromosomes are significantly different based on ANOVA test. Significantly different homoeologs are depicted by significance codes "***", "**", and "•" showing the p-value $p < 0.001$, $p < 0.01$, and $p < 0.1$, respectively.

Chromosome	l (%)		r_1	i		Category
1a	3.78		0.73	42.10	•	m
1b	3.79		0.76	43.15		m
2a	3.11	**	0.59	37.04	**	sm
2b	3.20		0.63	38.67		m
3a	2.98	***	0.20	16.58		st
3b	2.80		0.20	16.74		st
4a	2.65	***	0.60	37.48		sm
4b	2.80		0.62	38.42		m
5a	2.73	**	0.49	33.11	***	sm
5b	2.63		0.38	27.33		sm
6a	2.69	***	0.88	46.94		m
6b	2.54		0.87	46.63		m
7a	2.48	***	0.77	43.38		m
7b	2.16		0.78	43.78		m
8a	2.47	***	0.17	14.73		st
8b	2.28		0.18	15.47		st
9a	1.47		0.80	44.31		m
9b	1.48		0.80	44.54		m
10a	0.98	**	0.75	42.78		m
10b	0.93		0.75	42.90		m

submetacentric, and if the i value was equal to or greater than 12.5 and lower than 25, the chromosome was categorized as subtelocentric. The karyotype of *X. calcaratus* consists of 12 pairs of metacentric, four pairs of submetacentric, and four pairs of subtelocentric chromosomes.

We found that pairs of homoeologs tend to have similar chromosomal morphology in terms of l and i values (Fig. 7a). For example, chromosomes 3a, 3b, 8a, and 8b had low centromeric indexes (between 12.5–25) and were therefore both subtelocentric. Chromosomes 5a and 5b had centromeric indexes between 25–37.5 and were therefore both submetacentric. However, chromosomes 2a and 4a were in the submetacentric category whereas their homoeologous chromosomes 2b and 4b were in the metacentric category. The rest of chromosomes fell into the category of metacentric chromosomes (centromeric indexes of 37.5–50). Acrocentric chromosomes (centromeric indexes interval 0–12.5) and telocentric chromosomes withouta p arm (centromeric indexes = 0) were not present in the *X. calcaratus* karyotype.

The l and i values were assigned to each individual chromosome 1a–10b from each metaphase and plotted (Figs. 7b and 7c). A measure of statistical dispersion, the interquartile range (Q_1–Q_3), was used to evaluate the extent of morphological divergence of each homoeologous chromosomal pair. The highest divergence in l between homoeologous chromosomes was found between XCA 7a and 7b. The Q_1–Q_3 of XCA 7a and 7b l ranged from 2.37% to 2.61% and from 2.06% to 2.27%, respectively (Supplementary material, Box plot statistics of l, matrix `$stats` in `R` output, columns `[,13]` and `[,14]`, rows `[2,]-[4,]`). The second highest divergence in l was measured within homoeologous pairs XCA 6a (2.62% to 2.77%) and 6b (2.38% to 2.59%) (Supplementary material, Box plot statistics of l, matrix `$stats` in `R` output, columns `[,11]` and `[,12]`, rows `[2,]-[4,]`). The largest difference in i of homoeologous chromosomes was between XCA 5a and 5b, which differed within Q_1–Q_3 by 29.98–35.08 and 25.39–29.31, respectively (Supplementary material, Box plot statistics of i, `$stats` in `R` output, columns `[,9]` and `[,10]`, rows `[2,]-[4,]`). The second largest difference based on the Q_1–Q_3 interval of i was between XCA 2a (34.69–38.39) and 2b (37.07–41.53, Supplementary material, Box plot statistics of i, `$stats` in `R` output, columns `[,3]` and `[,4]`, rows `[2,]-[4,]`). Based on l or i, the four most differentiated homoeologous pairs (2a and 2b, 5a and 5b, 6a and 6b, 7a and 7b) are identifiable based on arms lengths.

The median values of l (%), r_1 and i are shown in Table 1, where these values are assigned to each chromosome.

Chromosome 7a and 7b of *X. calcaratus* can be distinguished because 7a has a secondary nucleolar constriction in the same position as XTR 7, whereas this feature is absent from XCA 7b. This inference is further supported by a higher intensity of Zoo-FISH and GISH signals with *X. tropicalis* probes on XCA 7a compared to 7b. The l values of some chromosomes were substantially different between "a" and "b" homoeologs (Table 1, significance codes). Based on the cytogenetic information presented here that was obtained from multiple methods, we defined a chromosome nomenclature for *X. calcaratus* that could extend to other tetraploid *Silurana* species depending on their phylogenetic relationships discussed below.

4. Discussion

We used a combination of conventional (C- and CMA_3-banding) and more advanced molecular cytogenetic techniques (rDNA FISH, intra- and cross-species painting FISH, FISH-TSA, and GISH) to study the allotetraploid karyotype architecture of *X. calcaratus*. Our results, together with previous cytogenetic findings (Tymowska and Fischberg, 1982; Schmid and Steinlein, 2015; Knytl et al., 2017), enabled us to distinguish and define the a- and b-subgenomes of *X. calcaratus*. We identified several cytogenetic changes discussed below in the b-subgenome that were not present in the a-subgenome of *X. calcaratus* or in *X. tropicalis*, which indicate that the b-subgenome has undergone more rapid (and asymmetric) evolution compared to the a-subgenome.

4.1. Localization of the heterochromatin, NOR, and other components of the ribosomes

The allotetraploid species *X. laevis* has one NOR on chromosome 3L*p* (Tymowska and Kobel, 1972; Schmid et al., 1987; Roco et al., 2021), with a homologous NOR on chromosome 3S thought to have been lost after allotetraploidization in subgenus *Xenopus* (Session et al., 2016). In the diploid *X. tropicalis* the NOR is on chromosome 7*q* (Tymowska, 1973; Tymowska and Fischberg, 1982; Uehara et al., 2002; Roco et al., 2021), the allotetraploid *X. epitropicalis* and *X. mellotropicalis* also have one NOR on chromosome 7a*q* (Tymowska and Fischberg, 1982; Tymowska, 1991), with the other on chromosome 7b hypothesized to have been lost after allotetraploidization (Knytl et al., 2017). In *X. calcaratus*, *28S* rDNA FISH identified nucleolar (secondary) constriction on XCA 7a*q* (Fig. 5a). There are at least two possible explanations for the conserved location and number of NORs in *X. mellotropicalis* and *X. calcaratus*. If these two species each evolved via independent allotetraploidization events (Fig. 1b), loss of one pair of NORs from the same ancestral species could have occurred twice independently after each allotetraploidization event. Under a scenario of one allotetraploidization in *Silurana* (Fig. 1a) it is also possible that one pair of NORs was lost only once after allopolyploidization in subgenus *Silurana*.

The *5S* ribosomal genes were localized to telomeric regions of most or perhaps all of the chromosomes of *X. laevis* (Pardue et al., 1973). Somatic and oocyte-specific types of *5S* ribosomal genes have been identified in *X. laevis* (Peterson et al., 1980). The somatic type of *5S* genes was localized to *X. laevis* chromosome 6L and the oocyte-specific type of *5S* genes was localized to subtelomeric regions of most chromosomes (Harper et al., 1983). Because somatic and oocyte-specific sequences have 95% sequence similarity (Ford and Brown, 1976), probes to both types of *5S* genes co-localize to somatic metaphase spreads (Harper et al., 1983). In *X. tropicalis* the *5S* is on subtelomeric regions of most of chromosomes (XTR 2, 3, 4, 5, 6, 7, 8, and 9) with the most intense fluorescent signal on XTR 6 (Knytl et al., 2017). In *X. mellotropicalis 5S* genes were mapped to chromosomes 4a, 5b, and 8b (Knytl et al., 2017) but *X. calcaratus* bears *5S* loci on chromosomes 2b, 4a, 5a, 6a, and 8b (Fig. 5a). These findings indicate independent

evolution of the *5S* genes in allotetraploid *X. mellotropicalis* and *X. calcaratus* with more frequent deletions in *X. mellotropicalis*.

C- and CMA_3- banding identified a prominent heterochromatic block in the form of a non-nucleolar secondary constriction, but some of these signals may co-localize with NORs (e.g. *28S*- and CMA_3-positive signals on XCA 7a, Figs. 5a and 5c). Several *Silurana* tetraploids have one intensely labeled non-nucleolar secondary constriction: for *X. tropicalis* it is on chromosome 9*q* (Tymowska and Fischberg, 1982; Knytl et al., 2017), for *X. mellotropicalis* it is on 2a*p* (re-designated below to be 2b*p*) (Knytl et al., 2017), for *X. epitropicalis* it is on the pericentromeric region of 2a (re-designated below to be 2b) involving both *p* and *q* arms (Tymowska and Fischberg, 1982), and for *X. calcaratus* it is on 1b*p*. Different sizes and positions of non-nucleolar secondary constrictions within *Silurana* species indicate that these constrictions are dynamic structures with independent evolution; the most similar positions are in *X. epitropicalis* and *X. mellotropicalis* (chromosome 2b), which is consistent with their close evolutionary relationship (Evans et al., 2005).

The number and position of NORs have been extensively explored in both diploid and polyploid animals. Amphibians and fish are good groups with which to explore the effect of whole genome duplication on the evolution of NOR and other ribosomal structures, such as *5S* and *45S* rRNA genes (Knytl et al., 2017; Knytl et al., 2018a), because both include a diversity of diploid and polyploid species (Evans et al., 2015; Knytl et al., 2022). The number and position of NORs and other ribosomal structures together with cytogenetic mapping of single-copy genes in polyploids may reflect the extent of rediploidization (Symonová et al., 2017). In most diploid and polyploid amphibians, only one homologous chromosome pair bears a NOR (Schmid, 1982; Schmid et al., 1987; Alves et al., 2012). However, in fish there is more extensive variation in the number of NORs, including observations ranging from one (Alves et al., 2012) to seven pairs (Gromicho et al., 2006). For instance, some tetraploid fish possess two pairs of NORs located on one homoeologous set of chromosomes, which is consistent with ancient tetraploidy (Diniz et al., 2009; Knytl et al., 2013a; Symonová et al., 2017). One NOR pair may therefore reflect functional diploidization, wherein bivalents rather than multivalents form during meiosis, which appears to be the case for all *Xenopus* (Tymowska, 1991).

Another possible explanation for among species variation in the number of nucleolar loci is that some have been transcriptionally inactive in the preceding interphase. Therefore, these loci have not been transcribed, and might not be detected by ribosomal probes (Schmid, 1982). The number of nucleolar loci could be also changed via translocation of individual rDNA copies from clusters via viruses or transposons (Gromicho et al., 2006).

4.2. *Silurana* subgenomes with different cytogenetic characteristics

Previous chromosome nomenclature of *X. mellotropicalis* and *X. epitropicalis* designated the larger of the homoeologous pairs as "a" and the smaller pair as "b" (Tymowska and Fischberg, 1982; Tymowska, 1991; Knytl et al., 2017). Although the relative size of homoeologous pairs corresponds to subgenomes in *X. laevis* (Session et al., 2016), this is not necessarily the case in other groups. Because the relative intensities of fluorescence signal in FISH correspond with phylogenetic distance between the probe and the genome being interrogated, evolutionary affinities of chromosomes within each subgenome can be inferred based on the intensity of the probe fluorescence (Markova et al., 2007; Liu et al., 2015). Here, we distinguished homoeologous chromosomes in the *X. calcaratus* a- and b-subgenomes based on measurements of chromosomal *p* and *q* arm length, and comparative cytogenetic findings from Zoo-FISH and GISH using probes from the diploid species *X. tropicalis*. This approach allowed for an evolutionary-based classification system based on divergence from *X. tropicalis* orthologous chromosomes. Chromosomes from the *X. calcaratus* a-subgenome are more similar and closely related to *X. tropicalis* orthologs than chromosomes from the *X. calcaratus* b-subgenome. With this approach, we identified one homoeologous pair – chromosome 2 – where the larger chromosome was actually from the b-subgenome, warranting revision of this aspect of the chromosomal nomenclature (Table 2). Consistent with this reappraisal, the intensity of the Zoo-FISH signal on the longer *X. mellotropicalis* chromosome 2 (2a sensu Knytl et al. (2017)) is lower than intensity of the smaller *X. mellotropicalis* chromosome 2 (2b sensu Knytl et al. (2017); see Fig. 4B in Knytl et al. (2017)). Based on results presented here for *X. calcaratus*, *X. mellotropicalis* 2a (XME 2a) and 2b should thus be reclassified as XME 2b and 2a, respectively.

Table 2
r_1 values (p/q arm ratio) for each chromosome in *X. tropicalis* (Tymowska, 1973), *X. calcaratus* (this study), and *X. mellotropicalis* (Knytl et al., 2017). *Xenopus tropicalis* chromosome nomenclature according Khokha et al. (2009) was used. Each *X. tropicalis* ortholog is divided into the "a" and "b" homoeologous chromosomes in tetraploid *Silurana* karyotypes ("homoeolog" column). Asterisks highlight changes in chromosome nomenclature.

Chromosome	*X. tropicalis* r_1	Homoeolog	*X. calcaratus* r_1	*X. mellotropicalis* r_1
1	0.72	a	0.73	0.70
		b	0.76	0.67
2	0.61	a	0.59	0.62*
		b	0.63	0.81*
3	0.31	a	0.20	0.20
		b	0.20	0.20
4	0.57	a	0.60	0.60
		b	0.62	0.62
5	0.58	a	0.49	0.42
		b	0.38	0.41
6	0.88	a	0.88	0.88
		b	0.87	0.88
7	0.71	a	0.77	0.66
		b	0.78	0.79
8	0.22	a	0.17	0.21
		b	0.18	0.21
9	0.68	a	0.80	0.88
		b	0.80	0.72
10	0.68	a	0.75	0.70
		b	0.75	0.72

Additionally, our findings indicate that chromosomes XCA 1b and 2b had higher p/q arm ratio, centromeric index and chromosomal length than XCA 1a and 2a, respectively. This is also inconsistent with previous designations based on conventional staining such as Giemsa, C-banding, or replication banding (Tymowska, 1991; Schmid and Steinlein, 2015).

Thus far, *X. calcaratus* and *X. mellotropicalis* a-subgenomes have no reported translocations, although the b-subgenome of *X. mellotropicalis* contains large-scale rearrangements between XME 2b and 9b (Knytl et al., 2017). Heterochromatin is evident on XCA 1b (Figs. 5b and 5c) but not on XTR 1 or XME 1b. Knytl et al. (2017) hypothesized that the heterochromatin transpositions occurred within b-subgenome. That the nucleolar *28S* rRNA loci (a part of *45S* rRNA) were detected only on XCA 7a*q* but not on 7b*q* indicates gene loss within *X. calcaratus* b-subgenome. Overall, these results suggest asymmetric subgenome evolution in *Silurana*, with the a-subgenome being more stable and resembling the *X. tropicalis* diploid genome, and the b-subgenome having experienced more chromosomal rearrangements. As discussed above, asymmetric subgenome evolution has also been reported in allotetraploid *X. laevis* which is in subgenus *Xenopus* (Session et al., 2016).

The p/q arm ratio of XTR 5 is more similar to the p/q arm ratio of XCA 4a, 4b, XME 4a, and 4b than to the p/q arm ratio of XCA 5a, 5b, XME 5a, and 5b (Table 2). It is not clear whether *X. tropicalis* chromosomes were identified correctly by Tymowska (1973) and Khokha et al. (2009), or whether both *X. calcaratus* and *X. mellotropicalis* homoeologs 5a and 5b have undergone changes that were undetectable by our experimental approaches. It is also possible that intraspecies variability in chromosome structure exists among geographically separated African populations of *Xenopus*. These possibilities might be distinguished by additional FISH mapping of loci on XTR 5, XCA 5a, 5b, XME 5a, and 5b or by new measurements of the XTR 5 arm length. Using chromosomal

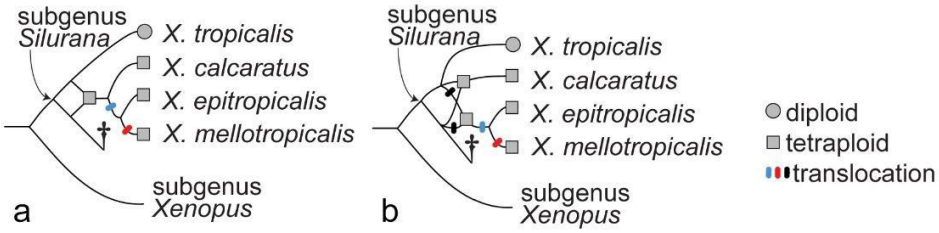

Fig. 8. Evolutionary scenarios in subgenus *Silurana* for the origin of a translocation that is observed in *X. mellotropicalis*, not observed in *X. calcaratus*, and for which no data exists for *X. epitropicalis*. **(a)** if one allotetraploidization event gave rise to all three tetraploid species then the translocation could have occurred after diverged of *X. calcaratus* but before speciation of *X. mellotropicalis* and *X. epitropicalis* (blue) or after this speciation in the ancestor of *X. mellotropicalis* (red). **(b)** if instead two independent allotetraploidizations occurred, the translocation could additionally have occurred in either diploid ancestor of the most recent common ancestor of *X. mellotropicalis* and *X. epitropicalis* (both are shown in black, but only one would have occurred).

length, arm ratio, and centromeric indexes alone, it was not possible to conclusively distinguish all homoeologous chromosomes from the a- and b-subgenomes of *X. calcaratus*, although these differences were readily distinguishable by FISH.

The sex chromosomes of *X. tropicalis* and *X. mellotropicalis* are homologous (XTR 7 and probably XME 7a, respectively (Olmstead et al., 2010; Roco et al., 2015; Mitros et al., 2019; Furman et al., 2020; Cauret et al., 2020)). On XTR 7, XME 7a, and XCA 7a the position of the nucleolar secondary constriction on the *q* arm and the *p*/*q* arm ratio (ranged from 0.66–0.77) are conserved. Because a master sex determining gene has not yet been identified in any *Silurana* species, we were not able to probe this gene and the sex chromosomes of *X. calcaratus* remain unidentified.

4.3. Timing of chromosomal translocation between chromosomes 9 and 2

Zoo-FISH with *X. tropicalis* WCP probes on *X. mellotropicalis* chromosomes and gene mapping using FISH-TSA revealed a large-scale interchromosomal translocation of heterochromatic block from chromosome 9b to 2b, abbreviated t(9b;2b) (Knytl et al., 2017; Knytl et al., 2018b). This translocation was not identified in *X. calcaratus* based on Zoo-FISH (Fig. 3) and also was not present in *X. tropicalis* (Knytl et al., 2018b). More specifically, we found that rearrangement-associated genes in *X. mellotropicalis* did not all map to the corresponding chromosomes of *X. calcaratus*. In Knytl et al. (2018b), *sf3b1α* mapped to XME 2a (which with the proposed revised nomenclature is XME 2b) but in *X. calcaratus* this gene mapped to XCA 9a. In *X. tropicalis*, *sf3b1* is localized on XTR 9 (Knytl et al., 2018b). The most parsimonious explanation for these observations is that the t(9b;2b) occurred in an ancestor of *X. mellotropicalis* after the divergence of *X. calcaratus* (Fig. 8). It is not clear whether t(9b;2b) occurred in the most recent common ancestor of *X. epitropicalis* and *X. mellotropicalis* (Fig. 8, black and blue spots), or if the translocation occurred solely in the *X. mellotropicalis* lineage after the divergence from the common ancestor with *X. epitropicalis* (Fig. 8, red spots). Another possible scenario is that the translocation occurred between ancestral chromosomes in a diploid ancestor of *X. epitropicalis* and *X. mellotropicalis* (Fig. 8b, black spots). A caveat to this interpretation is that we lack cytogenetic information from a diploid descendant of the other ancestor of *Silurana* allotetraploids, and we are therefore unable to rule out the possibility that some of these changes in the b-subgenome (all except the loss of the NOR) occurred in that ancestor before allotetraploidization. Further resolution of the evolutionary history of this translocation could be achieved via Zoo-FISH analysis of *X. epitropicalis* chromosomes. So far, cytogenetic studies of *X. epitropicalis* are limited to conventional banding (Tymowska, 1991; Schmid and Steinlein, 2015). Heterochromatic blocks identified by chromosome banding suggest that the t(9b;2b) of *X. mellotropicalis* is associated with repetitive sequences (Knytl et al., 2017). Extensive rearrangements and GC-rich secondary constrictions were not identified on the XCA 2b (CMA_3 or C-banding positive, Figs. 5b and 5c) which suggests the repetitive regions associated with the t(9b;2b) of *X. mellotropicalis* also accumulated after divergence from the ancestor of *X. calcaratus*. The effects on recombination of a rearrangement may not be bounded by the breakpoints of the rearrangement (Xia et al., 2020). It is thus conceivable that this translocation influenced speciation through the suppression of chromosomal pairing and recombination (Fishman et al., 2013).

5. Conclusions

Allopolyploid genomes are interesting subjects for cytogenetic investigation because evolutionary phenomena in each subgenome can be distinguished and compared. In this study, we identified two subgenomes in the allotetraploid frog *X. calcaratus*, and found them to be distinguished by cytogenetic characteristics that are consistent with asymmetric evolution. Results are consistent with the proposed allopolyploid origin of *X. calcaratus* (*X.* new tetraploid 2 in (Evans et al., 2005)), with one progenitor species also being an ancestor of *X. tropicalis* and another ancestral species either extinct or undiscovered. To better understand genome evolution in subgenus *Silurana* it is necessary to perform further cytogenetic analyses of *X. epitropicalis*, the remaining member of a group of allotetraploid species.

Ethics approval

Charles University has registered experimental breeding facilities for pipid frogs (16OZ12891/2018–17214, 37428/2019-MZE-18134). All experimental procedures involving frogs were approved by the Institutional Animal Care and Use Committee of Charles University, according to the directives from the State Veterinary Administration of the Czech Republic. MK is a holder of the Certificate of professional competence to design experiments according to §15d(3) of the Czech Republic Act No. 246/1992 coll. on the Protection of Animals against Cruelty (Registration number CZ 03973), provided by the Ministry of Agriculture of the Czech Republic.

Declaration of Competing Interest

The authors declare that they have no known competing financial interests or personal relationships that could have appeared to influence the work reported in this paper.

Acknowledgements

The research was funded by the institutional support from the IVB CAS, RVO: 68081766 (VG), institutional support from the Ministry of Agriculture of the Czech Republic, MZE-RO0518 (HC, SK), the Natural Science and Engineering Research Council of Canada, RGPIN-2017–05770 (BJE), and Charles University, Faculty of Science,

Cooperatio (VK). We thank two anonymous reviewers for their helpful comments on this manuscript.

Appendix A. Supplementary material

Supplementary data associated with this article can be found, in the online version, at https://doi.org/10.1016/j.gene.2022.146974.

References

Alves, A.L., de Borba, R.S., Pozzobon, A.P.B., Oliveira, C., Nirchio, M., Granado, A., Foresti, F., 2012. Localization of 18S ribosomal genes in suckermouth armoured catfishes Loricariidae (Teleostei, Siluriformes) with discussion on the Ag-NOR evolution. Compar. Cytogenet. 6, 315–321. https://doi.org/10.3897/CompCytogen.v6i3.2667.

Bi, K., Bogart, J.P., 2006. Identification of intergenomic recombinations in unisexual salamanders of the genus *Ambystoma* by genomic in situ hybridization (GISH). Cytogenet. Genome Res. 112, 307–312. https://doi.org/10.1159/000089885.

Biémont, C., Vieira, C., 2006. Genetics: junk DNA as an evolutionary force. Nature 443, 521–524. https://doi.org/10.1038/443521a.

Brunet, F.G., Crollius, H.R., Paris, M., Aury, J.M., Gibert, P., Jaillon, O., Laudet, V., Robinson-Rechavi, M., 2006. Gene loss and evolutionary rates following whole-genome duplication in teleost fishes. Mol. Biol. Evol. 23, 1808–1816. https://doi.org/10.1093/molbev/msl049.

Cauret, C.M.S., Gansauge, M.T., Tupper, A.S., Furman, B.L.S., Knytl, M., Song, X.Y., Greenbaum, E., Meyer, M., Evans, B.J., 2020. Developmental systems drift and the drivers of sex chromosome evolution. Mol. Biol. Evol. 37, 799–810. https://doi.org/10.1093/molbev/msz268.

Courtet, M., Flajnik, M., Du Pasquier, L., 2001. Major histocompatibility complex and immunoglobulin loci visualized by in situ hybridization on Xenopus chromosomes. Dev. Comp. Immunol. 25, 149–157. https://doi.org/10.1016/S0145-305X(00)00045-8.

Diniz, D., Laudicina, A., Bertollo, L.A.C., 2009. Chromosomal location of 18S and 5S rDNA sites in Triportheus fish species (Characiformes, Characidae). Genet. Mol. Biol. 32, 37–41. https://doi.org/10.1590/S1415-47572009005000017.

Evans, B.J., 2007. Ancestry influences the fate of duplicated genes millions of years after polyploidization of clawed frogs (*Xenopus*). Genetics 176, 1119–1130. https://doi.org/10.1534/genetics.106.069690.

Evans, B.J., 2008. Genome evolution and speciation genetics of clawed frogs (*Xenopus* and *Silurana*). Frontiers in Bioscience 13, 4687–4706. https://doi.org/10.2741/3033.

Evans, B.J., Carter, T.F., Greenbaum, E., Gvoždík, V., Kelley, D.B., McLaughlin, P.J., Pauwels, O.S.G., Portik, D.M., Stanley, E.L., Tinsley, R.C., Tobias, M.L., Blackburn, D.C., 2015. Genetics, morphology, advertisement calls, and historical records distinguish six new polyploid species of African clawed frog (*Xenopus*, Pipidae) from West and Central Africa. PloS ONE 10, e0142823.

Evans, B.J., Kelley, D.B., Melnick, D.J., Cannatella, D.C., 2005. Evolution of RAG-1 in polyploid clawed frogs. Mol. Biol. Evol. 22, 1193–1207. https://doi.org/10.1093/molbev/msi104.

Feder, J.L., Gejji, R., Powell, T.H., Nosil, P., 2011. Adaptive chromosomal divergence driven by mixed geographic mode of evolution. Evolution 65, 2157–2170. https://doi.org/10.1111/j.1558-5646.2011.01321.x.

Fishman, L., Stathos, A., Beardsley, P.M., Williams, C.F., Hill, J.P., 2013. Chromosomal rearrangements and the genetics of reproductive barriers in *Mimulus* (monkey flowers). Evolution 67, 2547–2560. https://doi.org/10.1111/evo.12154.

Ford, P.J., Brown, R.D., 1976. Sequences of 5S ribosomal RNA from *Xenopus mulleri* and the evolution of 5S gene-coding sequences. Cell 8, 485–493. https://doi.org/10.1016/0092-8674(76)90216-6.

Furman, B.L.S., Cauret, C.M.S., Knytl, M., Song, X.Y., Premachandra, T., Ofori-Boateng, C., Jordan, D.C., Horb, M.E., Evans, B.J., 2020. A frog with three sex chromosomes that co-mingle together in nature: *Xenopus tropicalis* has a degenerate W and a Y that evolved from a Z chromosome. PLOS Genet. 16, e1009121 https://doi.org/10.1371/journal.pgen.1009121.

Gromicho, M., Coutanceau, J.P., Ozouf-Costaz, C., Collares-Pereira, M.J., 2006. Contrast between extensive variation of 28S rDNA and stability of 5S rDNA and telomeric repeats in the diploid-polyploid Squalius alburnoides complex and in its maternal ancestor *Squalius pyrenaicus* (Teleostei, Cyprinidae). Chromosome Res. 14, 297–306. https://doi.org/10.1007/s10577-006-1047-4.

Harper, M.E., Price, J., Korn, L.J., 1983. Chromosomal mapping of Xenopus 5S genes: somatic-type versus oocyte-type. Nucleic Acids Res. 11, 2313–2323. https://doi.org/10.1093/nar/11.8.2313.

Hellsten, U., Harland, R.M., Gilchrist, M.J., Hendrix, D., Jurka, J., Kapitonov, V., Ovcharenko, I., Putnam, N.H., Shu, S., Taher, L., Blitz, I.L., Blumberg, B., Dichmann, D.S., Dubchak, I., Amaya, E., Detter, J.C., Fletcher, R., Gerhard, D.S., Goodstein, D., Graves, T., Grigoriev, I.V., Grimwood, J., Kawashima, T., Lindquist, E., Lucas, S.M., Mead, P.E., Mitros, T., Ogino, H., Ohta, Y., Poliakov, A.V., Pollet, N., Robert, J., Salamov, A., Sater, A.K., Schmutz, J., Terry, A., Vize, P.D., Warren, W.C., Wells, D., Wills, A., Wilson, R.K., Zimmerman, L.B., Zorn, A.M., Grainger, R., Grammer, T., Khokha, M.K., Richardson, P.M., Rokhsar, D.S., 2010. The genome of the Western clawed frog *Xenopus tropicalis*. Science 328, 633–636. https://doi.org/10.1126/science.1183670.

Janko, K., Pačes, J., Wilkinson-Herbots, H., Costa, R.J., Roslein, J., Drozd, P., Iakovenko, N., Rídl, J., Hroudová, M., Kočí, J., Reifová, R., Šlechtová, V., Choleva, L., 2018. Hybrid asexuality as a primary postzygotic barrier between nascent species: On the interconnection between asexuality, hybridization and speciation. Mol. Ecol. 27, 248–263. https://doi.org/10.1111/mec.14377.

Khokha, M.K., Krylov, V., Reilly, M.J., Gall, J.G., Bhattacharya, D., Cheung, C.Y.J., Kaufman, S., Lam, D.K., Macha, J., Ngo, C., Prakash, N., Schmidt, P., Tlapakova, T., Trivedi, T., Tumova, L., Abu-Daya, A., Geach, T., Vendrell, E., Ironfield, H., Sinzelle, L., Sater, A.K., Wells, D.E., Harland, R.M., Zimmerman, L.B., 2009. Rapid gynogenetic mapping of *Xenopus tropicalis* mutations to chromosomes. Dev. Dyn. 238, 1398–1406. https://doi.org/10.1002/dvdy.21965.

Knytl, M., Fornaini, N.R., 2021. Measurement of chromosomal arms and FISH reveal complex genome architecture and standardized karyotype of model fish, genus *Carassius*. Cells 10, 2343. https://doi.org/10.3390/cells10092343.

Knytl, M., Forsythe, A., Kalous, L., 2022. A fish of multiple faces, which show us enigmatic and incredible phenomena in nature: biology and cytogenetics of the genus *Carassius*. Int. J. Mol. Sci. 23, 8095. https://doi.org/10.3390/ijms23158095.

Knytl, M., Kalous, L., Rab, P., 2013a. Karyotype and chromosome banding of endangered crucian carp, *Carassius carassius* (Linnaeus, 1758) (Teleostei, Cyprinidae). Comp. Cytogenet. 7, 205–213.

Knytl, M., Kalous, L., Rylková, K., Choleva, L., Merilä, J., Ráb, P., 2018a. Morphologically indistinguishable hybrid Carassius female with 156 chromosomes: A threat for the threatened crucian carp, *C. carassius*, L. PLOS ONE 13, e0190924.

Knytl, M., Kalous, L., Symonová, R., Rylková, K., Ráb, P., 2013b. Chromosome studies of European cyprinid fishes: Cross-species painting reveals natural allotetraploid origin of a Carassius female with 206 chromosomes. Cytogenet. Genome Res. 139, 276–283.

Knytl, M., Smolík, O., Kubíčková, S., Tlapáková, T., Evans, B.J., Krylov, V., 2017. Chromosome divergence during evolution of the tetraploid clawed frogs, *Xenopus mellotropicalis* and *Xenopus epitropicalis* as revealed by Zoo-FISH. PLOS ONE 12, e0177087. https://doi.org/10.1371/journal.pone.0177087.

Knytl, M., Tlapakova, T., Vankova, T., Krylov, V., 2018. Silurana chromosomal evolution: A new piece to the puzzle. Cytogenet. Genome Res. 156, 223–228.

Krylov, V., Kubickova, S., Rubes, J., Macha, J., Tlapakova, T., Seifertova, E., Sebkova, N., 2010. Preparation of Xenopus tropicalis whole chromosome painting probes using laser microdissection and reconstruction of X. laevis tetraploid karyotype by Zoo-FISH. Chromosome Res. 18, 431–439. https://doi.org/10.1007/s10577-010-9127-x.

Krylov, V., Tlapakova, T., Macha, J., 2007. Localization of the single copy gene Mdh2 on Xenopus tropicalis chromosomes by FISH-TSA. Cytogenet. Genome Res. 116, 110–112. https://doi.org/10.1159/000097427.

Kubickova, S., Cernohorska, H., Musilova, P., Rubes, J., 2002. The use of laser microdissection for the preparation of chromosome-specific painting probes in farm animals. Chromosome Res. 10, 571–577. https://doi.org/10.1023/A:1020914702767.

Levan, A., Fredga, K., Sandberg, A.A., 1964. Nomenclature for centromeric position on chromosomes. Hereditas 52, 201–220. https://doi.org/10.1111/j.1601-5223.1964.tb01953.x.

Li, J.T., Wang, Q., Huang Yang, M.D., Li, Q.S., Cui, M.S., Dong, Z.J., Wang, H.W., Yu, J.H., Zhao, Y.J., Yang, C.R., Wang, Y.X., Sun, X.Q., Zhang, Y., Zhao, R., Jia, Z.Y., Wang, X.Y., 2021. Parallel subgenome structure and divergent expression evolution of allo-tetraploid common carp and goldfish. Nat. Genet. 53, 1493–1503. https://doi.org/10.1038/s41588-021-00933-9.

Liu, B., Poulsen, E.G., Davis, T.M., 2015. Insight into octoploid strawberry (*Fragaria*) subgenome composition revealed by GISH analysis of pentaploid hybrids. Genome 59, 79–86. https://doi.org/10.1139/gen-2015-0116.

Markova, M., Michu, E., Vyskot, B., Janousek, B., Zluvova, J., 2007. An interspecific hybrid as a tool to study phylogenetic relationships in plants using the GISH technique. Chromosome Res. 15, 1051–1059. https://doi.org/10.1007/s10577-007-1180-8.

Mitros, T., Lyons, J.B., Session, A.M., Jenkins, J., Shu, S., Kwon, T., Lane, M., Ng, C., Grammer, T.C., Khokha, M.K., Grimwood, J., Schmutz, J., Harland, R.M., Rokhsar, D.S., 2019. A chromosome-scale genome assembly and dense genetic map for *Xenopus tropicalis*. Dev. Bio. 452, 8–20. https://doi.org/10.1016/j.ydbio.2019.03.015.

Olmstead, A.W., Lindberg Livingston, A., Degitz, S.J., 2010. Genotyping sex in the amphibian, *Xenopus* (*Silurana*) *tropicalis*, for endocrine disruptor bioassays. Aquat. Toxicol. 98, 60–66. https://doi.org/10.1016/j.aquatox.2010.01.012.

Pardue, M.L., Brown, D.D., Birnstiel, M.L., 1973. Location of the genes for 5S ribosomal RNA in *Xenopus laevis*. Chromosoma 42, 191–203. https://doi.org/10.1007/BF00320940.

Peterson, R.C., Doering, J.L., Brown, D.D., 1980. Characterization of two Xenopus somatic 5S DNAs and one minor oocyte-specific 5S DNA. Cell 20, 131–141. https://doi.org/10.1016/0092-8674(80)90241-X.

R Core Team, 2020. R: a language and environment for statistical computing. R Foundation for Statistical Computing, Vienna, Austria. https://www.r-project.org/.

Rábová, M., Völker, M., Pelikánová, Š., Ráb, P., 2015. Sequential chromosome banding in fishes. In: Ozouf-Costaz, C., Pisano, E., Foresti, F., Foresti, L.d.A.T. (Eds.), Fish cytogenetic techniques. CRC Press, Boca Raton, pp. 102–112. https://doi.org/10.1201/B18534-17.

Roco, Á.S., Liehr, T., Ruiz-García, A., Guzmán, K., Bullejos, M., 2021. Comparative distribution of repetitive sequences in the karyotypes of *Xenopus tropicalis* and *Xenopus laevis* (Anura, Pipidae). Genes 12, 617. https://doi.org/10.3390/genes12050617.

Roco, Á.S., Olmstead, A.W., Degitz, S.J., Amano, T., Zimmerman, L.B., Bullejos, M., 2015. Coexistence of Y, W, and Z sex chromosomes in *Xenopus tropicalis*. Proc. Natl. Acad. Sci. U.S.A. 112, E4752–E4761. https://doi.org/10.1073/pnas.1505291112.

Schiavinato, M., Bodrug-Schepers, A., Dohm, J.C., Himmelbauer, H., 2021. Subgenome evolution in allotetraploid plants. Plant J. 106, 672–688. https://doi.org/10.1111/tpj.15190.

Schmid, M., 1982. Chromosome banding in Amphibia. Chromosoma 87, 327–344. https://doi.org/10.1007/BF00327634.

Schmid, M., Steinlein, C., 2015. Chromosome banding in Amphibia. XXXII. The genus *Xenopus* (Anura, Pipidae). Cytogenet. Genome Res. 145, 201–217. https://doi.org/10.1159/000433481.

Schmid, M., Vitelli, L., Batistoni, R., 1987. Chromosome banding in Amphibia. Chromosoma 95, 271–284. https://doi.org/10.1007/BF00294784.

Schneider, C.A., Rasband, W.S., Eliceiri, K.W., 2012. NIH Image to ImageJ: 25 years of image analysis. Nat. Methods 9, 671–675. https://doi.org/10.1038/nmeth.2089.

Seifertova, E., Zimmerman, L.B., Gilchrist, M.J., Macha, J., Kubickova, S., Cernohorska, H., Zarsky, V., Owens, N.D.L., Sesay, A.K., Tlapakova, T., Krylov, V., 2013. Efficient high-throughput sequencing of a laser microdissected chromosome arm. BMC Genom 14, 357. https://doi.org/10.1186/1471-2164-14-357.

Sember, A., Bohlen, J., Šlechtová, V., Altmanová, M., Symonová, R., Ráb, P., 2015. Karyotype differentiation in 19 species of river loach fishes (Nemacheilidae, Teleostei): extensive variability associated with rDNA and heterochromatin distribution and its phylogenetic and ecological interpretation. BMC Evol. Biol. 15, 1–22. https://doi.org/10.1186/s12862-015-0532-9.

Seroussi, E., Knytl, M., Pitel, F., Elleder, D., Krylov, V., Leroux, S., Morisson, M., Yosefi, S., Miyara, S., Ganesan, S., Ruzal, M., Andersson, L., Friedman-Einat, M., 2019. Avian expression patterns and genomic mapping implicate leptin in digestion and TNF in immunity, suggesting that their interacting adipokine role has been acquired only in mammals. Int. J. Mol. Sci. 20, 4489. https://doi.org/10.3390/ijms20184489.

Session, A.M., Uno, Y., Kwon, T., Chapman, J.A., Toyoda, A., Takahashi, S., Fukui, A., Hikosaka, A., Suzuki, A., Kondo, M., van Heeringen, S.J., Quigley, I., Heinz, S., Ogino, H., Ochi, H., Hellsten, U., Lyons, J.B., Simakov, O., Putnam, N., Stites, J., Kuroki, Y., Tanaka, T., Michiue, T., Watanabe, M., Bogdanovic, O., Lister, R., Georgiou, G., Paranjpe, S.S., van Kruijsbergen, I., Shu, S., Carlson, J., Kinoshita, T., Ohta, Y., Mawaribuchi, S., Jenkins, J., Grimwood, J., Schmutz, J., Mitros, T., Mozaffari, S.V., Suzuki, Y., Haramoto, Y., Yamamoto, T.S., Takagi, C., Heald, R., Miller, K., Haudenschild, C., Kitzman, J., Nakayama, T., Izutsu, Y., Robert, J., Fortriede, J., Burns, K., Lotay, V., Karimi, K., Yasuoka, Y., Dichmann, D.S., Flajnik, M.F., Houston, D.W., Shendure, J., DuPasquier, L., Vize, P.D., Zorn, A.M., Ito, M., Marcotte, E.M., Wallingford, J.B., Ito, Y., Asashima, M., Ueno, N., Matsuda, Y., Veenstra, G.J.C., Fujiyama, A., Harland, R.M., Taira, M., Rokhsar, D.S., 2016. Genome evolution in the allotetraploid frog *Xenopus laevis*. Nature 538, 336–343. https://doi.org/10.1038/nature19840.

Sinzelle, L., Thuret, R., Hwang, H.Y., Herszberg, B., Paillard, E., Bronchain, O.J., Stemple, D.L., Dhorne-Pollet, S., Pollet, N., 2012. Characterization of a novel *Xenopus tropicalis* cell line as a model for in vitro studies. Genesis (New York, N.Y.: 2000) 50, 316–324. https://doi.org/10.1002/dvg.20822.

Symonová, R., Havelka, M., Amemiya, C.T., Howell, W.M., Kořínková, T., Flajšhans, M., Gela, D., Ráb, P., 2017. Molecular cytogenetic differentiation of paralogs of Hox paralogs in duplicated and re-diploidized genome of the North American paddlefish (*Polyodon spathula*). BMC Genet. 18, 19. https://doi.org/10.1186/s12863-017-0484-8.

Tymowska, J., 1973. Karyotype analysis of Xenopus tropicalis Gray, Pipidae. Cytogenet. cell genet 12, 297–304. https://doi.org/10.1159/000130468.

Tymowska, J., 1991. Polyploidy and cytogenetic variation in frogs of the genus *Xenopus*. In: Green, D.M., Sessions, S.K. (Eds.), Amphibian cytogenetics and evolution. Academic Press, San Diego, pp. 259–297.

Tymowska, J., Fischberg, M., 1982. A comparison of the karyotype, constitutive heterochromatin, and nucleolar organizer regions of the new tetraploid species *Xenopus epitropicalis* Fischberg and Picard with those of *Xenopus tropicalis* Gray (Anura, Pipidae). Cytogenet. cell genet. 34, 149–157. https://doi.org/10.1159/000131803.

Tymowska, J., Kobel, H.R., 1972. Karyotype analysis of *Xenopus muelleri* (Peters) and *Xenopus laevis* (Daudin), Pipidae. Cytogenetics 11, 270–278. https://doi.org/10.1159/000130197.

Uehara, M., Haramoto, Y., Sekizaki, H., Takahashi, S., Asashima, M., 2002. Chromosome mapping of *Xenopus tropicalis* using the G- and Ag-bands: Tandem duplication and polyploidization of larvae heads. Dev. Growth Differ. 44, 427–436. https://doi.org/10.1046/j.1440-169X.2002.00656.x.

Uno, Y., Nishida, C., Tarui, H., Ishishita, S., Takagi, C., Nishimura, O., Ishijima, J., Ota, H., Kosaka, A., Matsubara, K., Murakami, Y., Kuratani, S., Ueno, N., Agata, K., Matsuda, Y., 2012. Inference of the protokaryotypes of amniotes and tetrapods and the evolutionary processes of microchromosomes from comparative gene mapping. PLoS ONE 7, 2–13. https://doi.org/10.1371/journal.pone.0053027.

Vierna, J., Wehner, S., Höner Zu Siederdissen, C., Martínez-Lage, A., Marz, M., 2013. Systematic analysis and evolution of 5S ribosomal DNA in metazoans. Heredity 111, 410–421. https://doi.org/10.1038/hdy.2013.63.

Wolfe, K.H., 2001. Yesterday's polyploids and the mystery of diploidization. Nat. Rev. Genet. 2, 333–341. https://doi.org/10.1038/35072009.

Xia, Y., Yuan, X., Luo, W., Yuan, S., Zeng, X., 2020. The origin and evolution of chromosomal reciprocal translocation in *Quasipaa boulengeri* (Anura, Dicroglossidae). Front. Genet. 10, 1–13. https://doi.org/10.3389/fgene.2019.01364.

Paper 3: **Consequences of polyploidy and divergence as revealed by cytogenetic mapping of tandem repeats in African clawed frogs (*Xenopus*, Pipidae)**

European Journal of Wildlife Research (2023) 69:81
https://doi.org/10.1007/s10344-023-01709-8

RESEARCH

Consequences of polyploidy and divergence as revealed by cytogenetic mapping of tandem repeats in African clawed frogs (*Xenopus*, Pipidae)

Nicola R. Fornaini[1] · Barbora Bergelová[1] · Václav Gvoždík[2,3] · Halina Černohorská[4] · Vladimír Krylov[1] · Svatava Kubíčková[4] · Eric B. Fokam[5] · Gabriel Badjedjea[6] · Ben J. Evans[7] · Martin Knytl[1,7]

Received: 1 February 2023 / Revised: 13 May 2023 / Accepted: 27 June 2023 / Published online: 21 July 2023

Abstract
Repetitive elements have been identified in several amphibian genomes using whole genome sequencing, but few studies have used cytogenetic mapping to visualize these elements in this vertebrate group. Here, we used fluorescence in situ hybridization and genomic data to map the U1 and U2 small nuclear RNAs and histone H3 in six species of African clawed frog (genus *Xenopus*), including, from subgenus *Silurana*, the diploid *Xenopus tropicalis* and its close allotetraploid relative *X. calcaratus* and, from subgenus *Xenopus*, the allotetraploid species *X. pygmaeus*, *X. allofraseri*, *X. laevis*, and *X. muelleri*. Results allowed us to qualitatively evaluate the relative roles of polyploidization and divergence in the evolution of repetitive elements because our focal species include allotetraploid species derived from two independent polyploidization events — one that is relatively young that gave rise to *X. calcaratus* and another that is older that gave rise to the other (older) allotetraploids. Our results demonstrated conserved loci number and position of signals in the species from subgenus *Silurana*; allotetraploid *X. calcaratus* has twice as many signals as diploid *X. tropicalis*. However, the content of repeats varied among the other allotetraploid species. We detected almost same number of signals in *X. muelleri* as in *X. calcaratus* and same number of signals in *X. pygmaeus*, *X. allofraseri*, *X. laevis* as in the diploid *X. tropicalis*. Overall, these results are consistent with the proposal that allopolyploidization duplicated these tandem repeats and that variation in their copy number was accumulated over time through reduction and expansion in a subset of the older allopolyploids.

Keywords Amphibians · Anura · snRNA · Histone H3 · Allopolyploidization · In situ hybridization

✉ Martin Knytl
martin.knytl@natur.cuni.cz

[1] Department of Cell Biology, Faculty of Science, Charles University, Viničná 7, Prague 12843, Czech Republic

[2] Institute of Vertebrate Biology of the Czech Academy of Sciences, Brno, Czech Republic

[3] Department of Zoology, National Museum of the Czech Republic, Prague, Czech Republic

[4] Department of Genetics and Reproduction, CEITEC - Veterinary Research Institute, Hudcova 296/70, Brno 62100, Czech Republic

[5] Department of Animal Biology and Conservation, University of Buea, PO Box 63, Buea 00237, Cameroon

[6] Department of Aquatic Ecology, Biodiversity Monitoring Center, University of Kisangani, Kisangani, Democratic Republic of the Congo

[7] Department of Biology, McMaster University, 1280 Main Street West, Hamilton, ON L8S4K1, Canada

Introduction

Repetitive elements are genomic sequences that are present in multiple copies and are found in all eukaryotic genomes, but with varying abundances and genomic distributions. Content of repetitive DNA ranges from less than 10% in some fishes (e.g., *Tetraodon nigroviridis* and *Cynoglossus semilaevis*) and birds (e.g., *Phoenicopterus ruber*, *Struthio camelus*, *Haliaeetus albicilla*) to > 90% in some plants, such as *Allium cepa* (Chalopin et al. 2015; Chen et al. 2014; Zhang et al. 2014; Canapa et al. 2016; Fu et al. 2019).

Repetitive elements in eukaryotes are categorized into transposable elements (TEs) and tandem repeats. TEs, which are scattered throughout the genome, include retroelements/retrotransposons and DNA transposons. Retrotransposons are reversely transcribed to DNA and replicated using a copy and paste mechanism. Therefore, they may increase genome size (Yampolsky 2016; Clark et al. 2019). Among

retrotransposons, the LINEs (Long Interspersed Nuclear Elements) are classified into many subcategories (Valente et al. 2011; Chalopin et al. 2015; Gama et al. 2022). In contrast, tandem repeats are found as tandem arrays or head-to-tail motifs from several to more than a hundred copies (Myers 2007). Tandem repeats are present in clusters within the genome on single chromosomal locus or multiple loci and include microsatellite, minisatellite, satellite DNA, ribosomal genes (minor 5S and major 45S), histone genes, and small nuclear RNA (snRNA) (Symonová et al. 2017b; Knytl et al. 2018a; Sember et al. 2020; Gazoni et al. 2021; Schott et al. 2022). These loci often undergo concerted evolution (Elder and Turner 1995; Liao 1999), causing intraspecific paralogous repetitive elements to be more similar to each other than to their orthologs, even when the origin of repetitive elements precedes speciation (Liao 1999). Repetitive loci on chromosomes show dynamic evolution in terms of where in the genome and how frequently they are found, and they often have a high rate of rearrangement (Bruschi et al. 2014; Liu et al. 2019).

Due to their repetitive nature, short read sequences typically pose challenges to mapping and repeat quantification, including using genomic data. However, localization of repetitive DNA can be achieved using fluorescent in situ hybridization (FISH) cytogenetic techniques. Cytogenetic mapping of repetitive sequences has been studied in teleost fishes (Bishani et al. 2021; Knytl et al. 2022), reptiles (Oliveira et al. 2021; Altmanová et al. 2022), birds (De Oliveira et al. 2017; Kretschmer et al. 2021), and mammals (Milioto et al. 2019; Gerbault-Seureau et al. 2018). In amphibians, cytogenetic mapping of repetitive sequences has identified inter- and intraspecific rearrangements and other features of karyotype evolution (da Silva et al. 2021; Phimphan et al. 2021; Guzmán et al. 2022).

African clawed frogs of the genus *Xenopus* (Pipidae) include almost 30 species and are divided into two subgenera (*Xenopus* and *Silurana*) (Evans et al. 2015) that each is sometimes considered to be a genus (e.g., Dubois et al. 2021). Subgenus *Silurana* includes four described species, the diploid *Xenopus* (*Silurana*) *tropicalis* and three allotetraploids *X. calcaratus*, *X. epitropicalis*, and *X. mellotropicalis*. For practical reasons, we use the name *Silurana* throughout this article, but present it at the subgenus level in accordance with Evans et al. (2015). Subgenus *Xenopus* includes 25 tetraploid, octoploid, or dodecaploid species (Tymowska 1991) that are divided into three species groups: *amieti*, *laevis*, and *muelleri* (Evans et al. 2015). In genus *Xenopus*, at least eight independent allopolyploidization events occurred, including at least one allotetraploidization event in each subgenus (Fig. 1; for an alternative scenario in *Silurana*, see Knytl et al. 2023). This variation in independently evolved ploidy levels offers a compelling opportunity to explore how tandem repeats evolve in the context of genome duplications.

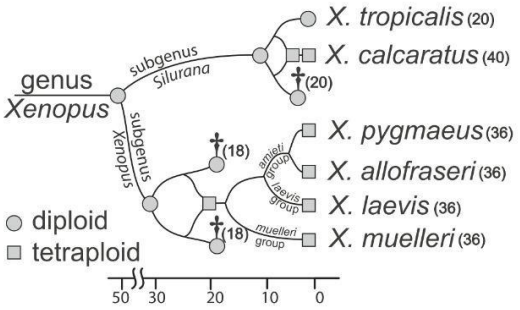

Fig. 1 Inferred phylogenetic relationships and approximate divergence times among our focal taxa based on Evans et al. (2015), Session et al. (2016), and Feng et al. (2017). Allotetraploidization (depicted as reticulating lineages) occurred independently in each subgenus; inferred diploid lineages with no known extant diploid descendants are indicated with daggers. Time scale is in millions of years ago; chromosome numbers are shown in parentheses

About 34.5% and 40% of the *X. tropicalis* and *X. laevis* genomes are repetitive (Hellsten et al. 2010; Session et al. 2016). Ribosomal DNAs (rDNAs) have been cytogenetically mapped on *Xenopus* chromosomes (Schmid and Steinlein 2015; Knytl et al. 2017, 2023; Roco et al. 2021). In allotetraploid species of subgenus *Silurana*, rDNA FISH analysis identified nucleolar organizer region (NOR) on chromosome 7a where the letter "a" refers to the "a subgenome" within the allotetraploid genome (Knytl et al. 2017, 2023). That only one pair of homologous chromosomes contains the NOR locus in *Xenopus* allotetraploids suggests deletion of NOR on chromosome 7b (of the b subgenome) after allotetraploidization (Knytl et al. 2023) because a NOR would have been required in each diploid ancestral species. There is limited cytogenetic information from other repetitive sequences in *Xenopus*, and thus, it is also not known whether non-rDNA repeats vary among *Xenopus* species.

Small nuclear RNAs are components of the spliceosome that perform pre-mRNA splicing. The spliceosome is composed of five RNA tandem-repeat units (U1, U2, U4, U5, and U6 snRNAs) (Valadkhan 2005). Histones are components of the nucleosome that are present in tandem repeat families of five major genes: H1/H5, H2A, H2B, H3, and H4. Here, we used FISH for mapping U1 and U2 snRNA and histone H3 loci on chromosomes from six species of *Xenopus*, including members of both subgenera which diverged from one another approximately 45–50 Mya (Session et al. 2016; Feng et al. 2017). The allotetraploidization event in subgenus *Xenopus* is estimated to have occurred earlier (17–18 Mya) than the one in subgenus *Silurana* and the onset of the polyploid radiation in subgenus *Xenopus* at approximately 17 Mya (Session et al. 2016). Specifically, we examined the diploid *X. tropicalis* and its tetraploid close relative *X. calcaratus*, which are from

subgenus *Silurana*, and the allotetraploids *X. pygmaeus*, *X. allofraseri* (both from the *amieti* species group), *X. laevis* (*laevis* species group), and *X. muelleri* (*muelleri* species group) which belong to subgenus *Xenopus* and arose from the older allotetraploidization. In the subgenus *Xenopus*, the L and S subgenomes diverged from one another about 30–35 Mya, whereas the subgenomes a and b in the tetraploid *Silurana* diverged from one another about 10 Mya (Evans et al. 2015; Session et al. 2016). With an overarching goal of exploring the effect of polyploidization and divergence on the evolution of tandem repeats, we used cytogenetic methods and a genome database to test the hypotheses that (i) the number of the repeat loci in diploid *X. tropicalis* is half that in the allotetraploid species, and (ii) the locations of repeat loci in the studied species are homologous.

Materials and methods

Primary cell cultures and metaphase spread preparations

Primary cell cultures were derived from laboratory strains of *X. tropicalis* (strain 'Ivory Coast'), *X. laevis*, and *X. muelleri*, and wild-derived stains of *X. calcaratus* and *X. allofraseri* from Cameroon (Bakingili, where they occur in syntopy, 4.0684°N, 9.0682°E) and *X. pygmaeus* from the Democratic Republic of the Congo (Kokolopori, Yalokole, near Luo River, 0.2056°N, 22.8884°E). *Xenopus muelleri* animals were originally obtained from the Institute of Zoology at the University of Geneva (Switzerland). All species were bred at Charles University, Faculty of Science, Prague, Czech Republic. Briefly, tadpoles were anesthetized, hind limbs removed and homogenized (Sinzelle et al. 2012) in a cultivation medium (Knytl et al. 2017) modified according to Knytl et al. (2023). The explants were then cultivated at 29.5 °C with 5.5% CO_2 for five days without disturbance. The media was then changed every day for one week. Passages were performed with trypsin-ethylenediaminetetraacetic acid (Knytl et al. 2017).

Chromosomal suspensions were prepared following Krylov et al. (2010) and stored in fixative solution (methanol/acetic acid, 3:1, v/v) at – 20 °C. For cytogenetic analysis, a chromosome suspension was dropped onto a slide (Courtet et al. 2001). Chromosome preparations were aged at – 20 °C for at least one week. For each experiment, mitotic metaphase spreads were counterstained with ProLong™ Diamond Antifade Mountant with the fluorescent 4′,6-diamidino-2-phenylindole, DAPI stain (Invitrogen by Thermo Fisher Scientific, Waltham, MA, USA). From ten to 20 metaphase spreads were analyzed per probe. Microscopy and processing of metaphase images were conducted using a Leica Microsystem (Wetzlar, Germany) as detailed in Seroussi et al. (2019).

Fluorescent in situ hybridization with repetitive DNA probes

In order to generate probes for FISH, genomic DNA from *X. tropicalis* was used as a template for amplification of the repetitive small nuclear DNA regions (snDNA) U1 and U2, and histone H3. DNA was extracted from tadpole tail tissue using the DNeasy Blood and Tissue Kit (Qiagen, Hilden, Germany) according to manufacturer's instructions. Primers used for amplification are listed in Table 1. The annealing temperature was 54 °C and the elongation step 30 s for all PCR reactions; other conditions for PCR amplification with PPP Master Mix (Top-Bio, Prague, Czech Republic) followed the manufacturer's recommendations. Labeling PCR was performed as described in Knytl and Fornaini (2021). Digoxigenin-11-dUTP (Jena Bioscience, Jena, Germany) was used for U2 and H3 labeling, and biotin-16-dUTP (Jena Bioscience) was used for U1 labeling. *Xenopus tropicalis* U1 and U2 snDNA and H3 probes were then hybridized to chromosome spreads of *X. tropicalis*, *X. calcaratus*, *X. pygmaeus*, *X. allofraseri*, *X. laevis*, and *X. muelleri*. The procedures for hybridization mixture preparation, denaturation, and the subsequent overnight hybridization were described previously for rDNA FISH (Knytl et al. 2023). Post-hybridization

Table 1 Genes used for FISH analysis, their GenBank accession numbers, lengths, sequences of primers, and studies in which primers were designed

Gene Symbol	Gene Name	Accession No	Length (bp)	Primer Sequence	Citation
U1	Small nuclear RNA U1	OQ714817	119	U1F: 5′-GCAGTCGAGATTCCCACATT-3′	Silva et al. (2015)
				U1R: 5′-CTTACCTGGCAGGGGAGATA-3′	
U2	Small nuclear RNA U2	OQ714818	177	U2F: 5′-ATCGCTTCTCGGCCTTATG-3′	Bueno et al. (2013)
				U2R: 5′-TCCCGGCGGTACTGCAATA-3′	
H3	Histone H3	OQ714819	364	H3F: 5′-ATGGCTCGTACCAAGCAGAC(ACG)GC-3′	Colgan et al. (1998)
				H3R: 5′-ATATCCTT(AG)GGCAT(AG)AT(AG)GTGAC-3′	

washing and blocking reactions were performed as described for painting FISH in Krylov et al. (2010). Probe visualization was performed following Knytl et al. (2017). Slides were then de-stained according to the following protocol: nail polish was removed using xylene (2 min) and benzoin (2 min). Slides with cover slip were incubated in 4×SSC/0.1% Tween for 10 min with agitation, and then cover slips were manually removed. Slides without cover slip were then incubated in 4×SSC/0.1% Tween for 30 min with agitation followed by dehydration with methanol series (70, 90, 100% for 3 min each) and then air dried. After slide incubation in fixative solution for 30 min, slides were rinsed with distilled water, air dried, and then aged for 90 min at 60 °C.

Painting FISH

We used whole chromosome painting probes generated by laser microdissection of *X. tropicalis* chromosomes from previous study by Knytl et al. (2023). Whole chromosome painting probes from *X. tropicalis* chromosomes 1 and 8 were newly labeled with digoxigenin-11-dUTP (Krylov et al. 2010) and biotin-16-dUTP (both Jena Bioscience) (Knytl et al. 2023), respectively. De-stained slides (after FISH with the U1 and U2 probes) of *X. tropicalis*, *X. calcaratus*, and *X. laevis* were used for cross-species painting FISH (Zoo-FISH) with a digoxigenin-labeled probe according to the protocols described in Krylov et al. (2010) and modified in Knytl et al. (2017). Subsequently, slides were de-stained again and used for Zoo-FISH with biotin-labeled probe. Detection of signal was carried as detailed for double-color painting in Knytl et al. (2023). The *X. tropicalis* FISH experiments were performed in the reverse order from the other species (i.e., painting FISH first followed by de-staining and snDNA FISH).

Results

Sanger sequencing and BLAST searching

Amplification of the U1 and U2 snDNA and H3 nuclear genes yielded 119 and 177 and 364 bp long amplicons, respectively. Based on BLASTn searches of the *X. tropicalis* "Nigeria" strain genome, the U1 amplicon had 98.3% identity (query cover 100%) with the sequence of U1 spliceosomal RNA, LOC116408489 (accession number XR_004220992.1); U2 amplicon had 98.3% identity (query cover 100%) with U2 spliceosomal RNA, LOC116407440 (accession number XR_004220346.1); and the H3 amplicon had 97.2% identity (query cover 98%) with histone H3, LOC100497127, mRNA (accession number XM_012953339.3). Our sequences were deposited to the NCBI GenBank database: U1 snDNA accession number OQ714817, U2 snDNA accession number OQ714818, H3 accession number OQ714819.

Fig. 2 Double-color FISH with U1 and U2 snDNA probes. The U1 probe (red) reveals one clear signal (= a pair of homologous chromosomes) in **a** *X. tropicalis*, **c** *X. pygmaeus*, **d** *X. allofraseri*, and **e** *X. laevis*, while the same FISH shows two signals, each within homoeologous chromosomes in **b** *X. calcaratus* and **f** *X. muelleri*. The U2 (green) probe shows one signal in **a** *X. tropicalis*, **c** *X. pygmaeus*, **d** *X. allofraseri*, and **e** *X. laevis*, while the U2 probe shows two signals, each of them within homoeologous chromosomes in **b** *X. calcaratus* and **f** *X. muelleri*. Green and red arrows correspond to the U2 and U1 repeat loci, respectively. Painting probes were used for identification of chromosomes 1 (green) and 8 (red) in **a** *X. tropicalis*. Chromosomes were counterstained with DAPI in blue/gray. Scale bars represent 10 µM

FISH with U1 and U2 snDNA probes and their genomic locations in available Xenopus genome assemblies

When hybridized on the diploid species *X. tropicalis*, the U1 and U2 snDNA probes had intense signals on the distal region of the long (q) arm of chromosomes 1 and 8 (Fig. 2(a)), respectively. The number of copies was determined based on matches at least 50% of the query sequence length and 85% of the query sequence identity. BLAST results using the U1 sequence as a query to the *X. tropicalis* genome identified ~ 20 copies of U1 snDNA on chromosome 1. Using the U2 sequence as a query, we identified ~ 40 copies on *X. tropicalis* chromosome 8. In the allotetraploid species *X. calcaratus*, the U1 and U2 snDNA probes hybridized to the q arms of the chromosomes 1a, 1b and 8a, 8b (Fig. 2(b)), respectively. Chromosomes 1a and 1b are homoeologous to each other, and they are orthologous to *X. tropicalis* chromosome 1, and the mapped U1 region in *X. calcaratus* is thus homologous to the orthologous U1 region of *X. tropicalis* (both species have U1 gene on the distal part of the same chromosome). The U2 snRNA locus also was detected on both homoeologous chromosomes of *X. calcaratus* (chromosomes 8a and 8b) and in a homologous location to the orthologous U2 gene of *X. tropicalis*. For detailed definitions of homologous, homoeologous, and orthologous genes and chromosomes in *Xenopus*, see Song et al. (2021).

These U1 and U2 snDNA probes thus each hybridized to both homoeologous chromosomes in *X. calcaratus* as expected if copy number of each repeat was doubled by allopolyploidization. Similarly, in *X. muelleri*, U1 and U2 snDNA probes mapped to the expected homoeologous chromosomes (U1 on 1Lq and 1Sq; U2 on 8Lq and 8Sq; Fig. 2(f)).

In the allotetraploid species *X. pygmaeus*, *X. allofraseri*, and *X. laevis* only one signal was detected for U1 and U2 snDNAs. For the more closely related pair — *X. pygmaeus* and *X. allofraseri* — the U1 snDNA probe hybridized

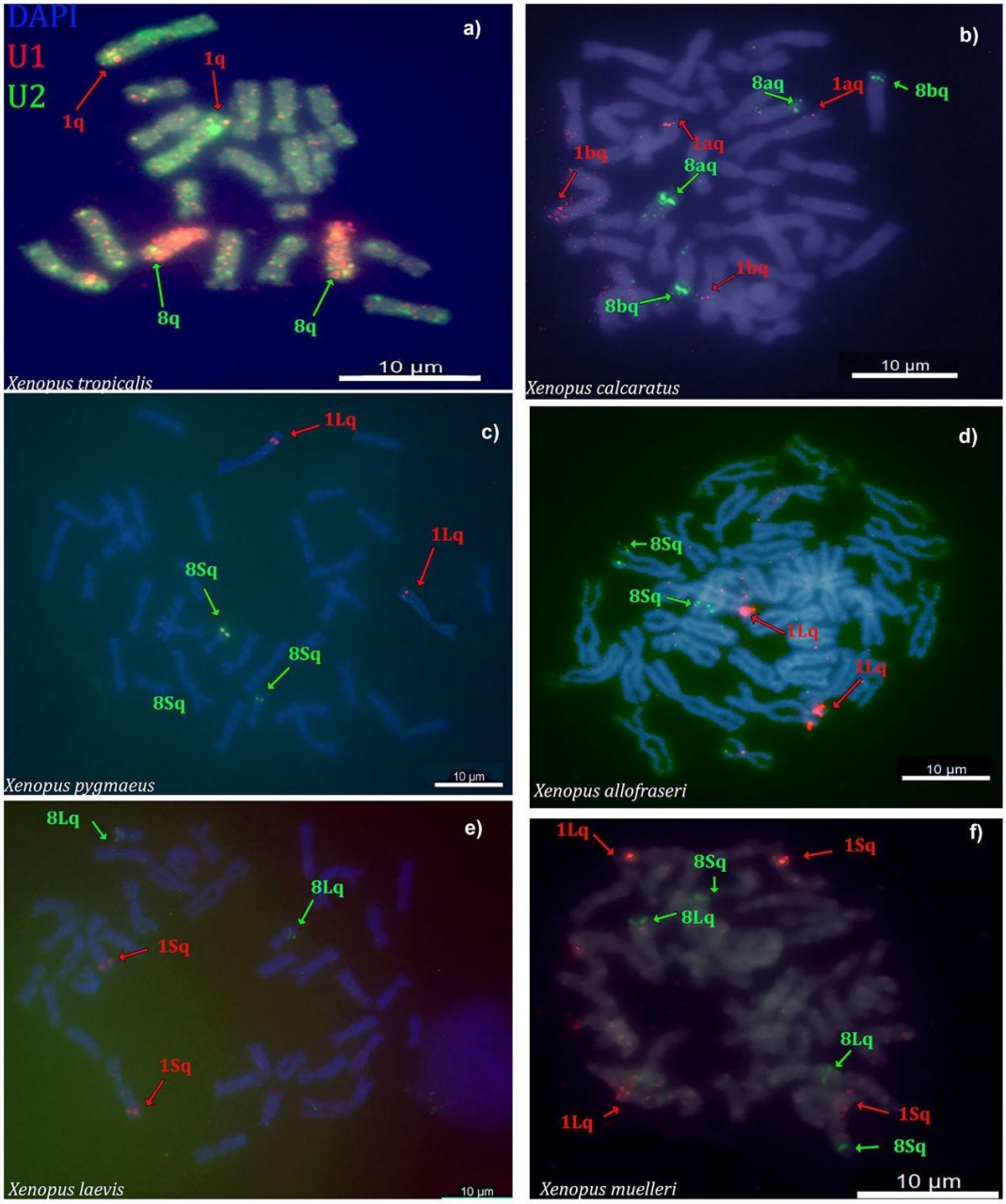

most conspicuously to the q arms of chromosome 1L and the U2 snDNA probe hybridized to the q arms of chromosome 8S (Fig. 2(c, d)). In *X. laevis*, the signal of the U1 and U2 snDNA probes was most conspicuous on the q arms of chromosomes 1S and 8L, respectively (Fig. 2(e)). Both U1 and U2 snRNA signals in *X. laevis* were located on chromosomes (1S and 8L) that are homoeologous to the chromosomes that bear U1 and U2 snRNA signals in *X. pygmaeus*

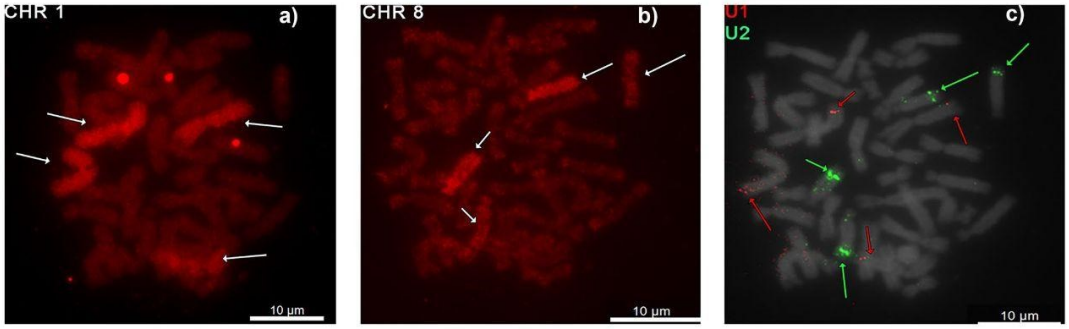

Fig. 3 Sequential FISH in *X. calcaratus* chromosomes. Cross-species painting FISH experiments with the whole chromosome painting probes from *X. tropicalis* **a** chromosome 1 (XTR 1) and **b** XTR 8 highlight chromosome-bearing U1 and U2 snRNA loci, respectively. **c** snDNA FISH illustrates that the U1 locus (in red) is localized on *X. calcaratus* chromosomes 1 (XCA 1a and 1b) and the U2 locus (in green) on XCA 8a and 8b. **a** and **b** are shown in the red channel, **c** is merged in the red-green-blue (RGB) channels. **c** chromosomes were counterstained with DAPI in gray. Scale bars represent 10 µM

and *X. allofraseri* (1L and 8S) and vice versa. The number of loci did not support the expectation that all tetraploid species should have twice as many snRNA loci as the diploid *X. tropicalis*, a result that could indicate copy number reduction or loss. Consistent with a scenario of reduction in copy number as opposed to complete loss, a BLAST search using U1 snDNA sequence as a query to the *X. laevis* genome recovered 11 copies on chromosome 1L and ~ 35 copies on chromosome 1S. Using the U2 sequence as a query against the *X. laevis* genome sequence, we identified ~ 40 copies on *X. laevis* chromosome 8L and 12 copies on chromosome 8S.

Painting FISH

To identify chromosomes bearing U1 and U2 loci, we employed FISH with the whole chromosome painting probes from *X. tropicalis* chromosomes 1 and 8. We successfully identified chromosomes 1 and 8 in *X. tropicalis* (Fig. 2(a)); chromosomes 1a, 1b, 8a, and 8b in *X. calcaratus* (Fig. 3); and chromosomes 1L, 1S, 8L, and 8S in *X. laevis* (Fig. 4). Homoeologous chromosomes of *X. calcaratus* and *X. laevis* were identified based on the intensity of the fluorescence signal (Knytl et al. 2023) and in the other studied species in subgenus *Xenopus* in which the painting FISH approach was not conducted; instead, homoeologous chromosomes were distinguished based on chromosome length (the L homoeologous chromosomes are longer than the S chromosomes; Matsuda et al. 2015; Session et al. 2016).

FISH with histone H3 probe and its genomic locations in available *Xenopus* genome assemblies

We then hybridized H3 probe to chromosome spreads of *X. tropicalis*, *X. calcaratus*, *X. pygmaeus*, *X. allofraseri*, *X. laevis*, and *X. muelleri*. In all species, signals were present in small patches on multiple chromosomes (Fig. 5). We found signals in all chromosomes in *X. tropicalis*, *X. calcaratus*, and *X. muelleri*. However, *X. pygmaeus*, *X. allofraseri*, and *X. laevis* had signals on about half of chromosomes. The H3 probes mapped to telomeric and pericentromeric regions.

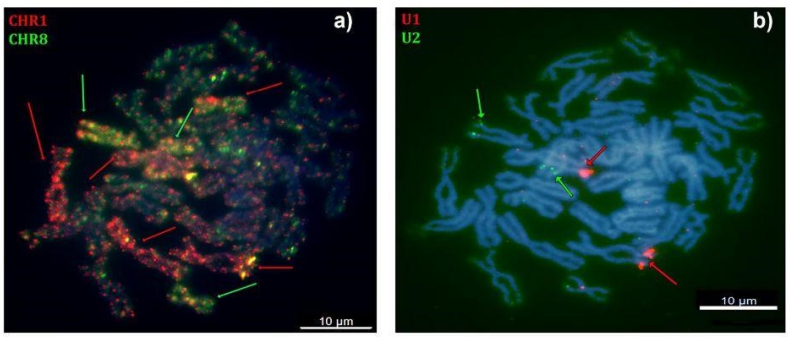

Fig. 4 Sequential FISH in *X. laevis* chromosomes. Cross-species painting FISH experiments with whole chromosome painting probes from **a** XTR 1 (in red) and XTR 8 (in green) illustrate that **b** the U1 locus (in red) is localized on *X. laevis* chromosomes 1S (XLA 1S), and the U2 locus (in green) on XLA 8L. Both **a** and **b** are merged in the RGB channels. Chromosomes were counterstained with DAPI in blue. Scale bars represent 10 µM

Based on BLAST searches, the H3 sequence occurs on *X. tropicalis* chromosomes 3 (11 hits), 6 (11 hits), and 9 (27 hits), and on chromosomes 5, 8, and 10, the matches were less than 50% of the query length. In *Xenopus laevis*, the H3 sequence occurs on chromosomes 3S (12 hits), 5L (6 hits), 5S (3 hits), 6L (2 hits), 6S (1 hit), 9_10L (15 hits), and 9_10S (5 hits). *Xenopus laevis* chromosomes 1L and 8L show some hits being less than 50% of the query sequence. All U1 and U1 snRNA and H3 loci mapped by FISH and BLAST are shown in Table 2.

Discussion

Quantification and localization of repetitive sequences using high-quality genome sequencing and assembly is an expensive and challenging undertaking as compared to using multiple cytogenetic approaches for gene mapping (Knytl et al. 2018b; Symonová et al. 2017a). As an alternative, we cytogenetically mapped non-rDNA tandem repeats (U1 and U2 snRNA and H3 histone) to one diploid and five allotetraploid *Xenopus* species with the aim of testing how repetitive elements were affected by genome duplication and divergence. At least two allotetraploidization events occurred in genus *Xenopus* with respect to our focal species and both — including studied species and their diploid extinct or yet undescribed predecessors — are depicted in Fig. 1.

Barring loss or movement of tandem repeats, we expected allotetraploid species to have twice as many tandem repeats as the diploid *X. tropicalis*, and that the locations of these elements would be unchanged (i.e., on the same region of both homoeologous chromosomes). In general, the cytogenetic results recovered no evidence for long-range movement of the U1, U2 snRNA or H3 loci. In the allotetraploids *X. calcaratus* and *X. muelleri*, the observed number of signals for each of the U1 and U2 snRNA loci matched our expectation based on allopolyploidization. However, for the three other allotetraploids (*X. pygmaeus*, *X. allofraseri*, and *X. laevis*), this expectation was not supported because, although in homologous locations, we found the same number of these tandem repeats as in the diploid *X. tropicalis* (Table 2). Furthermore, the snRNA signals in *X. pygmaeus* and *X. allofraseri* were on a different subgenome (U1 on L, U2 on S) than in *X. laevis* (U1 on S, U2 on L). Overall, this is consistent with an increased variation in copy number over time following allopolyploidization. BLAST searches of the *X. laevis* genome recovered each of these loci in both subgenomes, and it appears that the lower-than-expected number of cytogenetic signals is thus a consequence of differences in copy number, at least in this species. That the signals in *X. pygmaeus* and *X. allofraseri* are on different subgenomes than in *X. laevis* suggests that changes in copy number have been an ongoing phenomenon during *Xenopus* diversification. During diversification of African clawed frogs, the ancestor of *X. muelleri* diverged from the common ancestor of *X. pygmaeus*, *X. allofraseri*, and *X. laevis* soon after allotetraploidization in subgenus *Xenopus*, around 17 Mya (Fig. 1; Evans et al. 2015; Session et al. 2016). Thus, a parsimonious interpretation of these results posits that changes in copy number arose independently in an ancestor of *X. laevis* and again in the most recent common ancestor of *X. pygmaeus* and *X. allofraseri*.

In amphibians, U2 snRNA tandem repeats have also been localized in the cycloramphid genus *Thoropa* (Cholak et al. 2020) and the leptodactylid genus *Leptodactylus* (Gazoni et al. 2021), and the H3 gene has been localized in the pipid genus *Pipa* (Zattera et al. 2020). To our knowledge, there are no other cytogenetic studies that localize the U1, U2 snRNA, or H3 gene loci in this vertebrate group.

In frog genus *Thoropa*, U2 snRNA was detected cytogenetically on chromosomes 6 and 7 in some species, but others had U2 locus only on chromosome 6 or only on chromosome 7 (Cholak et al. 2020). The explanation for this variation might be that U2 loci are universally situated on both chromosomes 6 and 7 in all investigated *Thoropa* species but with different copy numbers on each of these chromosomes. We found similar variability in the location and number of FISH signals. Using BLAST, we identified locations where the sequence of our probe matched the *X. laevis* genome sequence and found that the number of U1 and U2 snRNAs detected by BLAST did not match the number of snRNAs detected by FISH. This inconsistency may be due to variation in the copy number of tandem repeats in each *X. laevis* subgenome and the lack of sensitivity of FISH to detect the locus with a low copy number of repeats. The U1 and U2 snRNA FISH signals were cytogenetically detected on those *X. laevis* chromosomes that contain ~ 15 and more copies of U1 and U2 repeats. In *Leptodactylus*, the U2 loci were identified on chromosome 6 in eight species, but one of them had signals on chromosomes 4, 6, 9, and 10 (Gazoni et al. 2021). These authors proposed that the additional signals on chromosomes 4, 9, and 10 can be the result of transposition by TEs followed amplification of the gene. We did not map TEs on *Xenopus* chromosomes and are thus unable to evaluate the possibility of TE transposition in this genus.

We also evaluated the effects of allotetraploidization and divergence on the evolution of H3 repeats. As expected, due to allotetraploidization, the allotetraploids *X. calcaratus* and *X. muelleri* possessed H3 repeats on twice as many chromosomes as the diploid *X. tropicalis*. However, in the allotetraploid *X. pygmaeus*, *X. allofraseri*, and *X. laevis*, we found signals on eight homologous pairs, which are fewer than expected based on allotetraploidization. This presumably is due to a decreased copy number or deletion of H3 repeats on several chromosomes, possibly in an ancestor of *X. pygmaeus*, *X. allofraseri*, and *X. laevis* based on phylogenetic

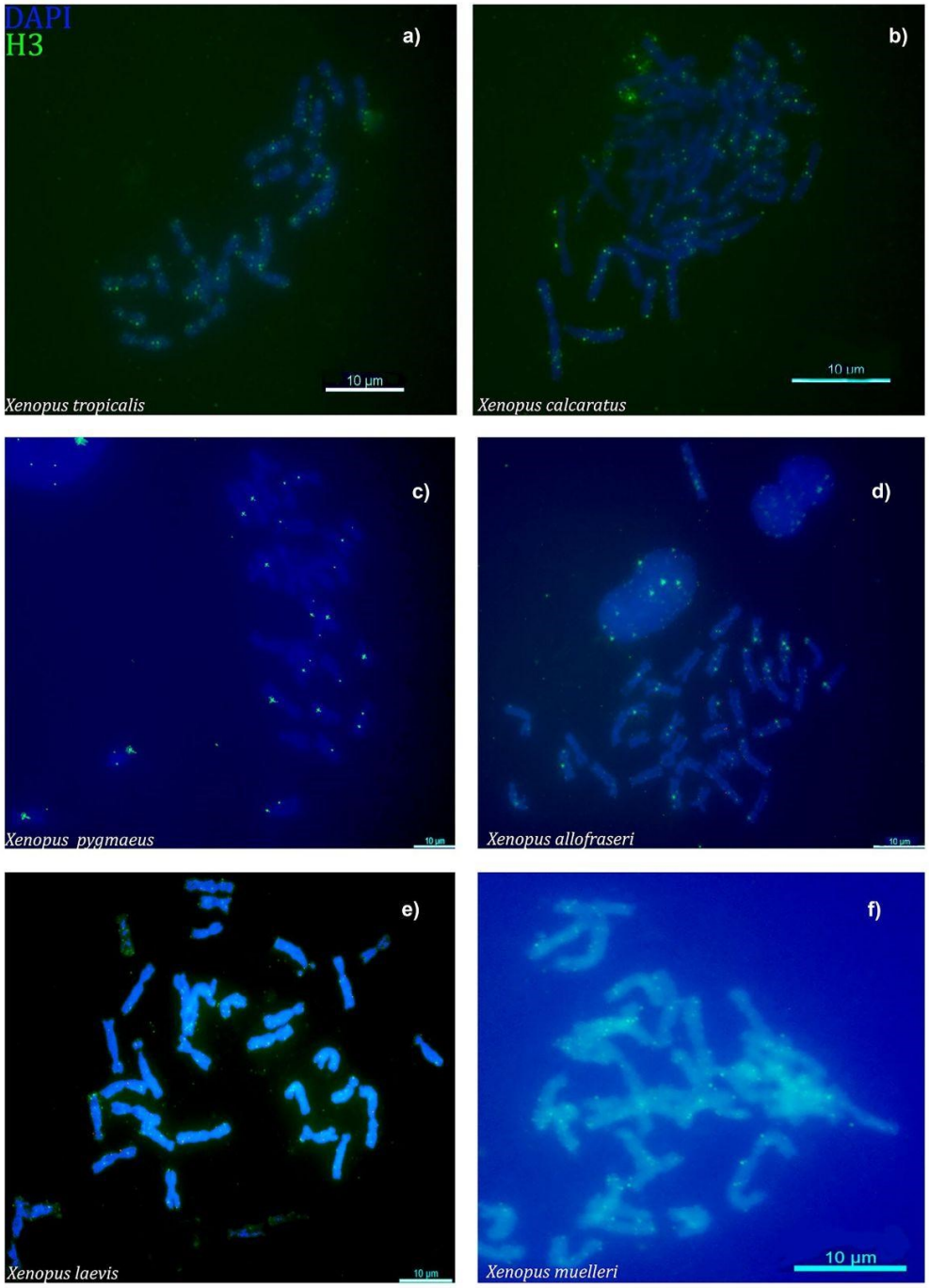

Fig. 5 FISH with histone H3 probe. The probe (green) shows multiple signals in **a** *X. tropicalis*, **b** *X. calcaratus*, **c** *X. pygmaeus*, **d** *X. allofraseri*, **e** *X. laevis*, and **f** *X. muelleri*. Chromosomes were counterstained with DAPI in blue/gray. Scale bars represent 10 µM

Table 2 Numbers and chromosomal positions of U1 and U2 snRNA and H3 loci per haploid genome in diploid *X. tropicalis* (subgenus *Silurana*) and reduced genome (half of the somatic set) in allotetraploid *X. calcaratus* (subgenus *Silurana*), *X. pygmaeus*, *X. allofraseri* (both in the *amieti* species group), *X. laevis* (*laevis* species group), and *X. muelleri* (*muelleri* species group). The numbers of loci are given according to the FISH results and the genomic database. The XTR, XCA, XPY, XAL, XLA, and XMU abbreviations correspond to chromosome of *X. tropicalis*, *X. calcaratus*, *X. pygmaeus*, *X. allofraseri*, *X. laevis*, and *X. muelleri*, respectively. *NA* means that information is not available in the genome database

Species	Number of chromosomes	U1 snRNA by FISH	U1 snRNA genomic database	U2 snRNA revealed by FISH	U2 snRNA genomic database	H3 by FISH	H3 genomic database
X. tropicalis	$n=10$	1 (XTR 1)	1 (XTR 1)	1 (XTR 8)	1 (XTR 8)	10	6
X. calcaratus	$n=20$	2 (XCA 1a and 1b)	NA	2 (XCA 8a and 8b)	NA	20	NA
X. pygmaeus	$n=18$	1 (XPY 1L)	NA	1 (XPY 8S)	NA	8	NA
X. allofraseri	$n=18$	1 (XAL 1L)	NA	1 (XAL 8S)	NA	8	NA
X. laevis	$n=18$	1 (XLA 1S)	2 (XLA 1L, XLA 1S)	1 (XLA 8L)	2 (XLA 8L, XLA 8S)	8	9
X. muelleri	$n=18$	2 (XMU 1L and 1S)	NA	2 (XMU 8L and 8S)	NA	18	NA

relationships among these species. Despite the variability associated with allopolyploidization followed by divergence in evolution of tandem repeats, the relative dosages of signals of U1, U2, and H3 with respect to *X. tropicalis* are similar in each allotetraploid species we examined.

Until recently, there was only one study in which the H3 gene was mapped on amphibian chromosomes (Zattera et al. 2020). In *Pipa carvalhoi*, a representative of the same family as *Xenopus* but deeply phylogenetically divergent by about 115–120 My (Feng et al. 2017; Hime et al. 2021), H3 signals were detected on chromosomes 1, 5, 6, 8, and 9, and less intense signals were visible on other chromosomes. Multiple distributions of H3 locus on all chromosomes have been observed, for example, in insect species of the family Acrididae (Oliveira et al. 2011; Bueno et al. 2013) where the distribution of the H3 locus may be related to the transposition of 5S ribosomal RNA (rRNA). In *Xenopus*, 5S rRNA is situated on telomeres of multiple chromosomes (Knytl et al. 2017, 2023), and therefore, the observed distribution of the H3 locus on multiple *Xenopus* chromosomes may also be associated to the distribution of 5S rRNA.

Co-localization of repetitive elements

An interesting finding that emerged from this study is a genomic association of various repetitive elements with rRNA; this can potentially provide evolutionary insights into genome organization. Synteny exists between As51 satellite DNA (originating from TEs) and NORs (Vicari et al. 2008) or between U1 snRNA and 5S rRNA in the characid fish genus *Astyanax* (Silva et al. 2015). One of possible roles of a co-localization can be a silencing of ribosomal genes by TEs (Vicari et al. 2008). All *Xenopus* species have NOR on a single homologous pair (Tymowska 1991). *Xenopus tropicalis* has NOR on chromosome 7, tetraploids from subgenus *Silurana* on 7a, and tetraploids from subgenus *Xenopus* on 3L (Tymowska 1991; Session et al. 2016; Roco et al. 2021; Knytl et al. 2023). We have not identified any snRNA loci on chromosomes 7, 7a, or 3L, and this finding argues against a genomic association between distinct NOR and snRNA repeats. The 5S ribosomal genes have been detected at the distal regions of the *X. mellotropicalis* and *X. calcaratus* (*Silurana* tetraploids) chromosomes 8bq (Knytl et al. 2017, 2023) which is the same position as the U2 snRNA locus in *X. calcaratus* (this study), supporting a genomic association between 5S rRNA and U2 snRNA. The NOR locus presumably was deleted on chromosome 7b in tetraploids of subgenus *Silurana* and on chromosome 3S in tetraploids of subgenus *Xenopus* (Session et al. 2016; Knytl et al. 2023). However, U1 and U2 loci map to both homoeologs in some tetraploids, and thus, deletion of snRNA in an ancestor of *Xenopus* tetraploids did not take place. There is the possibility that all our investigated *Xenopus* tetraploids have twice as many snRNA repeat loci as the diploid *X. tropicalis* but that these loci have unequal copy number within individual subgenomes, meaning that copy number of snRNA repeats was reduced in one subgenome (11 copies of U1 snRNA on *X. laevis* chromosome 1L is less than 20 copies on *X. tropicalis* chromosome 1; thus, the copy number of U1 snRNA on *X. laevis* chromosome 1L was reduced) but expanded in the other subgenome (35 copies of U1 snRNA on *X. laevis* chromosome 1S versus 20 copies in *X. tropicalis*). Moreover, some tandem repeat loci maintain a stable number of copies, for example, 40 copies of U2 snRNA on *X. tropicalis* chromosome 8 and *X. laevis* chromosomes 8L). These stable copy numbers within the U2 gene are consistent with studies that observed a higher evolutionary conservation of the *X. laevis* subgenome L than subgenome S, compared to *X. tropicalis* genome (Session et al. 2016). Reduction, expansion, and stability in the copy number of non-rDNA tandem repeats and complete loss of rRNA locus are the possible events that occur after polyploidization (Session et al. 2016;

Knytl et al. 2023). Genes retained as duplicates have distinct evolution leading to loss of function, subfunctionalization, or neofunctionalization and are under strong purifying selection (Force et al. 1999; Lynch et al. 2001), often followed by intra- and/or interchromosomal translocations, inversions, deletions, or degenerations (Evans 2007; Sémon and Wolfe 2007; Session et al. 2016; Knytl et al. 2017). Our study highlighted that copy number reduction and expansion of tandem repeats can be an important driver of evolution following allopolyploidization such as translocation, inversion, deletion, and degeneration.

Conclusion

Repetitive elements are integral components of a genome, and their evolution can be affected by mechanism of polyploidization or divergence among species. We used cytogenetic approaches to study repetitive elements in six species of *Xenopus* frogs (one diploid, five allotetraploids) with an aim of localizing and quantifying tandem repeats in their genomes. For U1 and U2 snRNA, and H3 tandem repeats, the locations were generally homologous, but we detected variation in copy numbers that resulted from reduction and expansion after allotetraploidization. The dynamic evolution of tandem repeats was most apparent in allotetraploid species that arose from the older allotetraploidization event.

Acknowledgements We thank two anonymous reviewers for their constructive comments on early versions of the manuscript. Also, we thank Xenbase (Karimi and Vize 2014) for making available the high-quality genome assemblies of *X. tropicalis* (v10.1) and *X. laevis* (v9.2).

Author contributions Laboratory experiments [Nicola R. Fornaini], [Barbora Bergelová], [Václav Gvoždík] and [Halina Černohorská]; Graphic design [Nicola R. Fornaini] and [Ben J. Evans]; Fieldwork [Václav Gvoždík], [Eric B. Fokam], [Gabriel Badjedjea] and [Ben J. Evans]; Funding acquisition [Václav Gvoždík], [Halina Černohorská], [Svatava Kubíčková], [Ben J. Evans] and [Martin Knytl]; Conceptualization of the study [Václav Gvoždík], [Ben J. Evans], [Martin Knytl]; Visualization [Martin Knytl]; Data curation and validation [Martin Knytl]; Project administration [Martin Knytl]; Writing – original draft preparation [Martin Knytl]; Supervision [Martin Knytl]; All authors reviewed, edited, and approved the final version of the manuscript.

Funding Open access publishing supported by the National Technical Library in Prague. The research was supported by the institutional support from the IVB CAS (RVO: 68081766); the Ministry of Culture of the Czech Republic (DKRVO 2019–2023/6.VII.e, National Museum, 00023272) (both VG); institutional support from the Ministry of Agriculture of the Czech Republic (MZE-RO0518) (HČ, SK); the Natural Science and Engineering Research Council of Canada (RGPIN-2017–05770) (BJE); the P JAC project CZ.02.01.01/00/22_010/0002902 MSCA Fellowships CZ – UK (MK).

Data availability The Sanger sequences that support the findings of this study are openly available in GenBank (accession numbers OQ714817-9).

Declarations

Statement of ethics Charles University has registered experimental breeding facilities for pipid frogs (16OZ12891/2018–17214, 37428/2019-MZE-18134). All experimental procedures involving frogs were approved by the Institutional Animal Care and Use Committee of Charles University, according to the directives from the State Veterinary Administration of the Czech Republic, reference number MSMT-20585/2022–4 issued by the Ministry of Education, Youth and Sport of the Czech Republic (MK is a manager of the experimental project on living *Xenopus* animals). MK is a holder of the Certificate of professional competence to design experiments according to §15d(3) of the Czech Republic Act No. 246/1992 coll. on the Protection of Animals against Cruelty (Registration number CZ 03973), provided by the Ministry of Agriculture of the Czech Republic.

Conflict of interest The authors declare no competing interests.

References

Altmanová M, Doležálková-Kaštánková M, Jablonski D, Strachinis I, Vergilov V, Vacheva E et al (2022) Karyotype stasis but species-specific repetitive DNA patterns in Anguis lizards (Anguidae), in the evolutionary framework of Anguiformes, PREPRINT (Version 1) available at Research Square. https://doi.org/10.21203/rs.3.rs-2413537/v1

Bishani A, Prokopov DY, Romanenko SA, Molodtseva AS, Perelman PL, Interesova EA et al (2021) Evolution of tandemly arranged repetitive DNAs in three species of Cyprinoidei with different ploidy levels. Cytogenet Genome Res 161(1–2):32–42. https://doi.org/10.1159/000513274

Bruschi DP, Rivera M, Lima AP, Zúñiga AB, Recco-Pimentel SM (2014) Interstitial telomeric sequences (ITS) and major rDNA mapping reveal insights into the karyotypical evolution of Neotropical leaf frogs species (Phyllomedusa, Hylidae, Anura). Mol Cytogenet 7(1):1–12. https://doi.org/10.1186/1755-8166-7-22

Bueno D, Palacios-Gimenez OM, Cabral-de-Mello DC (2013) Chromosomal mapping of repetitive DNAs in the grasshopper Abracris flavolineata reveal possible ancestry of the B chromosome and H3 histone spreading. PLoS One 8(6). https://doi.org/10.1371/journal.pone.0066532

Canapa A, Barucca M, Biscotti MA, Forconi M, Olmo E (2016) Transposons, genome size, and evolutionary insights in animals. Cytogenet Genome Res 147(4):217–239. https://doi.org/10.1159/000444429

Chalopin D, Naville M, Plard F, Galiana D, Volff JN (2015) Comparative analysis of transposable elements highlights mobilome diversity and evolution in vertebrates. Genome Biol Evol 7(2):567–580. https://doi.org/10.1093/gbe/evv005

Chen S, Zhang G, Shao C, Huang Q, Liu G, Zhang P et al (2014) Whole-genome sequence of a flatfish provides insights into ZW sex chromosome evolution and adaptation to a benthic lifestyle. Nat Genet 46:253–260. https://doi.org/10.1038/ng.2890

Cholak LR, Haddad CFB, Parise-Maltempi PP (2020) Cytogenetic analysis of the genus Thoropa Cope, 1865 (Anura-Cycloramphidae) with evolutionary inferences based on repetitive sequences. Genet Mol Biol 43(3):e20190364. https://doi.org/10.1590/1678-4685-GMB-2019-0364

Clark DP, Pazdernik NJ, McGehee MR (2019) Molecular biology. Elsevier, Academic Cell. https://doi.org/10.1016/C2015-0-06229-3

Colgan DJ, McLauchlan A, Wilson GDF, Livingston SP, Edgecombe GD, Macaranas J et al (1998) Histone H3 and U2 snRNA DNA sequences and arthropod molecular evolution. Aust J Zool 46:419–437. https://doi.org/10.1071/ZO98048

Courtet M, Flajnik M, Du Pasquier L (2001) Major histocompatibility complex and immunoglobulin loci visualized by in situ hybridization on *Xenopus* chromosomes. Dev Comp Immunol 25(2):149–157. https://doi.org/10.1016/S0145-305X(00)00045-8

Da Silva DS, Da Silva Filho HF, Cioffi MB, De Oliveira EHC, Gomes AJB (2021) Comparative cytogenetics in four leptodactylus species (Amphibia, Anura, Leptodactylidae): evidence of inner chromosomal diversification in highly conserved karyotypes. Cytogenet Genome Res 161(1–2):52–62. https://doi.org/10.1159/000515831

De Oliveira FI, Kretschmer R, Dos Santos MS, De Lima Carvalho CA, Gunski RJ, O'Brien PCM et al (2017) Chromosomal mapping of repetitive DNAs in Myiopsitta monachus and Amazona aestiva (Psittaciformes, Psittacidae) with emphasis on the sex chromosomes. Cytogenet Genome Res 151(3):151–160. https://doi.org/10.1159/000464458

Dubois A, Ohler A, Pyron RA (2021) New concepts and methods for phylogenetic taxonomy and nomenclature in zoology, exemplified by a new ranked cladonomy of recent amphibians (Lissamphibia). Megataxa 5(1):1–738. https://doi.org/10.1159/000464458

Elder JF, Turner BJ (1995) Concerted evolution of repetitive DNA sequences in eukaryotes. Q Rev Biol 70(3):297–320. https://doi.org/10.1086/419073

Evans BJ (2007) Ancestry influences the fate of duplicated genes millions of years after polyploidization of clawed frogs (*Xenopus*). Genetics 176(2):1119–1130. https://doi.org/10.1534/genetics.106.069690

Evans BJ, Carter TF, Greenbaum E, Gvoždík V, Kelley DB, McLaughlin PJ et al (2015) Genetics, morphology, advertisement calls, and historical records distinguish six new polyploid species of African clawed frog (*Xenopus*, Pipidae) from West and Central Africa. PLoS One 10(12):e0142823. https://doi.org/10.1371/journal.pone.0142823

Feng YJ, Blackburn DC, Liang D, Hillis DM, Wake DB, Cannatella DC et al (2017) Phylogenomics reveals rapid, simultaneous diversification of three major clades of Gondwanan frogs at the Cretaceous-Paleogene boundary. Proc Natl Acad Sci USA 114(29):E5864–E5870. https://doi.org/10.1073/pnas.1704632114

Force A, Lynch M, Pickett FB, Amores A, Yan YL, Postlethwait J (1999) Preservation of duplicate genes by complementary, degenerative mutations. Genetics 151(4):1531–1545. https://doi.org/10.1093/genetics/151.4.1531

Fu J, Zhang H, Guo F, Ma L, Wu J, Yue M et al (2019) Identification and characterization of abundant repetitive sequences in Allium cepa. Sci Rep 9(1):1–7. https://doi.org/10.1038/s41598-019-52995-9

Gama JM, Ludwig A, Gazolla AB, Guizelini D, Recco-Pimentel SM, Bruschi DP (2022) A genomic survey of LINE elements in Pipidae aquatic frogs shed light on Rex-elements evolution in these genomes. Mol Phylogenet Evol 168:107393. https://doi.org/10.1016/j.ympev.2022.107393

Gazoni T, Dorigon NS, Da Silva MJ, Cholak LR, Haddad CFB, Parise-Maltempi PP (2021) Chromosome mapping of U2 snDNA in species of Leptodactylus (Anura, Leptodactylidae). Cytogenet Genome Res 161(1–2):63–69. https://doi.org/10.1159/000515047

Gerbault-Seureau M, Cacheux L, Dutrillaux B (2018) The relationship between the (in-)stability of NORs and their chromosomal location: the example of cercopithecidae and a short review of other primates. Cytogenet Genome Res 153(3):138–146. https://doi.org/10.1159/000486441

Guzmán K, Roco ÁS, Stöck M, Ruiz-García A, García-Muñoz E, Bullejos M (2022) Identification and characterization of a new family of long satellite DNA, specific of true toads (Anura, Amphibia, Bufonidae). Sci Rep 12(1). https://doi.org/10.1038/s41598-022-18051-9

Hellsten U, Harland RM, Gilchrist MJ, Hendrix D, Jurka J, Kapitonov V et al (2010) The genome of the Western clawed frog *Xenopus tropicalis*. Science (80-) 328(5978):633–6. https://doi.org/10.1126/science.1183670

Hime PM, Lemmon AR, Lemmon ECM, Prendini E, Brown JM, Thomson RC et al (2021) Phylogenomics reveals ancient gene tree discordance in the Amphibian Tree of Life. Syst Biol 70:49–66. https://doi.org/10.1093/sysbio/syaa034

Karimi K, Vize PD (2014) The Virtual Xenbase: transitioning an online bioinformatics resource to a private cloud. Database (Oxford) 2014:bau108. https://doi.org/10.1093/database/bau108

Knytl M, Fornaini NR (2021) Measurement of chromosomal arms and FISH reveal complex Genome architecture and standardized karyotype of model fish, genus Carassius. Cells 10(9):2343. https://doi.org/10.3390/cells10092343

Knytl M, Smolík O, Kubíčková S, Tlapáková T, Evans BJ, Krylov V (2017) Chromosome divergence during evolution of the tetraploid clawed frogs, *Xenopus mellotropicalis* and *Xenopus epitropicalis* as revealed by Zoo-FISH. PLoS One 12(5):e0177087. https://doi.org/10.1371/journal.pone.0177087

Knytl M, Kalous L, Rylková K, Choleva L, Merilä J, Ráb P (2018a) Morphologically indistinguishable hybrid Carassius female with 156 chromosomes: a threat for the threatened crucian carp, C. carassius, L. PLoS One 13(1):e0190924. https://doi.org/10.1371/journal.pone.0190924

Knytl M, Tlapakova T, Vankova T, Krylov V (2018b) Silurana chromosomal evolution: a new piece to the puzzle. Cytogenet Genome Res 156(4):223–228. https://doi.org/10.1159/000494708

Knytl M, Forsythe A, Kalous L (2022) A fish of multiple faces, which show us enigmatic and incredible phenomena in nature: biology and cytogenetics of the genus Carassius. Int J Mol Sci 23(15):8095. https://doi.org/10.3390/ijms23158095

Knytl M, Fornaini NR, Bergelová B, Gvoždík V, Černohorská H, Kubíčková S et al (2023) Divergent subgenome evolution in the allotetraploid frog *Xenopus calcaratus*. Gene 851:146974. https://doi.org/10.1016/j.gene.2022.146974

Kretschmer R, Rodrigues BS, Barcellos SA, Costa AL, de Cioffi M, B, Garnero ADV, et al (2021) Karyotype evolution and genomic organization of repetitive DNAs in the saffron finch, sicalis flaveola (Passeriformes, aves). Animals 11(5):1456. https://doi.org/10.3390/ani11051456

Krylov V, Kubickova S, Rubes J, Macha J, Tlapakova T, Seifertova E et al (2010) Preparation of *Xenopus tropicalis* whole chromosome painting probes using laser microdissection and reconstruction of *X. laevis* tetraploid karyotype by Zoo-FISH. Chromosom Res 18(4):431–439. https://doi.org/10.1007/s10577-010-9127-x

Liao D (1999) Concerted evolution: molecular mechanism and biological implications. Am J Hum Genet 64(1):24–30. https://doi.org/10.1086/302221

Liu Y, Song M, Luo W, Xia Y, Zeng X (2019) Chromosomal evolution in the Amolops mantzorum species group (Ranidae; Anura) narrated by repetitive DNAs. Cytogenet Genome Res 157(3):172–178. https://doi.org/10.1159/000499416

Lynch M, O'Hely M, Walsh B, Force A (2001) The probability of preservation of a newly arisen gene duplicate. Genetics 159(4):1789–1804. https://doi.org/10.1093/genetics/159.4.1789

Matsuda Y, Uno Y, Kondo M, Gilchrist MJ, Zorn AM, Rokhsar DS et al (2015) A new nomenclature of *Xenopus laevis* chromosomes based on the phylogenetic relationship to Silurana/*Xenopus tropicalis*. Cytogenet Genome Res 145(3–4):187–191. https://doi.org/10.1159/000381292

Milioto V, Vlah S, Mazzoleni S, Rovatsos M, Dumas F (2019) Chromosomal localization of 18S–28S rDNA and (TTAGGG)n sequences in wo South African dormice of the genus Graphiurus (Rodentia: Gliridae). Cytogenet Genome Res 158(3):145–151. https://doi.org/10.1159/000500985

Myers PZ (2007) Tandem repeats and morphological variation. Nat Educ 1(1):1. https://www.nature.com/scitable/topicpage/tandem-repeats-and-morphological-variation-40690/

Oliveira VCS, Altmanová M, Viana PF, Ezaz T, Bertollo LAC, Ráb P et al (2021) Revisiting the karyotypes of alligators and caimans (Crocodylia, Alligatoridae) after a half-century delay: bridging the gap in the chromosomal evolution of reptiles. Cells 10(6):1397. https://doi.org/10.1186/1755-8166-4-24

Oliveira NL, Cabral-de-Mello DC, Rocha MF, Loreto V, Martins C, Moura RC (2011) Chromosomal mapping of rDNAs and H3 histone sequences in the grasshopper rhammatocerus brasiliensis (acrididae, gomphocerinae): extensive chromosomal dispersion and co-localization of 5S rDNA/H3 histone clusters in the A complement and B chromosome. Mol Cytogenet 4:24. https://doi.org/10.1186/1755-8166-4-24

Phimphan S, Aiumsumang S, Tanomtong A (2021) Characterization of chromosomal and repetitive elements in the genome of "Rana nigrovittata" (Anura, Ranidae): revealed by classical and molecular techniques. Cytol Genet 55(6):583–589. https://doi.org/10.3103/S0095452721060104

Roco ÁS, Liehr T, Ruiz-García A, Guzmán K, Bullejos M (2021) Comparative distribution of repetitive sequences in the karyotypes of *Xenopus tropicalis* and *Xenopus laevis* (Anura, Pipidae). Genes (basel) 12(5):617. https://doi.org/10.3390/genes12050617

Schmid M, Steinlein C (2015) Chromosome banding in Amphibia. XXXII. The genus *Xenopus* (Anura, Pipidae). Cytogenet Genome Res 145:201–217. https://doi.org/10.1159/000433481

Schott SCQ, Glugoski L, Azambuja M, Moreira-Filho O, Vicari MR, Nogaroto V (2022) Comparative cytogenetic and sequence analysis of U small nuclear RNA genes in three Ancistrus species (Siluriformes: Loricariidae). Zebrafish 19(5):200–209. https://doi.org/10.1089/zeb.2022.0040

Sember A, Pelikánová Š, de Bello CM, Šlechtová V, Hatanaka T, Do Doan H et al (2020) Taxonomic diversity not associated with gross karyotype differentiation: the case of bighead carps, genus Hypophthalmichthys (Teleostei, Cypriniformes, Xenocyprididae). Genes (basel) 11(5):479. https://doi.org/10.3390/genes11050479

Sémon M, Wolfe KH (2007) Consequences of genome duplication. Curr Opin Genet Dev 17(6):505–512. https://doi.org/10.1016/j.gde.2007.09.007

Seroussi E, Knytl M, Pitel F, Elleder D, Krylov V, Leroux S et al (2019) Avian expression patterns and genomic mapping implicate leptin in digestion and TNF in immunity, suggesting that their interacting adipokine role has been acquired only in mammals. Int J Mol Sci 20(18):4489. https://doi.org/10.3390/ijms20184489

Session AM, Uno Y, Kwon T, Chapman JA, Toyoda A, Takahashi S et al (2016) Genome evolution in the allotetraploid frog Xenopus laevis. Nature 538(7625):336–343. https://doi.org/10.1038/nature19840

Silva DMZA, Utsunomia R, Pansonato-Alves JC, Oliveira C, Foresti F (2015) Chromosomal mapping of repetitive DNA sequences in five species of astyanax (Characiformes, Characidae) reveals independent location of U1 and U2 snRNA sites and association of U1 snRNA and 5S rDNA. Cytogenet Genome Res 146(2):144–152. https://doi.org/10.1159/000438813

Sinzelle L, Thuret R, Hwang H-Y, Herszberg B, Paillard E, Bronchain OJ et al (2012) Characterization of a novel *Xenopus tropicalis* cell line as a model for in vitro studies. Genesis 50(3):316–324. https://doi.org/10.1002/dvg.20822

Song XY, Furman BLS, Premachandra T, Knytl M, Cauret CMS, Wasonga DV et al (2021) Sex chromosome degeneration, turnover, and sex-biased expression of sex-linked transcripts in African clawed frogs (*Xenopus*). Philos Trans R Soc Lond B Biol Sci 376(1832):20200095. https://doi.org/10.1098/rstb.2020.0095

Symonová R, Havelka M, Amemiya CT, Howell WM, Kořínková T, Flajšhans M et al (2017a) Molecular cytogenetic differentiation of paralogs of Hox paralogs in duplicated and re-diploidized genome of the North American paddlefish (Polyodon spathula). BMC Genet 18(1):19. https://doi.org/10.1186/s12863-017-0484-8

Symonová R, Ocalewicz K, Kirtiklis L, Delmastro GB, Pelikánová Š, Garcia S et al (2017b) Higher-order organisation of extremely amplified, potentially functional and massively methylated 5S rDNA in European pikes (Esox sp.). BMC Genomics 18(1):391. https://doi.org/10.1186/s12864-017-3774-7

Tymowska J (1991) Polyploidy and cytogenetic variation in frogs of the genus Xenopus. In: Green DM, Sessions SK (eds) Amphibian cytogenetics and evolution. Academic Press, San Diego, pp 259–297

Valadkhan S (2005) snRNAs as the catalysts of pre-mRNA splicing. Curr Opin Chem Biol 9(6):603–608. https://doi.org/10.1016/j.cbpa.2005.10.008

Valente GT, Mazzuchelli J, Ferreira IA, Poletto AB, Fantinatti BEA, Martins C (2011) Cytogenetic mapping of the retroelements Rex1, Rex3 and Rex6 among cichlid Fish: new insights on the chromosomal distribution of transposable elements. Cytogenet Genome Res 133(1):34–42. https://doi.org/10.1159/000322888

Vicari MR, Artoni RF, Moreira-Filho O, Bertollo LAC (2008) Colocalization of repetitive DNAs and silencing of major rRNA genes. A case report of the fish Astyanax janeiroensis. Cytogenet Genome Res 122(1):67–72. https://doi.org/10.1159/000151318

Yampolsky LY (2016) Mutation and genome evolution. Encyclop Evol Biol 77–83. Elsevier. https://doi.org/10.1016/B978-0-12-800049-6.00170-0

Zattera ML, Gazolla CB, de Soares A, A, Gazoni T, Pollet N, Recco-Pimentel SM et al (2020) Evolutionary dynamics of the repetitive DNA in the karyotypes of Pipa carvalhoi and Xenopus tropicalis (Anura, Pipidae). Front Genet 11:1–10. https://doi.org/10.3389/fgene.2020.00637

Zhang G, Li B, Li C, Gilbert MTP, Jarvis ED, Wang J (2014) Comparative genomic data of the Avian phylogenomics project. Gigascience 3(1):1–8. https://doi.org/10.1186/2047-217X-3-26

Terms and Conditions

Paper 4: Tetraploidy in the Boettger's dwarf clawed frog (Pipidae: Hymenochirus boettgeri) from the Congo indicates non-conspecificity with the captive population

Zoological Journal of the Linnean Society, 2024, **200**, 1034–1047
https://doi.org/10.1093/zoolinnean/zlad119
Advance access publication 18 October 2023
Original Article

OXFORD

Original Article

Tetraploidy in the Boettger's dwarf clawed frog (Pipidae: *Hymenochirus boettgeri*) from the Congo indicates non-conspecificity with the captive population

Václav Gvoždík[1,2,*,‡], Martin Knytl[3,4,*,‡], Ange-Ghislain Zassi-Boulou[5], Nicola R. Fornaini[3], Barbora Bergelová[3]

[1]Institute of Vertebrate Biology of the Czech Academy of Sciences, Brno, Czech Republic
[2]National Museum of the Czech Republic, Department of Zoology, Prague, Czech Republic
[3]Department of Cell Biology, Faculty of Science, Charles University, Viničná 7, Prague 128 43, Czech Republic
[4]Department of Biology, McMaster University, 1280 Main Street West, Hamilton, Ontario, L8S 4K1, Canada
[5]Department of Biology, National Institute for Research in Exact and Natural Sciences, Brazzaville, Republic of the Congo

‡V. Gvoždík and M. Knytl are co-first and co-senior authors in alphabetical order.

*Corresponding authors. Institute of Vertebrate Biology of the Czech Academy of Sciences, Studenec 122, 675 02 Studenec, Czech Republic. E-mail: vaclav.gvozdik@gmail.com; Department of Cell Biology, Faculty of Science, Charles University, Viničná 7, 128 43 Prague, Czech Republic. E-mail: martin.knytl@natur.cuni.cz

ABSTRACT

Cytogenetics can be used as a tool to study the evolution of polyploidy and taxonomy. Here we focus on aquatic African pipids, dwarf clawed frogs (*Hymenochirus*). Our study reveals that dwarf clawed frogs, present for decades in captivity, are best referred to as *Hymenochirus* sp. instead of the commonly used name '*H. boettgeri*' or sometimes '*H. curtipes*'. We present the first karyotype from a morphologically identified specimen of *H. boettgeri* with a known locality in the north-western Congo, which is tetraploid with 2n = 36. The captive *Hymenochirus* species has been found diploid in previous studies with different reported chromosome numbers; here we reveal 2n = 20A + 1B chromosomes. Our findings suggest that the tetraploid *H. boettgeri* karyotype evolved through fusion of two biarmed chromosomes and subsequent allotetraploidization, and is functionally diploid, similar to the origin of tetraploid clawed frogs in the subgenus *Xenopus*. We observed the stable presence of a single B chromosome in both sexes of our individuals from the captive population of *Hymenochirus* sp. However, additional investigation is necessary to clarify whether there is variation in the number of A and B chromosomes among populations, individuals, and/or tissues. Further research is also needed to understand the evolution and taxonomy of the genus *Hymenochirus*.

Keywords: amphibia; Anura; chromosome; cytogenetics; FISH; karyotype; polyploidy; taxonomy

INTRODUCTION

Amphibians represent a vertebrate clade that contains >8600 species (AmphibiaWeb 2023; Frost 2023) and approximately 100 species from 19 families have been identified as polyploid (Mezzasalma *et al.* 2023). Polyploidy in amphibians has evolved independently several times in multiple families, unlike, for example, teleost fishes, where whole genome duplication arose in the whole group as an ancestral evolutionary process (Schmid *et al.* 2015). Amphibians form both diploid and polyploid populations/species with sexual reproduction, making them a unique group compared to other vertebrate lineages (Bogart 1980, Mezzasalma *et al.* 2023). There is, therefore, a great advantage that diploids can serve as reference material for evolutionary and cytogenetic studies of related polyploids (Bogart and Bi 2013, Knytl *et al.* 2018, Fornaini *et al.* 2023). Polyploidy can arise in two different ways. Autopolyploidy, less common in amphibians, arises within a single ancestor in which meiotic incompatibilities are caused by environmental factors. A second possible origin is allopolyploidization, initiated by hybridization of two or more ancestors divergent enough to promote meiotic incompatibilities that prevent following cytokinesis.

Pipid frogs (family Pipidae) represent an ancient evolutionary lineage of fully aquatic frogs that split from its sister-lineage Rhinophrynidae more than 150 Mya. The extant pipid frogs

Received 28 April 2023; revised 27 July 2023; accepted 2 August 2023

are divided into two subfamilies, the American Pipinae (*Pipa* Laurenti, 1768) and the African Dactylethrinae (split ~110 Mya) containing two deeply divergent tribes (split ~100 Mya), Dactylethrini (*Xenopus* Wagler, 1827) and Hymenochirini (*Hymenochirus* Boulenger, 1896 and *Pseudhymenochirus* Chabanaud, 1920); for evolutionary relationships, see Feng *et al.* (2017), Dubois *et al.* (2021), and Hime *et al.* (2021). The genus *Xenopus* is divided into two subgenera, *Xenopus* and *Silurana* Gray, 1864, which are sometimes considered valid genera (e.g. Dubois *et al.* 2021). Pipids are known as a group with highly variable karyotypes, particularly chromosome numbers, primarily due to the role of polyploidization in their evolutionary history (Tymowska 1991, Schmid *et al.* 2015). Mezzasalma *et al.* (2015) suggested that the ancestral karyotype of pipids was 2n = 20, which can be observed in *Xenopus* (subgenus *Silurana*), *Hymenochirus*, *Pseudhymenochirus*, and *Pipa* (*P. carvalhoi* (Miranda-Ribeiro, 1937)). These authors also proposed three mechanisms for the increase in chromosome number in pipid frogs: allopolyploidy, fission, and addition of B chromosomes. In pipids, polyploidy, especially allopolyploidy, has so far only been found in *Xenopus*, including *Silurana* (Schmid *et al.* 2015). The haploid number n = 10 is present in *Silurana* and n = 9 in the subgenus *Xenopus* in which fusion of chromosome 9 and 10 occurred (Session *et al.* 2016). Recently, a fusion of chromosome 8 and 10 was documented in *Hymenochirus* (Bredeson *et al.* 2021). It has been hypothesized that chromosome fissions occurred in *Pipa* (Mezzasalma *et al.* 2015), and potentially also occurred in Central African *Hymenochirus* (see results in: Morescalchi 1968, 1981, Scheel 1973).

The addition of B chromosomes was found in the captive (pet trade) population of '*Hymenochirus boettgeri*' (2n = 20A + 1B), with B chromosomes detected in approximately half of the karyotypes scored in the two males studied (30/66 metaphase spreads obtained from the intestine, spleen, gonads, and lung tips; the remainder had 2n = 20; Mezzasalma *et al.* 2015). On the other hand, previous, relatively old studies of '*H. boettgeri*' reported 2n = 24 chromosomes (Morescalchi 1968; republished by: Morescalchi 1981, Tymowska 1991), or Scheel (1973) stated karyotype 2n = 22. The latter only stated the chromosome number and provided no further details. Finally, a recent study found 2n = 18 chromosomes and no B chromosomes in '*H. boettgeri*' (Bredeson *et al.* 2021). It is unclear whether the differences in chromosome number represent variation in B chromosome number (with the exception of 2n = 18, where chromosome fusion occurred), as hypothesized by Mezzasalma *et al.* (2015), or whether earlier researchers (Morescalchi 1968, 1981, Scheel 1973) studied one or more different species in which chromosome fissions occurred.

The captive stock of dwarf clawed frogs (*Hymenochirus* spp.) probably originated in the 1950s, when dwarf clawed frogs were imported from the wild by pet fish companies to Europe and the USA (Sokol 1959, Olsson and Österdahl 1960). The only available geographic information states that dwarf clawed frogs 'were shipped from Leopoldville'—present-day Kinshasa in the Democratic Republic of the Congo (Rabb and Rabb 1963)—or 'from Stanley Pool' (Sokol 1962), an area north-east of Kinshasa. However, Leopoldville could only have been the place of shipment or Stanley Pool the place of arrival (collectors could have landed here, as it is an area with ports), not the actual area of origin. At least two species, traditionally referred to as *H. boettgeri* (Tornier, 1896) and *H. curtipes* Noble, 1924, were probably imported in the 1950s and possibly later (e.g. Sokol 1959, 1962), the latter species being less common (Rabb and Rabb 1963, Sokol 1969). *Hymenochirus curtipes* has been reported to be an open area species (Noble 1924), requiring higher temperature in captivity and especially for breeding, and its tadpoles require more space (Sokol 1962). Therefore, it has been hypothesized that *H. curtipes* gradually disappeared from captivity due to its more specialised breeding requirements (Kunz 2002). However, names of both species can still be found in the aquarium/herpetoculture literature, although only one species seems to have been found in aquaria in recent decades (Kunz 2002, 2003). It is usually called *H. boettgeri*, although it has been noted that a taxonomic revision of the genus is needed (Kunz 2004).

The conspecificity of the aquarium population with *H. boettgeri* has sometimes been questioned based on certain morphological differences, and it has even been hypothesized that the aquarium population may represent a 'domesticated' hybrid between *H. boettgeri* and *H. curtipes* (Cecere 1998). Typical morphological features of *H. boettgeri* are, for example, the sides of the body covered with enlarged tubercles, the body rather oval, the head broad, and the dorsum monochromatic (de Witte 1930, Perret 1966, Arnoult and Lamotte 1968). This does not correspond much to the aquarium population, which is characterized by the body sides with homogeneous tubercles, without differentiated verrucosity, the body oval to pear-shaped, the head not distinctly broad, and the dorsum often mottled (Kunz 2004). Dwarf clawed frogs from the aquarium population are usually kept as a hobby animal and usually not as a laboratory animal. Nevertheless, it has been used in several laboratory studies where frogs were typically obtained from the pet trade and the name '*H. boettgeri*' is usually used in publications (e.g. Mezzasalma *et al.* 2015, Höbel and Fellows 2016, Miller *et al.* 2019, Cauret *et al.* 2020). Bredeson *et al.* (2021) referred to this dwarf clawed frog as an emerging model species. However, given the confusion with the species identification of the captive population since its establishment in aquaria (Rabb and Rabb 1963, von Filek 1967, Cecere 1998, Kunz 2002), we recommend naming the captive population of dwarf clawed frogs as *Hymenochirus* sp. We will use this name hereafter.

To date, all cytogenetic findings in the tribe Hymenochirini have been based on conventional and Giemsa staining, and banding techniques (Morescalchi 1968, Mezzasalma *et al.* 2015). No fluorescent *in situ* hybridization (FISH) experiments have been performed to study chromosome evolution in Hymenochirini. Furthermore, sex chromosomes were unknown in the genus *Hymenochirus* until Cauret *et al.* (2020) identified the male heterogametic system on chromosome 4 of '*H. boettgeri*' (= *Hymenochirus* sp.) using whole-genome sequencing. However, no study has focused on the cytogenetic delineation of sex chromosomes in the tribe Hymenochirini. Pipid frogs have homomorphic sex chromosomes, meaning that the sex chromosomes look identical and are morphologically indistinguishable from each other, e.g. the Z chromosome from the W chromosome in *Xenopus laevis* (Daudin, 1802) (see: Tymowska 1991). Despite the homomorphic nature of the sex chromosomes, there is great diversity in sex determination systems/mechanisms and

genetic differentiation of sex chromosomes in pipids (Roco *et al.* 2015, Cauret *et al.* 2020, Furman *et al.* 2020, Song *et al.* 2021).

Here, for the first time, we cytogenetically investigated the Boettger's dwarf clawed frog (*H. boettgeri*) from the wild with a known locality in comparison to *Hymenochirus* sp. from the captive population, including the first information on karyotype in females. We aimed to test whether polymorphism exists in the chromosome number, morphology and size, localization of ribosomal DNA (rDNA) and small nuclear DNA (snDNA) multigene families, i.e. tandem repeats, and occurrence of B chromosome(s) within our material. Our findings reveal the presence of allopolyploidization in the genus *Hymenochirus*, and also point to previously discussed uncertainties in the species' identification of the captive population. The unclear taxonomy is discussed in the context of new karyotype data, available molecular data, and comparison with type material.

MATERIAL AND METHODS

Karyotype sampling

One male of the Boettger's dwarf clawed frog (*H. boettgeri*) from the north-western part of the Republic of the Congo (Mindjong, Mbemba Forest; 1.4701°N 14.3556°E, 520 m) was compared with three males and three females from the aquarium population of *Hymenochirus* sp. obtained from a private breeder in the Czech Republic (Fig. 1; Supporting Information, Table S1). Voucher specimens are deposited in the herpetological collection of the Institute of Vertebrate Biology of the Czech Academy of Sciences (IVB-H), Research Facility Studenec, Brno, Czech Republic (IVB-H-CG17-356, IVB-H-Hsp01—Hsp06). Dwarf clawed frogs were identified following available keys (de Witte 1930, Perret 1966, Arnoult and Lamotte 1968) and by comparison with type material of all *Hymenochirus* species. Chromosomes were prepared according to Völker *et al.* (2006). A piece of foot interdigital webbing between the second and third toes was cut from each hind limb of an adult using fine laboratory scissors. After 2 weeks, a section of regenerated webbing tissue, about 2 mm wide, was cut off and incubated in Ringer's solution with colchicine, as described in detail, including subsequent hypotonization, in Völker *et al.* (2006). Tissue fixation was performed and metaphases were spread on glass slides in the same manner as described in the embryo preparation protocol (Völker and Kullmann 2006). Microscopy and processing of metaphase images were conducted using Leica Microsystem (Wetzlar, Germany) as detailed in Seroussi *et al.* (2019). Short (p) and long (q) arms were measured in pixels using ImageJ, v.1.53i (Schneider *et al.* 2012) and chromosome length was quantified as proposed by Knytl and Fornaini (2021). Chromosome size in μm was estimated using a scale bar generated by chromosome photography software. Chromosomes were identified according to a nomenclature based on the ratio of the p and q arms (Levan *et al.* 1964).

DNA barcoding

The seven karyotyped individuals were DNA barcoded targeting one mitochondrial DNA (mtDNA) and one nuclear DNA (nDNA) marker. A fragment of the mitochondrial 16S rRNA gene (*16S*) was amplified using a primer pair (16SL1 and 16SH1; adapted from: Palumbi *et al.* 1991; for details see: Gvoždík *et al.* 2010) commonly used in amphibian DNA barcoding (Vences *et al.* 2005, 2012). Consensus sequences were obtained from sequencing in both directions, resulting in a 579-bp long fragment. Our new sequences were combined with all available homologous *16S* fragments of *Hymenochirus* from GenBank, adding 11 specimens, and two outgroups—representatives of two other African pipid genera [*Pseudhymenochirus merlini* Chabanaud, 1920 and *Xenopus tropicalis* (Gray, 1864)] (see Supporting Information, Table S1). The sequences were aligned using the MAFFT algorithm (Katoh and Standley 2013), resulting in an alignment length of 583 bp. A best-fit model of nucleotide evolution (TIM2+F+G) was inferred in parallel with the maximum-likelihood phylogenetic tree, and branch support was obtained using 1000 standard bootstrap pseudoreplicates, all using IQ-TREE 2 (Kalyaanamoorthy *et al.* 2017, Minh *et al.* 2020).

A similar methodology was also applied to collect nuclear DNA data, a fragment of the recombination activating protein 1 (*rag1*) gene, using a pair of primers RAG-1_MartFl1 and RAG-1_AmpR1 (Pramuk 2006). All seven karyotyped individuals were sequenced from both sides, resulting in consensus sequences 933-bp long, but low-quality ends were trimmed in the Congo specimen of *H. boettgeri*, resulting in a fragment 879-bp long. No stop codons were present. Six additional *Hymenochirus* sequences and the same outgroups as defined above were added from GenBank (for details see Supporting Information, Table S1). The IQ-TREE 2 maximum likelihood tree was inferred using partitioned models (Chernomor *et al.* 2016) based on codon positions (best-fit models: F81 for codon positions 1 and 2, TPM2 for codon position 3). Branch support was obtained using 1000 bootstrap pseudoreplicates.

Since all six individuals from the aquarium population (*Hymenochirus* sp.) had the same haplotype, in both *16S* and *rag1*, only one representative sequence per each marker was deposited in the GenBank database along with data on *H. boettgeri* from the Congo (for Acc. Nos. see Supporting Information, Table S1).

Chromosome banding, and repetitive FISH with snDNA and rDNA probes

Five cytogenetic techniques were conducted sequentially on the same metaphase spread in the following order: (i) 5% Giemsa/PBS solution (v/v), (ii) chromomycin A_3, CMA_3 (Sigma–Aldrich, St. Louis, MO, USA), (iii) C-banding, (iv) double-colour FISH with the 5S and 28S rDNA probes, and (v) double-colour FISH with the U1 and U2 snDNA probes. The CMA_3/C-banding protocol followed Rábová *et al.* (2015) with the modifications described in Knytl *et al.* (2017). In order to generate probes for repetitive FISH, *X. tropicalis* and *H. boettgeri* were used as templates for amplification of U1 and U2 snDNAs, respectively, while *X. tropicalis* and *Hymenochirus* sp. were used for the 5S and 28S rDNA regions, respectively. The same *X. tropicalis* U1 amplicon from Fornaini *et al.* (2023) was used and labelled. Total genomic DNA (gDNA) was extracted from the webbing tissue of adult frogs using the DNeasy Blood and Tissue Kit (Qiagen, Hilden, Germany) according to manufacturer's instructions. Conditions for polymerase chain reaction (PCR) amplification

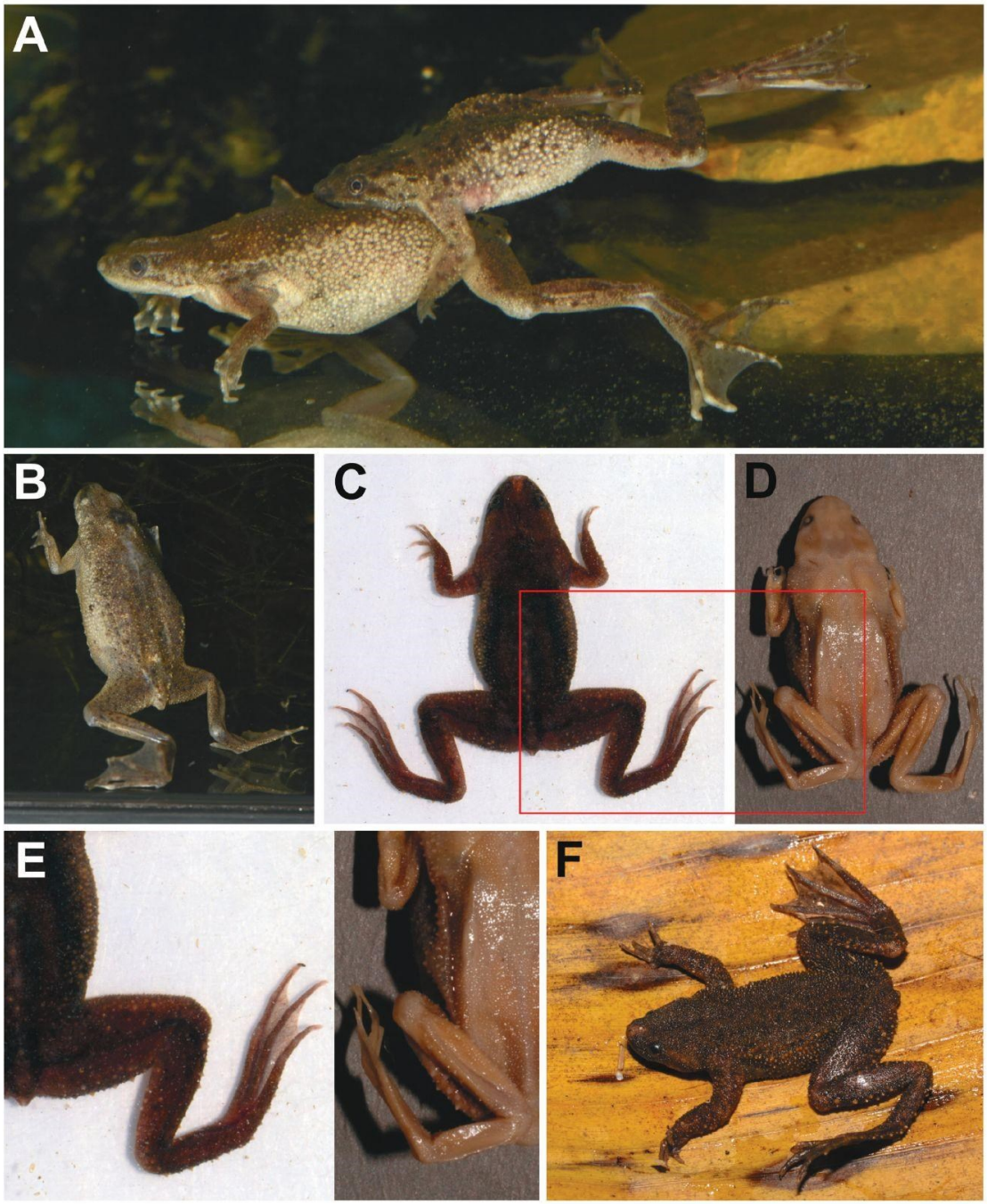

Figure 1. Dwarf clawed frogs, *Hymenochirus* sp. (captive population) and *H. boettgeri*. A, *Hymenochirus* sp., female (IVB-H-Hsp06) and male (IVB-H-Hsp02) in amplexus. B, *Hymenochirus* sp., female in dorsolateral view (IVB-H-Hsp04). In (A) and (B), note the relatively smooth flanks and hindlegs with homogeneous, unenlarged tubercles. C, *Hymenochirus boettgeri* from the north-western part of the Republic of the Congo (male, IVB-H-CG17-356). D, holotype of *H. boettgeri*, female (ZMB 11521). The area marked by the red rectangle is detailed in (E). F, *Hymenochirus boettgeri* from the same locality as the karyotyped individual (IVB-H-CG17-112, male). In (C–F), note the enlarged and spiny tubercles on the flanks and hindlegs typical for *H. boettgeri*.

were used according to PPP Master Mix (Top-Bio, Prague, Czech Republic) supplier recommendations. Primers used for amplification are listed in the Supporting Information, Table S2. The PCR conditions for the U1 and U2 snDNA amplifications were taken from Fornaini *et al.* (2023). Amplifications of the 5S and 28S rDNA loci and PCR labelling (5S, 28S, U1, and U2 probes) with digoxigenin-11-dUTP (Roche, Mannheim, Germany) and biotin-16-dUTP (Jena Bioscience, Jena, Germany), including purification steps, are detailed in Knytl and Fornaini (2021). Digoxigenin-11-dUTP was used for 5S and U2 labelling. Biotin-16-dUTP was used for 28S and U1 labelling. The 5S, 28S, U1, and U2 probes were hybridized with chromosome spreads of *H. boettgeri* and *Hymenochirus* sp. The contents of the hybridization mixture, denaturation, and the subsequent overnight hybridization were conducted as it was described in the rDNA FISH protocol (Knytl *et al.* 2023). Post-hybridization washing and blocking reactions were performed as described for painting FISH in Krylov *et al.* (2010). Biotin and digoxigenin probe signals were detected using CY3™-streptavidin (Invitrogen, Camarillo, CA, USA) and anti-digoxigenin-fluorescein (Roche), respectively (Knytl *et al.* 2017). After Giemsa staining, slides were de-stained in methanol and acetic acid solution (Rábová *et al.* 2015). Between techniques (ii)–(v), slides were de-stained as given in the protocol in Fornaini *et al.* (2023) and counterstained with ProLong™ Diamond Antifade Mountant with the fluorescent 4',6-diamidino-2-phenylindole, DAPI stain (Invitrogen by Thermo Fisher Scientific, Waltham, MA, USA).

Genomic *in situ* hybridization

Hymenochirus boettgeri and *Hymenochirus* sp. gDNAs were used as probes for genomic *in situ* hybridization (GISH) experiments. Whole-genome painting (WGP) probes were prepared using the GenomePlex Single Cell Whole Genome Amplification Kit (WGA4), Sigma–Aldrich, according to the manufacturer's whole genome amplification protocol with extracted gDNA. GenomePlex WGA Reamplification Kit (WGA3), Sigma–Aldrich, was used for labelling with digoxigenin-11-dUTP (Jena Bioscience), as described in Krylov *et al.* (2010). A combination of salmon sperm (Knytl *et al.* 2013) and autoclaved *H. boettgeri* and *Hymenochirus* sp. gDNAs (Bi and Bogart 2006) were used as a competitor DNA conspecifically to a probe. The highly concentrated competitor gDNAs were extracted using the DNeasy Blood and Tissue Kit (Qiagen) from liver and used 5 μg per ~500 ng of a probe. A total of ~500 ng of probe was used per hybridization mixture. A control GISH was performed with the *Hymenochirus* sp. probe hybridized on *Hymenochirus* sp. chromosomes, as detailed in the painting FISH method (Krylov *et al.* 2010), and cross-species GISH experiments were carried out with *Hymenochirus* sp. and *H. boettgeri* on *H. boettgeri* and *Hymenochirus* sp. chromosomes, respectively, as technically detailed in the Zoo-FISH methodology (Krylov *et al.* 2010), with minor changes (Knytl *et al.* 2017).

RESULTS

Species identification

In mtDNA (*16S*), the specimen obtained from the north-western Congo (IVB-H-CG17-356) closely matches with 99.5% identity the specimen from the south-western Congo retrieved from GenBank and originally identified as '*Hymenochirus* sp'. and deposited under the museum catalogue number USNM 584175 (Deichmann *et al.* 2017). Here, based on comparisons with type material (Fig. 1), we identify this lineage as *H. boettgeri*, as opposed to *Hymenochirus* sp., the naming we apply to the captive population (our new specimens IVB-H-Hsp01 to IVB-H-Hsp06; Fig. 2). *Hymenochirus boettgeri* forms a well-supported (bootstrap 82%) common clade with *H. curtipes* (from the wild, north-eastern Rep. Congo; Jackson and Beier 2006, Jackson *et al.* 2007, Deichmann *et al.* 2017) and this clade is sister to the captive population of *Hymenochirus* sp. Uncorrected *p*-distance in *16S* between *H. boettgeri* and *Hymenochirus* sp. is 8.6%.

For nDNA (*rag1*), less comparative data were available, and only two lineages (species) are identified (Fig. 2). Our specimens from the captive population (*Hymenochirus* sp.) share a clade with other specimens originating, or probably originating, from the pet trade, while our Congo *H. boettgeri* specimen shares a clade with a specimen originating from Cameroon (museum number CAS 249965), originally identified as '*Hymenochirus* sp.' (GenBank, online museum catalogue) or '*H. boettgeri*' (Feng *et al.* 2017). Interestingly, the *rag1* sequence of our *H. boettgeri* from the Congo has an unusually high proportion of heterozygous positions (3.4%), indicating—in agreement with the karyotype results—the allotetraploid nature of this specimen.

Morphologically, our specimen from the Congo corresponds closely with the type of *H. boettgeri* (e.g. enlarged and spiny tubercles on the flanks and hindlegs), while the specimens from the captive population do not correspond to any of the described species (Fig. 1).

Cytogenetic characterization of *Hymenochirus boettgeri* from the Congo

For both species of the genus *Hymenochirus*, we carried out the same methods. Giemsa staining shows better results than DAPI, thus we present Giemsa-stained karyotypes with consistently stained chromosomes. *Hymenochirus boettgeri* possesses 36 chromosomes with eight pairs of metacentric, two pairs of submetacentric, and seven pairs of subtelocentric chromosomes (Fig. 3A). All chromosomes are biarmed, the fundamental arm number (FN) is 72. The size of chromosome 1 is shown as the vertical scale bar and is estimated to be less than 10 μm.

DAPI (negative black band) and CMA_3 (positive green band) highlight the NOR locus on a single homologous pair, which is morphologically similar to *Hymenochirus* sp. chromosome 4 (Fig. 4A, B). C-banding identifies 14 heterochromatic blocks (on seven homologous pairs) (Fig. 4C). The rDNA FISH analysis shows the 28S NOR locus on the same chromosome on which the CMA_3 is displayed. The 5S probe does not highlight any locus (Fig. 4D), probably because of low efficacy of the used 5S probe. Unfortunately, we could not have repeated FISH with the 5S probe because chromosome structure on slide is broken after several attempts of staining and de-staining. The U1 locus is identified in the pericentromeric region of the q arm of the largest chromosome 1 (Fig. 4E), which is not homologous to the U1 locus of *Hymenochirus* sp. (the pericentromeric region of the p arm of chromosome 1). The U2 locus is found in the telomeric region of the q arm of chromosome 8 (Fig. 4E), which is homologous to the U2 locus of *Hymenochirus* sp. GISH analysis with the *Hymenochirus* sp. WGP probe and competitor

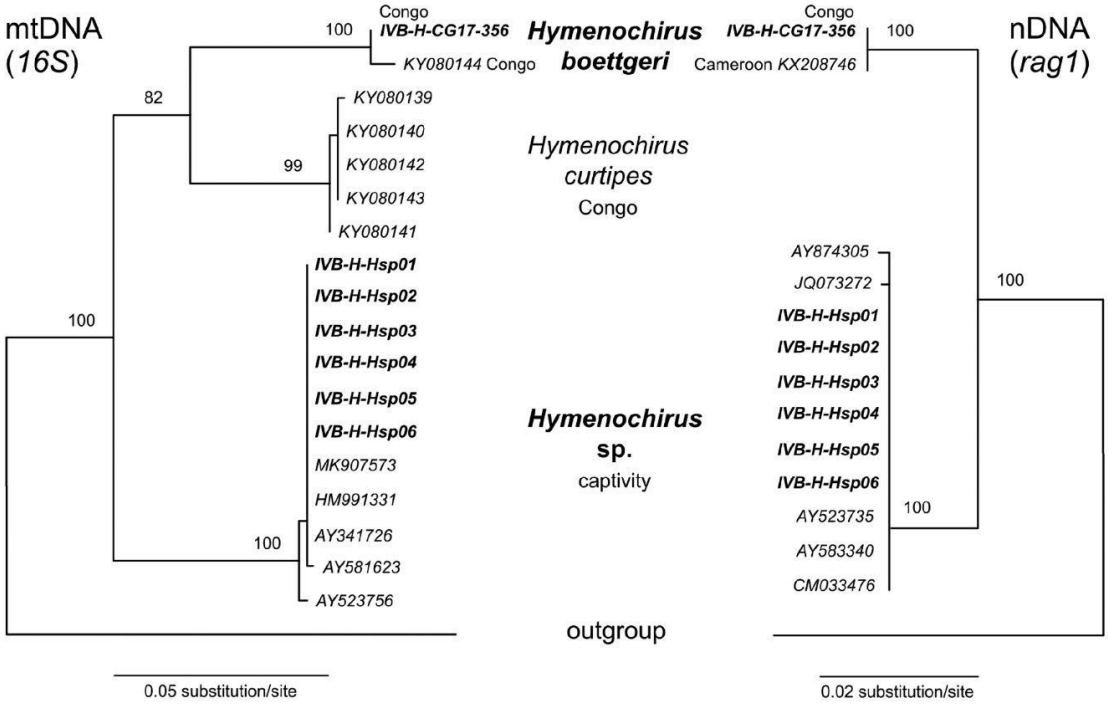

Figure 2. Phylogenetic trees of dwarf clawed frogs. Maximum likelihood mtDNA (*16S*, left) and nDNA (*rag1*, right) trees showing the positions of karyotyped individuals (in bold) in the context of available molecular sampling retrieved from GenBank (acc. nos. listed). For sampling details, see Supporting Information, Table S1.

Hymenochirus sp. DNA paint all 36 chromosomes of *H. boettgeri*, with some chromosomes having less intense signals (arrows in Fig. 4F). The difference in signal intensity is one of the other clues to determine the level of ploidy and homoeologous chromosomes. We find no heterochromatic B chromosomes in the karyotype of *H. boettgeri*.

Cytogenetic characterization of the captive *Hymenochirus* sp.

The number of chromosomes in *Hymenochirus* sp. is 21 (20A + 1B) with seven pairs of metacentric, one pair of submetacentric, and two pairs of subtelocentric chromosomes, and one extra B chromosome (Fig. 3B). All chromosomes are biarmed, FN = 42. The size of chromosome 1 is estimated to be 12–13 μm. Both males and females have the same number and general morphology of chromosomes. Sequential DAPI and CMA_3 analyses (Fig. 5A, B) show a single NOR on the p arm of submetacentric chromosome 4. DAPI consistently stains all 21 chromosomes but without staining of the NOR locus, which is CMA_3-positive. C-banding highlights telomeric and pericentromeric bands on most chromosomes, which helps to identify homologous chromosome pairs (Fig. 5C). Interestingly, the NOR locus is not stained using C-banding. The B chromosome is entirely painted and shows a high degree of heterochromatization (Fig. 5C, D, F; Supporting Information, Fig. S1A, B, D, E). FISH with rDNA probes identifies the 5S locus on the telomere and interstitial region of the q arm of chromosome 6. The 28S (NOR) locus is mapped to chromosome 4 (Fig. 5D) and is identical with CMA_3 bands. FISH with snDNA probes identifies the U1 locus on chromosome 1 and the U2 locus on chromosome 8 (Fig. 5E). GISH with the *H. boettgeri* WGP probe paints 20 chromosomes. Accessory B chromosome is stained with DAPI (DAPI-positive) but is not painted with the *H. boettgeri* WGP probe (Fig. 5F; Supporting Information, Fig. S1A). We performed two control GISH experiments with the *Hymenochirus* sp. WGP probe: the first with (Supporting Information, Fig. S1B) and the second without (Supporting Information, Fig. S1C) *Hymenochirus* sp. competitor DNA. Surprisingly, the WGP probe does not paint the B chromosome of *Hymenochirus* sp. in either control experiment (no red signal on the B chromosome). DAPI staining shows no signal on the B chromosome in the GISH experiment without the competitor (Supporting Information, Fig. S1C, F) compared to GISH with the competitor DNA where DAPI stains the entire B chromosome (Supporting Information, Fig. S1A, B, D, E).

DISCUSSION

Taxonomy

Our new molecular data, combined with the morphological characteristics of the specimen, such as enlarged tubercles on its body sides and hindlegs, confirms that our specimen from the northern Republic of the Congo is *H. boettgeri* (Fig. 1).

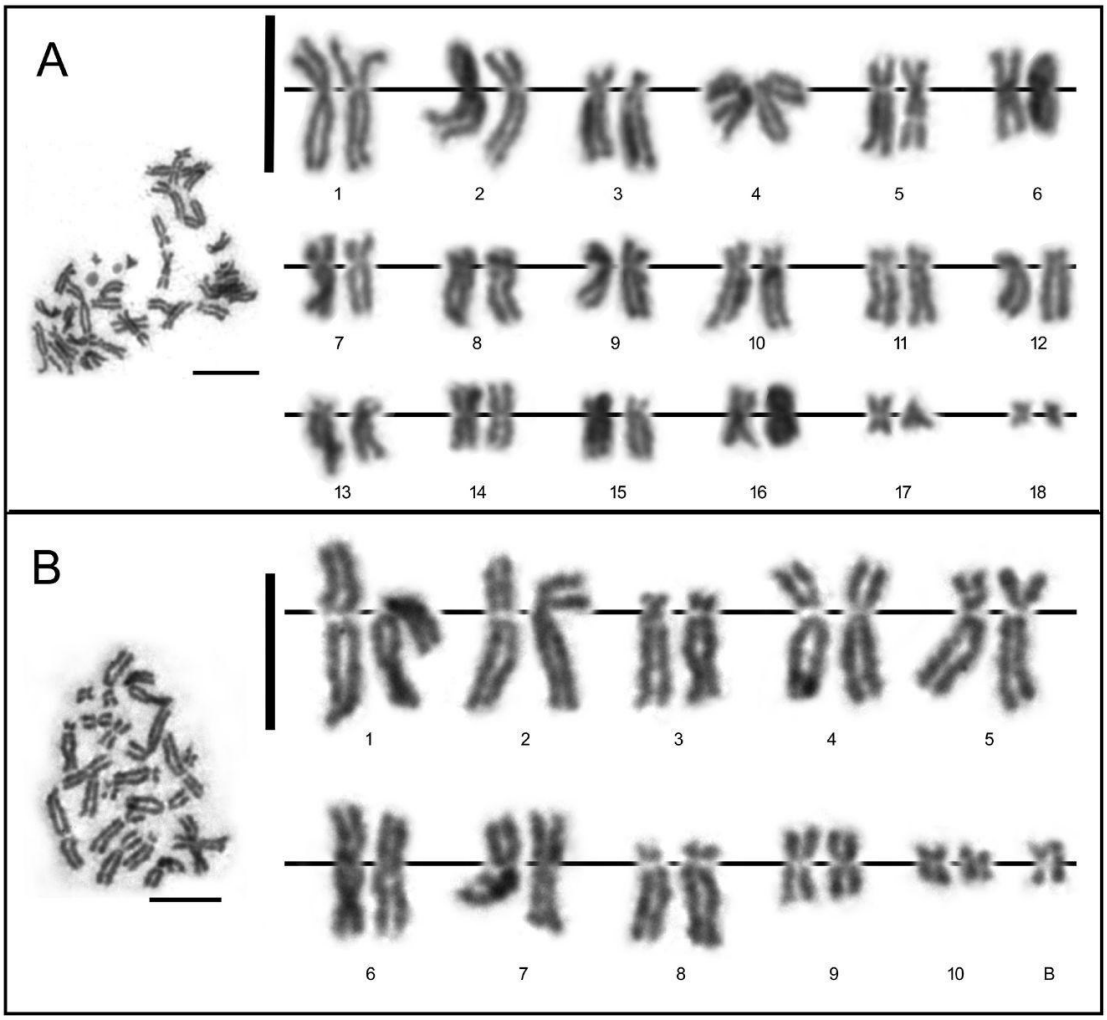

Figure 3. Karyotypes of (A) *Hymenochirus boettgeri* (IVB-H-CG17-356, male) with 18 homologous chromosome pairs, and (B) *Hymenochirus* sp. (IVB-H-Hsp06, female) with 10 pairs of A chromosomes and one B chromosome, arranged from Giemsa-stained chromosomes. Chromosomes were cut from metaphase spreads on the left. Long lines in karyotype arrangements indicate the position of chromosome centromere. Short vertical and horizontal lines correspond to the scale = 10 μm.

Two other specimens from the southern part of the Republic of the Congo and central Cameroon are very closely related with our specimen, and thus most probably conspecific, according to available molecular data (Deichmann *et al.* 2017, Feng *et al.* 2017; Fig. 2; Supporting Information, Table S1). The captive population, genetically deeply divergent from *H. boettgeri*, is not clearly identifiable as any described species (following identification keys in: de Witte 1930, Perret 1966, Arnoult and Lamotte 1968; and our unpublished data) and is most appropriately named as *Hymenochirus* sp. However, in literature and practice, captive dwarf clawed frogs are usually mistakenly referred to as '*H. boettgeri*' (e.g. Kunz 2003, 2004, Mezzasalma *et al.* 2015, Höbel and Fellows 2016, Miller *et al.* 2019, Cauret *et al.* 2020, Bredeson *et al.* 2021) or '*H. curtipes*' (e.g. Bewick *et al.* 2012; but see: Kunz 2002). Our molecular phylogenetic analysis suggests that *H. curtipes*, which used to occur in European and American aquaria in the past but probably became extinct in captivity (Sokol 1959, 1962, Rabb and Rabb 1963, Kunz 2002), is a sister-lineage of *H. boettgeri* (Fig. 2). However, data for other species are currently missing. A taxonomic revision is needed to properly understand the diversity and relationships within the genus *Hymenochirus* and to name the dwarf clawed frogs from the captive population.

Tetraploidy in *Hymenochirus boettgeri*

Our cytogenetic analysis detected 36 chromosomes in *H. boettgeri* from the Congo and confirmed 20 A chromosomes and one B chromosome in *Hymenochirus* sp. from the captive

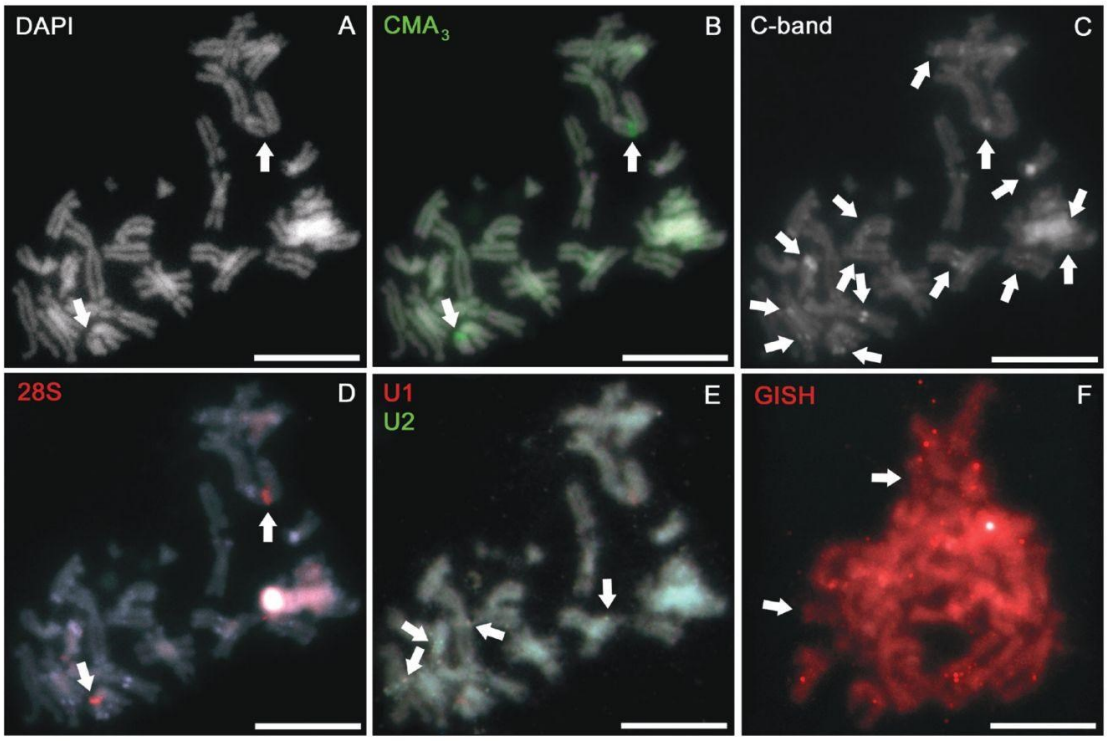

Figure 4. *Hymenochirus boettgeri* (IVB-H-CG17-356, male), sequential fluorescent chromosome mapping—DAPI, CMA_3, C-banding, ribosomal DNA (rDNA) FISH, small nuclear DNA (snDNA) FISH; and non-sequential whole-genome painting on metaphase spread. A, DAPI (black and white, B&W) consistently stains all 36 chromosomes. B, CMA_3 banding in green shows nucleolar secondary constriction (NOR locus) on the p arm of chromosome 4 that co-localizes with 28S. C, C-banding (B&W, brighter staining) highlights heterochromatic blocks on telomeric and pericentromeric regions of seven homologous chromosomes (14 arrows). D, FISH with 28S (red) ribosomal probes shows the p arm of chromosome 4. E, FISH with U1 (red) and U2 (green) snDNA probes shows very weak signals. The U1 probe maps to the q arm of chromosome 1, the U2 probe maps to the q arm of chromosome 8. F, genomic *in situ* hybridization (GISH) with *Hymenochirus* sp. whole-genome painting DNA probe that hybridizes to all 36 chromosomes with different intensity. Arrows show the less intensely painted chromosome pair. Scale bars represent 10 μm.

population (Fig. 3). The latter finding is consistent with that of Mezzasalma *et al.* (2015), but in contrast to an earlier study by Morescalchi (1968; republished by: Morescalchi 1981, Tymowska 1991), which found 24 chromosomes. However, the origin of Morescalchi's specimen is unknown and no details at all were given by Scheel (1973), who reported 22 chromosomes in '*H. boettgeri*'. As a possible explanation of this discrepancy, we hypothesize that Morescalchi (1968) and/or Scheel (1973) may have karyotyped one or eventually more different species, possibly *H. curtipes* that was present in captivity at the time of Morescalchi's and Scheel's analyses (Kunz 2002). Another explanation could be variation in chromosome number, especially in the number of B chromosomes, as suggested by Mezzasalma *et al.* (2015). See further discussion below, in the section about the B chromosomes.

Compared to all previous studies, our finding of 36 chromosomes is exceptional. The chromosome number of our *H. boettgeri* from the Congo is almost twice that of *Hymenochirus* sp. from the captive population, which has the putative ancestral number of A chromosomes in pipid frogs of 2n = 20 (Mezzasalma *et al.* 2015), and exactly twice the number of chromosomes found by Bredeson *et al.* (2021). The number, morphology, and composition of chromosomes of our *H. boettgeri* provide evidence that our specimen is tetraploid or allotetraploid, respectively, which is the first case of tetraploidy in pipids outside the genus *Xenopus* (Mezzasalma *et al.* 2015, Schmid *et al.* 2015). The size of the chromosomes also indirectly demonstrates the tetraploid nature of *H. boettgeri*, as its chromosomes are smaller than those of *Hymenochirus* sp. (Fig. 3). Polymorphism in chromosome size is also visible in the karyotypes of diploid *X. tropicalis* compared to allotetraploid *X. laevis*, *X. mellotropicalis* Evans, Carter, Greenbaum, *et al.*, 2015, or *X. calcaratus* Peters, 1875 (see: Session *et al.* 2016, Knytl *et al.* 2017, 2023). In *X. laevis*, the chromosomes of the S-subgenome (shorter homoeologues) have undergone losses and deletions, and, therefore, the size of these chromosomes has decreased (Session *et al.* 2016). In cyprinid fishes, for example, polyploids have chromosomes that are smaller than those of their

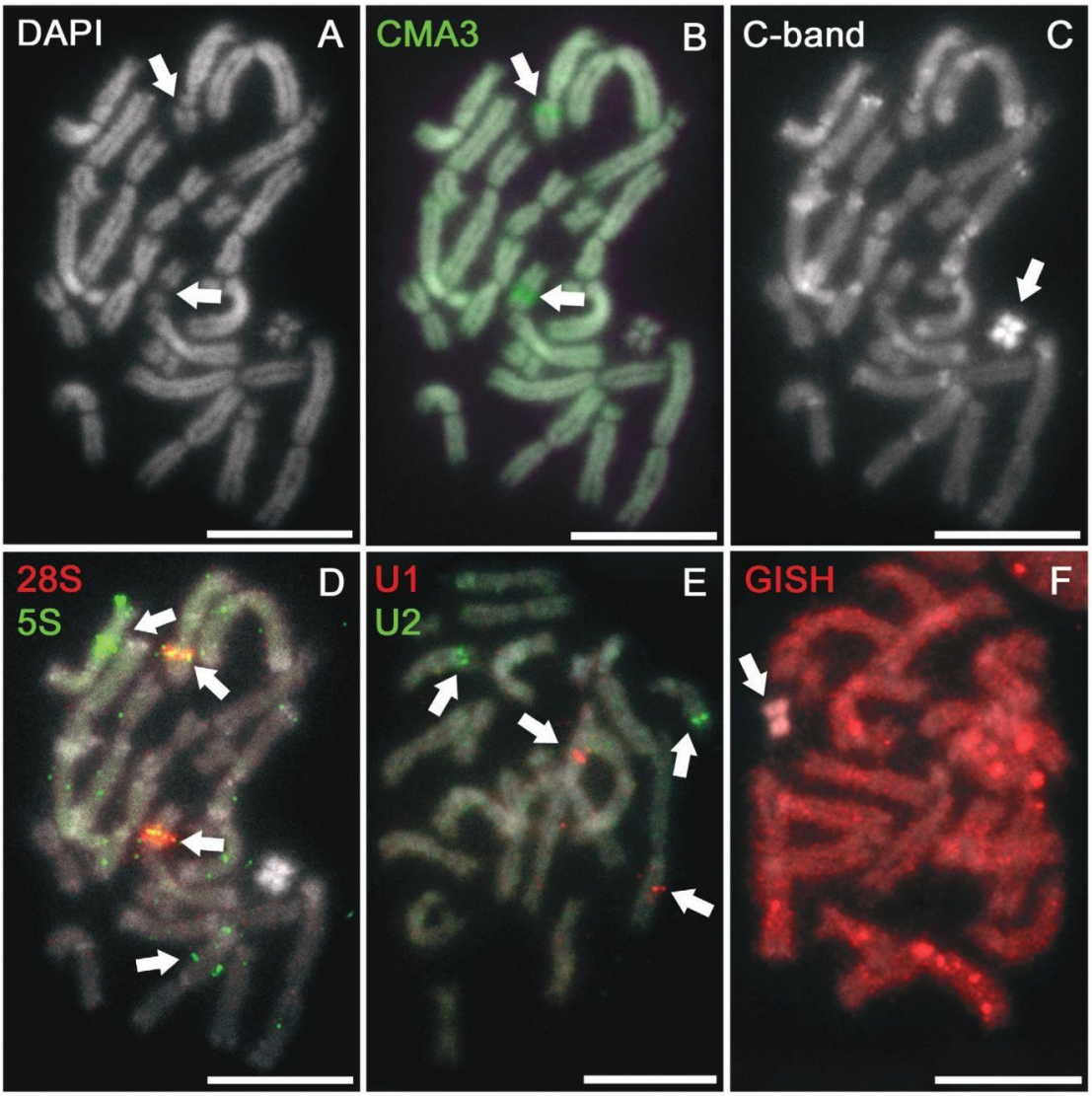

Figure 5. *Hymenochirus* sp. (IVB-H-Hsp06, female), sequential fluorescent chromosome mapping (DAPI, CMA_3, C-banding, rDNA FISH), non-sequential snDNA FISH, and whole-genome painting on metaphase spread. A, DAPI (B&W) counter-stained metaphase spread shows all 21 chromosomes. B, CMA_3 banding in green shows NOR locus on the p arm of chromosome 4. CMA_3 signal co-localizes with 28S locus. C, C-banding (B&W, brighter staining) highlights heterochromatic blocks on telomeric and pericentromeric regions of almost all chromosomes. In addition, the whole B chromosome is intensely banded (arrow). D, 5S (green) and 28S (red) rDNA loci are located on the q arm of chromosome 6 and p arm of chromosome 4, respectively. The 5S rDNA is situated on two different chromosomal loci within the single q arm. E, the snDNA loci U1 (red) and U2 (green) are located on the p arm of chromosome 1 and the q arm of chromosome 8, respectively. F, the GISH experiment of the *H. boettgeri* whole-genome painting probe, which hybridizes on *Hymenochirus* sp. chromosomes. All chromosomes are painted (red) except one, B chromosome, which shows no GISH signal and is DAPI-positive (arrow). Scale bars represent 10 μm.

diploid relatives (e.g. visible on karyotypes of diploid and triploid/tetraploid *Carassius* Nilsson, 1832; see: Kalous and Knytl 2011, Knytl *et al.* 2013, 2022). Further support for tetraploidy comes from GISH, where the tetraploid *H. boettgeri* probe consistently painted all 20 A chromosomes of *Hymenochirus* sp., while the diploid *Hymenochirus* sp. probe painted some *H. boettgeri* chromosomes more intensely than others, similar to what was observed in diploid and allotetraploid *Xenopus* (Knytl *et al.* 2023). This suggests that one subgenome of *H. boettgeri* may be evolutionarily closer to *Hymenochirus* sp. than the other

subgenome, indicating an allotetraploid origin. Further indirect evidence of allotetraploidy is the high frequency of heterozygous positions in the *rag1* nucleotide sequence, where a potential divergence of 3.4% between two paralogues is indicative of an allotetraploid origin.

The discovery of tetraploidy is based on a single male individual, which may open the question of whether tetraploidy is an autapomorphy of *H. boettgeri*, or whether there is geographic variation at the ploidy level within this supposedly widespread Central African species (Channing and Rödel 2019). To answer this question, multiple populations of *H. boettgeri* need to be cytogenetically examined. However, the genome size of *H. boettgeri* from the northern Democratic Republic of the Congo (DRC) is almost twice as large (3.77–4.29 pg; Liedtke *et al.* 2018) as that reported by King (1990; 2.45 pg). The latter most probably originated from the captive population, as virtually all dwarf clawed frogs used in research in recent decades have come from the captive population. Given that the locality of the DRC samples is approximately 800 km east of our karyotyped individual [one of us (V.G.) provided material for the Liedtke *et al.* (2018) study from a locality at 2.1228°N 21.3891°E], this is indicative of *H. boettgeri* being tetraploid throughout its range, or at least in a substantial portion of its populations.

Potential evolutionary origin of tetraploidy in *Hymenochirus boettgeri*

Hymenochirus sp. has the presumed pipid ancestral karyotype 2n = 20 (plus one B chromosome unique in this species), while tetraploid *H. boettgeri* has 36 chromosomes, which are probably secondarily organized as diploid (2n = 4x = 36; see below). Both karyotypes consist of biarmed chromosomes (no telocentrics), and, therefore, neither centric fusion of two telocentric chromosomes nor fission of a metacentric chromosome may be the evolutionary mechanism underlying the different chromosome numbers of the two *Hymenochirus* species. The same difference in chromosome number between diploid and allotetraploid pipids is known between two subgenera of the genus *Xenopus*: diploid *X.* (*Silurana*) *tropicalis* (2n = 20) and tetraploid species of the subgenus *Xenopus* (2n = 36), e.g. *X. laevis* (Tymowska 1991; Evans *et al.* 2004). The 36-chromosome karyotype of the subgenus *Xenopus* arose after the fusion of two metacentric chromosomes 9 and 10 in a common ancestor of both subgenomes (2n = 18) and subsequent allotetraploidization (Evans *et al.* 2005; Session *et al.* 2016). We assume that a similar mechanism may have occurred in *H. boettgeri*. Interesting, and still poorly understood, is a recent finding pointing to a polymorphism in the number of chromosomes in the captive population, where karyotype 2n = 18 was found in *Hymenochirus* sp. (see Fig. 2 and Supporting Information, Table S1 for molecular identification) after the fusion of chromosomes 8 and 10 (Bredeson *et al.* 2021).

The limited molecular phylogenetic data available support the hypothesis that the ancestral karyotype of the tribe Hymenochirini is 2n = 20, because *Hymenochirus* sp. with 20 A chromosomes represents the first diverging branch of the genus and the sister-genus *Pseudhymenochirus* also has 2n = 20 (Mezzasalma *et al.* 2015). Thus, tetraploidization in *Hymenochirus* is probably a derived state that occurred later in the evolution of the genus. However, because we lack information on karyotypes of other *Hymenochirus* species, we cannot formulate a more precise hypothesis about the evolutionary scenario of tetraploidization in this genus. For example, *H. curtipes* appears to be a sister-lineage to *H. boettgeri* (Fig. 2), but we lack information on its karyotype. We can only speculate that the karyotype of '*H. boettgeri*' with 2n = 24 presented by Morescalchi (1968; republished by: Morescalchi 1981, Tymowska 1991) could be misidentified *H. curtipes*, which was available in hobby aquaria in the 1960s (Sokol 1959, Rabb and Rabb 1963, von Filek 1967), and the increased chromosome number could have arisen by fissions (e.g. as in *Pipa parva* Ruthven and Gaige, 1923; see: Mezzasalma *et al.* 2015). However, this is only a speculation that is unlikely to be confirmed or refuted unless we know the karyotype of *H. curtipes*.

FISH in tetraploid *Hymenochirus boettgeri* and diploid *Hymenochirus* sp.

The numbers of FISH signals of multigene families are helpful to understand the functional diploidy of evolutionarily tetraploid *H. boettgeri*. The 28S rDNA (NOR), U1 and U2 snDNA loci are situated on a single chromosome, indicating rediploidization of a tetraploid ancestor, probably associated with a sexual mode of reproduction, and, therefore, the presence of a diploid–haploid cycle and crossing-over are expected in tetraploid *H. boettgeri*. This phenomenon has been described in all *Xenopus* polyploids (Tymowska 1991, Session *et al.* 2016, Knytl *et al.* 2017, 2023). On the other hand, the number and localization of U1 and U2 snDNAs are more diverse in *Xenopus* tetraploids, with one or two U1 and U2 loci detected by FISH, depending on the copy number of these tandemly repeated elements on the exact chromosome (Fornaini *et al.* 2023), which is not the case for the tetraploid *Hymenochirus* in this study.

The U1 snDNAs show the stable number but polymorphism in their position on *H. boettgeri* and *Hymenochirus* sp. chromosomes. *Hymenochirus boettgeri* has the U1 locus on the q arm of chromosome 1 and *Hymenochirus* sp. has this locus on the p arm of chromosome 1. *Xenopus* has the U1 locus close to the telomere on the q arm of chromosome 1 (Fornaini *et al.* 2023). A responsible mechanism for the rearrangement of the U1 locus in *Hymenochirus* can be pericentromeric inversion of a massive region, or a change of the position by a mechanism similar to transposition of transposons. An alternative explanation of this polymorphism is that the U1 locus is present on both chromosome arms but with a different number of copies—reduced copy number on the p arm and expanded copy number on the q arm of chromosome 1 in *H. boettgeri*. The diversity of the U1 locus localization points to its dynamic character, which is not the case of the U2 and NOR loci found constantly on the telomere of the q arm of chromosome 8 and pericentromeric region of the p arm of chromosome 4, respectively. All mapped loci are shown in Figure 6.

We analysed karyologically male and female individuals of *Hymenochirus* sp. (females for the first time) and male *H. boettgeri*. No sex-specific differences in karyotype and/or chromosome morphology have been found, suggesting that the sex chromosomes [most likely chromosome 4 as identified in *Hymenochirus* sp. by Cauret *et al.* (2020)] are homomorphic. This is consistent with previous findings within the family Pipidae (Tymowska 1991).

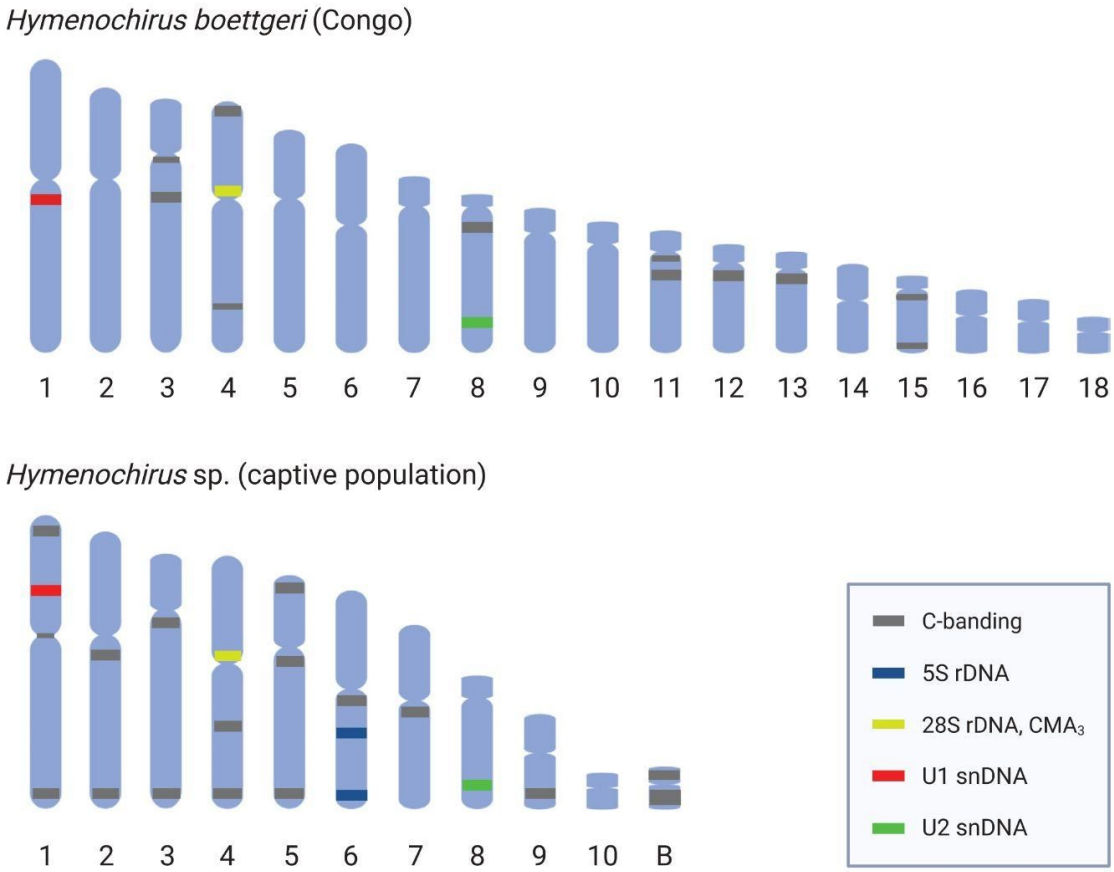

Figure 6. Schematic representation of the chromosomal location of the U1 (red) and U2 (green) snDNAs, 5S (dark blue) and 28S (yellow) rDNAs, and C-bands (dark grey) in *H. boettgeri* (Congo) and *Hymenochirus* sp. (captive population). The haploid A chromosome set of each species, 18 chromosomes in *H. boettgeri* and 10 chromosomes in *Hymenochirus* sp., is arranged in descending order of size. The B chromosome of *Hymenochirus* sp. is depicted separately from the A chromosomes and is entirely covered in grey, as revealed by C-banding. The 5S rDNA locus was not detected in *H. boettgeri* and is only depicted in the *Hymenochirus* sp. karyotype. Mapping of the U1 snDNA locus identified a pericentric inversion or copy number reduction/expansion visible on non-homologous regions of chromosome 1. Created with BioRender.com.

B chromosomes

B chromosomes, also known as accessory, supernumerary, or they may sometimes be referred to as microchromosomes, are often considered selfish or parasitic in nature. They are maintained in a cell through meiotic or mitotic drive, have a low gene content, and tend to have a high degree of heterochromatization and repetitive elements. In contrast to redundant traits, B chromosomes may be important for sex determination or protecting against parasites (reviewed in: Camacho *et al.* 2000, Johnson Pokorná and Reifová 2021). We were able to identify B chromosomes using C-banding, as the B chromosomes in *Hymenochirus* sp. are highly heterochromatized, as noted by Mezzasalma *et al.* (2015). An intensely highlighted B chromosome is visible in each nucleus, including nuclei where chromosomes are not fully condensed (data not shown). In amphibians, the number of B chromosomes can be stable (e.g. *Uraeotyphlus* Peters, 1880; see: Venu *et al.* 2021), or variable between different populations (e.g. *Leiopelma* Fitzinger, 1861;, see: Green 1991), or even variable between tissues within the same individual (e.g. *Dicamptodon* Strauch, 1870; see: Green 1991). In their study, Mezzasalma *et al.* (2015) found either the presence of a B chromosome or no B chromosome in various tissues of *Hymenochirus* sp. (previously referred to as '*H. boettgeri*'). We consistently found one B chromosome in all six individuals of both sexes (three males, three females) of *Hymenochirus* sp. However, we used only one source of somatic tissue—foot webbing. The variability in the presence/absence of B chromosomes in different tissues found by Mezzasalma *et al.* (2015) may be caused by uneven cell division of B chromosomes in some cells/tissues (Johnson Pokorná and Reifová 2021). During meiotic division, B chromosomes can be preferentially transferred to the germline (Camacho *et al.* 2000), but irregular chromosome pairing and nondisjunctions

can lead to polymorphisms, as found by Mezzasalma *et al.* (2015). The latter authors also discussed whether four of the 24 chromosomes found by Morescalchi (1968) in '*H. boettgeri*' could possibly represent B chromosomes. If this were true, then *Hymenochirus* sp. may contain a variable number of B chromosomes from zero to at least four, as can also be inferred from the uncommented brief report by Scheel (1973) on 2n = 22, where two chromosomes could potentially be B chromosomes. This hypothesis assumes that the material processed in the previous studies was conspecific with our *Hymenochirus* sp. However, another explanation may be that earlier studies (Morescalchi 1968, Scheel 1973) karyotyped (an)other species, as discussed above, and supernumerary chromosomes above the presumed ancestral number of 2n = 20 may or may not represent B chromosomes.

The preferred hypothesis for the evolutionary origin of B chromosomes is that they were derived from A chromosomes by rearrangements (Camacho *et al.* 2000). It is unclear whether B chromosomes are also present in other *Hymenochirus* species, but we have not detected them in tetraploid *H. boettgeri*. B chromosomes have not yet been identified in other genera of the family Pipidae. We attempted to reveal the origin of the B chromosome in *Hymenochirus* sp. using GISH analysis with a whole-genome painting probe from *H. boettgeri* hybridized on a chromosome spread of *Hymenochirus* sp. and vice versa. Neither B chromosome was painted by probe in any of the GISH experiments, including the control experiment with a conspecific whole-genome painting probe, which indicates that the *Hymenochirus* B chromosome may be highly stable during the denaturation process due to the high heterochromatin (shown by C-banding, Fig. 5C) and AT-specific (shown by DAPI in GISH, Fig. 5F) content and the low permeability of the B chromosome to the painting probe during hybridization. These characteristics make the *Hymenochirus* B chromosome unsuitable for painting *in situ* hybridization techniques. Other methodological approaches, such as high-throughput sequencing, may help to better study their evolution.

CONCLUSION

In this study, we demonstrate that the captive population of dwarf clawed frogs is best taxonomically named *Hymenochirus* sp. and not *H. boettgeri*, as is usually the case. We present for the first time the karyotype from a specimen with a known locality (NW Congo) that we identified as *H. boettgeri*. This species is tetraploid with 2n = 36, in contrast to diploid *Hymenochirus* sp. with 2n = 20 A chromosomes and one B chromosome according to our results. Based on several cytogenetic and molecular tools used, we hypothesize that the *H. boettgeri* karyotype evolved from a diploid ancestor with the original chromosome number 2n = 20 through fusion of two biarmed chromosomes and subsequent allotetraploidization resulting from hybridization of two diploid ancestors with 2n = 18. The scenario is similar to that proposed for the origin of tetraploid clawed frogs from the subgenus *Xenopus* (Evans *et al.* 2005, Session *et al.* 2016), and its probable relevance is supported by the recent finding of a karyotype with 2n = 18 with an identified fusion of two chromosomes in *Hymenochirus* sp. (Bredeson *et al.* 2021). Based on a comparison of the two *Hymenochirus* species and mapping of the U1 snDNA locus, we revealed that either pericentromeric inversion or reduction/expansion of U1 copies occurred on chromosome 1. In the captive population of *Hymenochirus* sp. we found the stable presence of a single B chromosome in both sexes, in contrast to the presence (one B chromosome) or absence found by Mezzasalma *et al.* (2015). Results of previous studies also indicate a possible higher number of B chromosomes in *Hymenochirus* (four or two; Morescalchi 1968, Scheel 1973). Further research is needed to assess patterns of variation in the number of A and B chromosomes among populations, individuals and/or tissues, as well as to better understand the (karyotype) evolution and taxonomy of the genus *Hymenochirus*.

SUPPLEMENTARY DATA

Supplementary data are available at *Zoological Journal of the Linnean Society* online.

ACKNOWLEDGEMENTS

We would like to thank the IRSEN (Brazzaville) authorities for issuing permits and logistical support, and Zdeňka Dittrichová (Brandýs nad Labem) for providing the material of *Hymenochirus* sp. We further thank M.-O. Rödel and F. Tillack (ZMB, Berlin) for providing access to the type specimen of *Hymenochirus boettgeri*, Matej Dolinay, Jérémy Thomas, and Alain S. Nzila for help in the field, and F. Snítilý for help in the laboratory.

ETHICS

Charles University has registered experimental breeding facilities for pipid frogs (16OZ12891/2018–17214, 37428/2019-MZE-18134). All experimental procedures involving frogs were approved by the Institutional Animal Care and Use Committee of Charles University, according to the directives from the State Veterinary Administration of the Czech Republic, reference number MSMT-20585/2022–4 issued by the Ministry of Education, Youth and Sport of the Czech Republic (M.K. is a manager of the experimental project on living *Xenopus* and *Hymenochirus* animals). M.K. and V.G. are holders of the certificate of professional competence to design experiments according to §15d(3) of the Czech Republic Act No. 246/1992 Coll., on the Protection of Animals against Cruelty (Registration numbers CZ 03973, CZ 02519), provided by the Ministry of Agriculture of the Czech Republic.

FUNDING

This study was supported by the P JAC project CZ.02.01.01/00/22_010/0002902 MSCA Fellowships CZ—UK, Ministry of Culture of the Czech Republic (DKRVO 2019–2023/6.VII.e, National Museum, 00023272), and the Czech Science Foundation (23-07331S). Open access publishing was supported by the National Technical Library in Prague.

CONFLICT OF INTEREST

The authors declare no conflict of interest.

DATA AVAILABILITY

All the data supporting the findings of this study are available within the article and its supplementary materials. DNA sequences are

deposited in GenBank (see Supporting Information, Table S1 for accession numbers).

REFERENCES

AmphibiaWeb. 2023. https://amphibiaweb.org. Berkeley, CA, USA: University of California (13 April 2023, date last accessed).

Arnoult J, Lamotte M. Les Pipidae de l'Ouest africain et du Cameroun. *Bulletin de l'Institut française d'Afrique Noire Série A* 1968;**30**:270–306.

Bewick AJ, Chain FJJ, Heled J *et al.* The pipid root. *Systematic Biology* 2012;**61**:913–26.

Bi K, Bogart JP. Identification of intergenomic recombinations in unisexual salamanders of the genus *Ambystoma* by genomic in situ hybridization (GISH). *Cytogenetic and Genome Research* 2006;**112**:307–12.

Bogart JP. Evolutionary implications of polyploidy in amphibians and reptiles. In: Lewis WH (ed.), *Polyploidy: Biological Relevance*. New York: Plenum Press, 1980, 341–78.

Bogart JP, Bi K. Genetic and genomic interactions of animals with different ploidy levels. *Cytogenetic and Genome Research* 2013;**140**:117–36.

Bredeson JV, Mudd AB, Medina-Ruiz S *et al.* Conserved chromatin and repetitive patterns reveal slow genome evolution in frogs. *bioRxiv* 2021:2021.10.18.464293.

Camacho JPM, Sharbel TF, Beukeboom LW. B-chromosome evolution. *Philosophical Transactions of the Royal Society of London, Series B: Biological Sciences* 2000;**355**:163–78.

Cauret CMS, Gansauge MT, Tupper AS *et al.* Developmental systems drift and the drivers of sex chromosome evolution. *Molecular Biology and Evolution* 2020;**37**:799–810.

Cecere DD. *Discrepancies in Observations of Hymenochirus boettgeri, Rabb vs. Sokol*, 1998. https://davidcecere.pipidae.org/discrepencies.htm (13 April 2023, date last accessed).

Channing A, Rödel MO. *Field Guide to the Frogs and Other Amphibians of Africa*. Cape Town, South Africa: Struik Nature, 2019.

Chernomor O, von Haeseler A, Minh BQ. Terrace aware data structure for phylogenomic inference from supermatrices. *Systematic Biology* 2016;**65**:997–1008.

Deichmann JL, Mulcahy DG, Vanthomme H *et al.* How many species and under what names? Using DNA barcoding and GenBank data for west Central African amphibian conservation. *PLoS One* 2017;**12**:e0187283.

Dubois A, Ohler A, Pyron RA. New concepts and methods for phylogenetic taxonomy and nomenclature in zoology, exemplified by a new ranked cladonomy of recent amphibians (Lissamphibia). *Megataxa* 2021;**5**:1–738.

Evans BJ, Kelley DB, Tinsley RC *et al.* A mitochondrial DNA phylogeny of African clawed frogs: phylogeography and implications for polyploid evolution. *Molecular Phylogenetics and Evolution* 2004;**33**:197–213.

Evans BJ, Kelley DB, Melnick DJ *et al.* Evolution of RAG-1 in polyploid clawed frogs. *Molecular Biology and Evolution* 2005;**22**:1193–207.

Feng YJ, Blackburn DC, Liang D *et al.* Phylogenomics reveals rapid, simultaneous diversification of three major clades of Gondwanan frogs at the Cretaceous–Paleogene boundary. *Proceedings of the National Academy of Sciences of the United States of America* 2017;**114**:E5864–70.

von Filek W. *Frösche im Aquarium*. Stuttgart: Franckh, 1967.

Fornaini NR, Bergelová B, Gvoždík V *et al.* Consequences of polyploidy and divergence as revealed by cytogenetic mapping of tandem repeats in African clawed frogs (*Xenopus*, Pipidae). *European Journal of Wildlife Research* 2023;**69**:81.

Frost DR. *Amphibian Species of the World: An Online Reference, v.6.1*, 2023. https://amphibiansoftheworld.amnh.org/index.php. New York, USA: American Museum of Natural History (13 April 2023, date last accessed).

Furman BLS, Cauret CMS, Knytl M *et al.* A frog with three sex chromosomes that co-mingle together in nature: *Xenopus tropicalis* has a degenerate W and a Y that evolved from a Z chromosome. *PLoS Genetics* 2020;**16**:e1009121.

Green DM. Supernumerary chromosomes in amphibians. In: Green DM, Sessions SK (eds), *Amphibian Cytogenetics and Evolution*. San Diego: Academic Press, 1991, 333–58.

Gvoždík V, Moravec J, Klütsch C *et al.* Phylogeography of the Middle Eastern tree frogs (*Hyla*, Hylidae, Amphibia) as inferred from nuclear and mitochondrial DNA variation, with a description of a new species. *Molecular Phylogenetics and Evolution* 2010;**55**:1146–66.

Hime PM, Lemmon AR, Moriarty Lemmon EC *et al.* Phylogenomics reveals ancient gene tree discordance in the amphibian tree of life. *Systematic Biology* 2021;**70**:49–66.

Höbel G, Fellows SR. Vocal repertoire and calling activity of a dwarf clawed frog (*Hymenochirus boettgeri*). *Herpetological Review* 2016;**47**:543–9.

Jackson K, Beier M. *Hymenochirus curtipes*: geographic distribution (Republic of Congo). *Herpetological Review* 2006;**37**:488.

Jackson K, Zassi-Boulou AG, Mavoungou LB *et al.* Amphibians and reptiles of the Lac Télé Community reserve, Likouala region, Republic of Congo (Brazzaville). *Herpetological Conservation and Biology* 2007;**2**:75–86.

Johnson Pokorná M, Reifová R. Evolution of B chromosomes: from dispensable parasitic chromosomes to essential genomic players. *Frontiers in Genetics* 2021;**12**:1–11.

Kalous L, Knytl M. Karyotype diversity of the offspring resulting from reproduction experiment between diploid male and triploid female of silver Prussian carp, *Carassius gibelio* (Cyprinidae, Actinopterygii). *Folia Zoologica* 2011;**60**:115–21.

Kalyaanamoorthy S, Minh BQ, Wong TKF *et al.* ModelFinder: fast model selection for accurate phylogenetic estimates. *Nature Methods* 2017;**14**:587–9.

Katoh K, Standley DM. MAFFT Multiple sequence alignment software v.7: improvements in performance and usability. *Molecular Biology and Evolution* 2013;**30**:772–80.

King M. *Animal Cytogenetics, Chordata 2. Amphibia* (Bernard J, Kayano H, Levan A, eds), Stuttgart, Germany: Schweizerbart Science Publishers, 1990.

Knytl M, Fornaini NR. Measurement of chromosomal arms and FISH reveal complex genome architecture and standardized karyotype of model fish, genus *Carassius*. *Cells* 2021;**10**:2343.

Knytl M, Kalous L, Symonová R *et al.* Chromosome studies of European cyprinid fishes: cross-species painting reveals natural allotetraploid origin of a *Carassius* female with 206 chromosomes. *Cytogenetic and Genome Research* 2013;**139**:276–83.

Knytl M, Smolík O, Kubíčková S *et al.* Chromosome divergence during evolution of the tetraploid clawed frogs, *Xenopus mellotropicalis* and *Xenopus epitropicalis* as revealed by Zoo-FISH. *PLoS One* 2017;**12**:e0177087.

Knytl M, Tlapakova T, Vankova T *et al. Silurana* chromosomal evolution: a new piece to the puzzle. *Cytogenetic and Genome Research* 2018;**156**:223–8.

Knytl M, Forsythe A, Kalous L. A fish of multiple faces, which show us enigmatic and incredible phenomena in nature: biology and cytogenetics of the genus *Carassius*. *International Journal of Molecular Sciences* 2022;**23**:8095.

Knytl M, Fornaini NR, Bergelová B*et al.* Divergent subgenome evolution in the allotetraploid frog *Xenopus calcaratus*. *Gene* 2023;**851**:146974.

Krylov V, Kubickova S, Rubes J *et al.* Preparation of *Xenopus tropicalis* whole chromosome painting probes using laser microdissection and reconstruction of *X. laevis* tetraploid karyotype by Zoo-FISH. *Chromosome Research* 2010;**18**:431–9.

Kunz K. Über einige Fehlbestimmungen von Zwergkrallenfröschen der Gattung *Hymenochirus* in der Literatur. *Reptilia* 2002;**7**:73–7.

Kunz K. *Krallenfrösche, Zwergkrallenfrösche, Wabenkröten—Pipidae in Natur und Menschenhand*. Münster: Natur und Tier, 2003.

Kunz K. *Der Zwergkrallenfrosch Hymenochirus boettgeri*. Münster: Natur und Tier, 2004.

Levan A, Fredga K, Sandberg AA. Nomenclature for centromeric position on chromosomes. *Hereditas* 1964;**52**:201–20.

Liedtke HC, Gower DJ, Wilkinson M *et al.* Macroevolutionary shift in the size of amphibian genomes and the role of life history and climate. *Nature Ecology and Evolution* 2018;**2**:1792–9.

Mezzasalma M, Glaw F, Odierna G *et al.* Karyological analyses of *Pseudhymenochirus merlini* and *Hymenochirus boettgeri* provide new insights into the chromosome evolution in the anuran family

Pipidae. *Zoologischer Anzeiger—A Journal of Comparative Zoology* 2015;**258**:47–53.
Mezzasalma M, Brunelli E, Odierna G *et al.* Evolutionary and genomic diversity of true polyploidy in tetrapods. *Animals* 2023;**13**:1033.
Miller KE, Session AM, Heald R. Kif2a scales meiotic spindle size in *Hymenochirus boettgeri*. *Current Biology* 2019;**29**:3720–7.e5.
Minh BQ, Schmidt HA, Chernomor O *et al.* IQ-TREE 2: new models and efficient methods for phylogenetic inference in the genomic era. *Molecular Biology and Evolution* 2020;**37**:1530–4.
Morescalchi A. I cromosomi di alcuni Pipidae (Amphibia Salientia). *Experientia* 1968;**24**:81–2.
Morescalchi A. Karyology of the main groups of African frogs. *Monitore Zoologico Italiano Supplemento* 1981;**15**:41–53.
Noble GK. Contributions to the herpetology of the Belgian Congo based on the collection of the American Museum Congo Expedition, 1909-1915. Part III. Amphibia. *Bulletin of the American Museum of Natural History* 1924;**49**:147–347.
Olsson R, Österdahl L. Aquarium behaviour and breeding of *Hymenochirus*. *Nature* 1960;**188**:869.
Palumbi S, Martin A, Romano S *et al. The Simple Fool's Guide to PCR, v.2.0.* Honolulu: University of Hawaii, 1991.
Perret JL. Les amphibiens du Cameroun. *Zoologische Jahrbücher. Abteilung für Systematik, Ökologie und Geographie* 1966;**93**:289–464.
Pramuk JB. Phylogeny of South American *Bufo* (Anura: Bufonidae) inferred from combined evidence. *Zoological Journal of the Linnean Society* 2006;**146**:407–52.
Rabb GB, Rabb MS. On the behavior and breeding biology of the African pipid frog *Hymenochirus boettgeri*. *Zeitschrift für Tierpsychologie* 1963;**20**:215–41.
Rábová M, Völker M, Pelikánová Š *et al.* Sequential chromosome banding in fishes. In: Ozouf-Costaz C, Pisano E, Foresti F, de Almeida Toledo LF (eds), *Fish Cytogenetic Techniques*. Boca Raton: CRC Press, 2015, 102–12.
Roco AS, Olmstead AW, Degitz SJ *et al.* Coexistence of Y, W, and Z sex chromosomes in *Xenopus tropicalis*. *Proceedings of the National Academy of Sciences* 2015;**112**:E4752–61.
Scheel JJ. The chromosomes of some African anuran species. In: Schröder JH (ed.), *Genetics and Mutagenesis of Fish*. Berlin, Heidelberg: Springer, 1973, 113–6.
Schmid M, Evans BJ, Bogart JP. Polyploidy in Amphibia. *Cytogenetic and Genome Research* 2015;**145**:315–30.
Schneider CA, Rasband WS, Eliceiri KW. NIH Image to ImageJ: 25 years of image analysis. *Nature Methods* 2012;**9**:671–5.
Seroussi E, Knytl M, Pitel F *et al.* Avian expression patterns and genomic mapping implicate leptin in digestion and TNF immunity, suggesting that their interacting adipokine role has been acquired only in mammals. *International Journal of Molecular Sciences* 2019;**20**:4489.
Session AM, Uno Y, Kwon T *et al.* Genome evolution in the allotetraploid frog *Xenopus laevis*. *Nature* 2016;**538**:336–43.
Sokol OM. Studien an pipiden Fröschen. I. Die Kaulquappe von *Hymenochirus curtipes* Noble. *Zoologischer Anzeiger* 1959;**162**:154–60.
Sokol OM. The tadpole of *Hymenochirus boettgeri*. *Copeia* 1962;**1962**:272.
Sokol OM. Feeding in the pipid frog *Hymenochirus boettgeri* (Tornier). *Herpetologica* 1969;**25**:9–24.
Song XY, Furman BLS, Premachandra T *et al.* Sex chromosome degeneration, turnover, and sex-biased expression of sex-linked transcripts in African clawed frogs (*Xenopus*). *Philosophical Transactions of the Royal Society B: Biological Sciences* 2021;**376**:20200095.
Tymowska J. Polyploidy and cytogenetic variation in frogs of the genus *Xenopus*. In: Green DM, Sessions SK (eds), *Amphibian Cytogenetics and Evolution*. San Diego: Academic Press, 1991, 259–97.
Vences M, Thomas M, van der Meijden A *et al.* Comparative performance of the 16S rRNA gene in DNA barcoding of amphibians. *Frontiers in Zoology* 2005;**2**:5.
Vences M, Nagy ZT, Sonet G *et al.* DNA barcoding amphibians and reptiles. In: Kress WJ, Erickson DL (eds), *DNA Barcodes: Methods and Protocols, Methods in Molecular Biology*, Vol. **858**. Totowa: Humana Press, 2012, 79–107.
Venu G, Rajendran A, Raju NG *et al.* First report of B chromosomes in caecilians (Amphibia: Gymnophiona). *Ichthyology and Herpetology* 2021;**109**:443–8.
Völker M, Kullmann H. Sequential chromosome banding from single acetic acid fixed embryos of *Chromaphyosemion* killifishes (Cyprinodontiformes, Nothobranchiidae). *Cybium* 2006;**30**:171–6.
Völker M, Sonnenberg R, Ráb P *et al.* Karyotype differentiation in *Chromaphyosemion* killifishes (Cyprinodontiformes, Nothobranchiidae). II: cytogenetic and mitochondrial DNA analyses demonstrate karyotype differentiation and its evolutionary direction in *C. riggenbachi*. *Cytogenetic and Genome Research* 2006;**115**:70–83.
de Witte G. Liste des batraciens du Congo Belge (collection du Musée du Congo Belge à Tervuren). Première partie. *Revue Zoologie et de Botanique Africaines* 1930;**19**:232–74.

Zoological Journal of the Linnean Society

Supporting Information

Tetraploidy in the Boettger's dwarf clawed frog (Pipidae: *Hymenochirus boettgeri*) from the Congo indicates non-conspecificity with the captive population

Václav GVOŽDÍK[‡,*], Martin KNYTL[‡,*], Ange-Ghislain ZASSI-BOULOU, Nicola R. FORNAINI, Barbora BERGELOVÁ

[‡]V. Gvoždík and M. Knytl are co-first and co-senior authors in alphabetical order.

*Corresponding authors. E-mail: vaclav.gvozdik@gmail.com (V. Gvoždík), martin.knytl@natur.cuni.cz (M. Knytl)

CONTENT **Page**

Table S1. Material used in cytogenetic and molecular analyses.

Species (updated identification)	*16S* GenBank	*rag1* GenBank	Specimen	Origin	Reference	Original identification	Remark
Hymenochirus boettgeri	OR360735	OR352008	IVB-H-CG17-356	Congo, Mindjong (Mbemba)	This study	-	Male, karyotyped
H. boettgeri	KY080144		USNM 584175	Congo, Simombondo	Deichmann *et al.* (2017)	*Hymenochirus* sp.	
H. boettgeri		KX208746	CAS 249965	Cameroon, Ndombam	Feng *et al.* (2017)	*Hymenochirus* sp. / *H. boettgeri*	
H. curtipes	KY080139		USNM 576617	Congo, Impongui	Deichmann *et al.* (2017)	*H. curtipes*	
H. curtipes	KY080140		USNM 576620	Congo, Impongui	Deichmann *et al.* (2017)	*H. curtipes*	
H. curtipes	KY080141		USNM 576618	Congo, Impongui	Deichmann *et al.* (2017)	*H. curtipes*	
H. curtipes	KY080142		USNM 563881	Congo, Ganganya Brousse	Deichmann *et al.* (2017)	*H. curtipes*	Jackson & Beier (2006)
H. curtipes	KY080143		USNM 576619	Congo, Impongui	Deichmann *et al.* (2017)	*H. curtipes*	
Hymenochirus sp.	OR360736*	OR352009*	IVB-H-Hsp01	Laboratory/Pet trade	This study	-	Male, karyotyped
Hymenochirus sp.	OR360736*	OR352009*	IVB-H-Hsp02	Laboratory/Pet trade	This study	-	Male, karyotyped
Hymenochirus sp.	OR360736*	OR352009*	IVB-H-Hsp03	Laboratory/Pet trade	This study	-	Male, karyotyped
Hymenochirus sp.	OR360736*	OR352009*	IVB-H-Hsp04	Laboratory/Pet trade	This study	-	Female, karyotyped
Hymenochirus sp.	OR360736*	OR352009*	IVB-H-Hsp05	Laboratory/Pet trade	This study	-	Female, karyotyped
Hymenochirus sp.	OR360736*	OR352009*	IVB-H-Hsp06/DNA	Laboratory/Pet trade	This study	-	Female, karyotyped
Hymenochirus sp.	AY341726		?	Laboratory/Pet trade	Vences *et al.* (2003)	*H. boettgeri*	
Hymenochirus sp.	AY523756	AY523735	VUB 0092	Laboratory/Pet trade	Roelants & Bossuyt (2005)	*H. boettgeri*	
Hymenochirus sp.		AY583340	?	Laboratory/Pet trade	San Mauro *et al.* (2005)	*H. boettgeri*	
Hymenochirus sp.	AY581623		Isolate BJE-2004	Laboratory/Pet trade	Evans *et al.* (2004)	*Hymenochirus* sp.	
Hymenochirus sp.		AY874305	Isolate BJE-2004‡	Laboratory/Pet trade	Evans *et al.* (2005) / Bewick *et al.* (2012)	*Hymenochirus* sp. / *H. curtipes*	
Hymenochirus sp.	HM991331		MNCN/ADN 28465	Laboratory/Pet trade	Irisarri *et al.* (2011)	*H. boettgeri*	
Hymenochirus sp.	MK907573		Isolate BJE3814	Laboratory/Pet trade	Cauret *et al.* (2020)	*H. boettgeri*	
Hymenochirus sp.		JQ073272	ZCMV 12658	Laboratory/Pet trade	Crottini *et al.* (2012)	*H. boettgeri*	
Hymenochirus sp.		CM033476†	Isolate Female2	Laboratory/Pet trade	Bredeson *et al.* (2021)	*H. boettgeri*	
Pseudhymenochirus merlini	HM991333	HM998975	MNCN/ADN 28467	Guinea Bissau	Irisarri *et al.* (2011)	-	Outgroup
Xenopus (*Silurana*) *tropicalis*	MN259067		Isolate R7931_AMNH17274	Sierra Leone	Evans *et al.* (2019)	-	Outgroup
X. (*S.*) *tropicalis*		AY874306	MHNG 2644.55	Sierra Leone	Evans *et al.* (2005)	-	Outgroup

* The same haplotype in all individuals within a genetic marker (*16S*, *rag1*).
‡ The voucher specimen is erroneously identified as KU 205801 in GenBank, but this represents a specimen of *Pipa pipa* (B.J. Evans, pers. comm., 7 August 2023).
† *rag1* extracted from the assembly of chromosome 8_10 (Bredeson *et al.*, 2021), genome UCB_Hboe_1.0 (University of California, Berkeley, 2021, GenBank: GCA_019447015.1).

1

Table S2. Markers used in FISH analysis, amplified gDNA templates, GenBank accession numbers, lengths, PCR primer sequences, and references to studies in which the primers were designed. The *U1* snDNA amplicon was used from Fornaini *et al.* (2023).

Gene Symbol	Gene Name	gDNA Template	Accession No.	Length (bp)	Primer Sequence	Reference
5S rRNA	5S ribosomal RNA	*Xenopus* (*Silurana*) *tropicalis*	OR360596	251	XTR 5S F: 5′-CAGGGTGGTATGGCCGTAGG-3′ XTR 5S R: 5′-AGCGCCCGATCTCGTCTGAT-3′	Knytl & Fornaini (2021)
28S rRNA	28S ribosomal RNA	*Hymenochirus* sp.	OR389490	290	28SA: 5′-AAACTGTGGTGGAGGTCCGT-3′ 28SB: 5′-CTTACCAAAAGTGGCCCACTA-3′	Naito *et al.* (1992)
U1 snRNA	U1 small nuclear RNA	*X.* (*S.*) *tropicalis*	OQ714817	119	U1F: 5′-GCAGTCGAGATTCCCACATT-3′ U1R: 5′-CTTACCTGGCAGGGGAGATA-3′	Silva *et al.* (2015)
U2 snRNA	U2 small nuclear RNA	*Hymenochirus boettgeri*	OR359290	177	U2F: 5′-ATCGCTTCTCGGCCTTATG-3′ U2R: 5′-TCCCGGCGGTACTGCAATA-3′	Bueno *et al.* (2013)

2

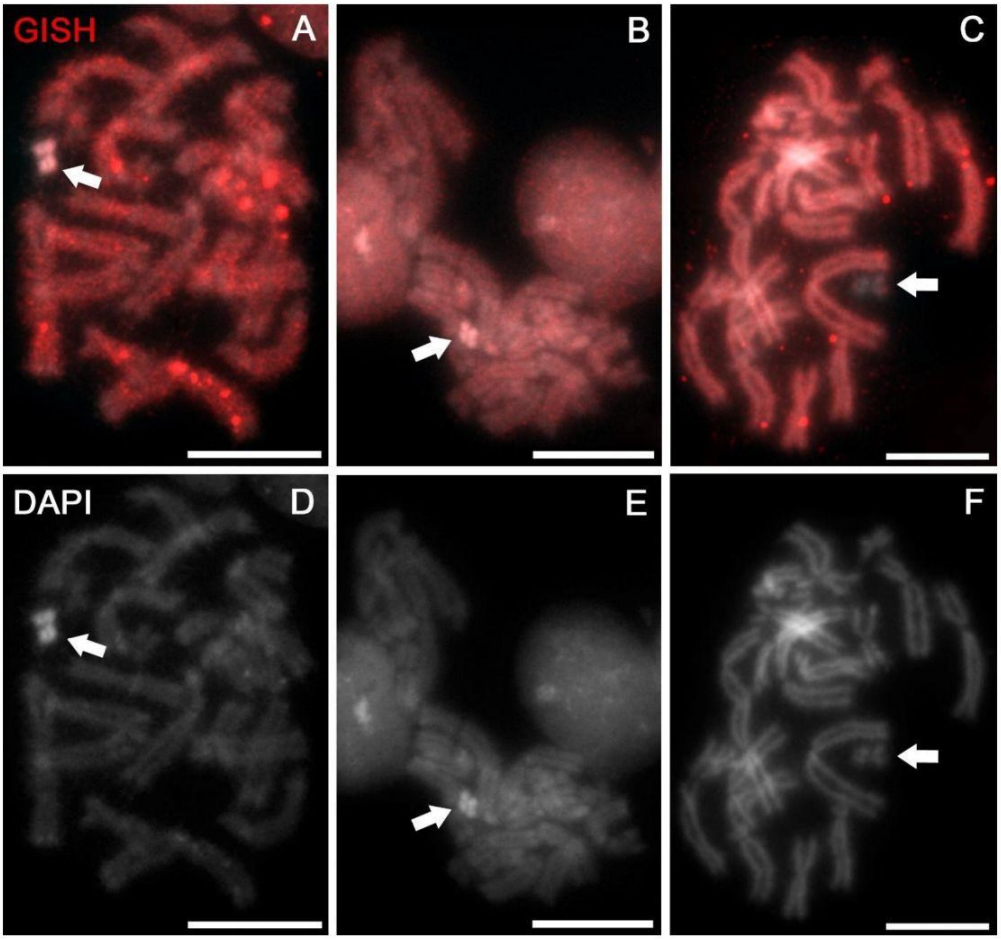

Figure S1. Genomic in situ hybridization (GISH) on *Hymenochirus* sp. (IVB-H-Hsp06) metaphase spreads. (A) The *H. boettgeri* whole genome painting (WGP) probe and *H. boettgeri* competitor DNA hybridize on all *Hymenochirus* sp. chromosomes (red) except one – the B chromosome shows no GISH signal (arrow). This is an identical figure as Fig. 5F. (B) Control GISH with the *Hymenochirus* sp. WGP probe and *Hymenochirus* sp. competitor DNA hybridized on all *Hymenochirus* sp. chromosomes (red) except one – the B chromosome shows no GISH signal (arrow). (C) Control GISH with the *Hymenochirus* sp. WGP probe without competitor DNA hybridized on all *Hymenochirus* sp. chromosomes (red) except one – the B chromosome shows no GISH signal (arrow). (D–F) DAPI channel (B&W) shows intensely painted B chromosomes (D, E, arrows) but no DAPI signal was found in the GISH experiment in which no competitor DNA was used (F, arrow). Scale bars represent 10 μm.

ADDITIONAL REFERENCES

Bueno D, Palacios-Gimenez OM, Cabral-de-Mello DC. 2013. Chromosomal mapping of repetitive DNAs in the grasshopper *Abracris flavolineata* reveal possible ancestry of the B chromosome and H3 histone spreading. *PLoS ONE* 8: e66532.

Crottini A, Madsen O, Poux C, Strauß A, Vieites DR, Vences M. 2012. Vertebrate time-tree elucidates the biogeographic pattern of a major biotic change around the K-T boundary in Madagascar. *Proceedings of the National Academy of Sciences of the United States of America* 109: 5358–5363.

Evans BJ, Gansauge M-T, Stanley EL, Furman BLS, Cauret CMS, Ofori-Boateng C, Gvoždík V, Streicher JW, Greenbaum E, Tinsley RC, Meyer M, Blackburn DC. 2019. *Xenopus fraseri*: Mr. Fraser, where did your frog come from? *PLoS ONE* 14: e0220892.

Irisarri I, Vences M, San Mauro D, Glaw F, Zardoya R. 2011. Reversal to air-driven sound production revealed by a molecular phylogeny of tongueless frogs, family Pipidae. *BMC Evolutionary Biology* 11: 114.

Naito E, Dewa K, Ymanouchi,H, Kominami R. 1992. Ribosomal ribonucleic acid (rRNA) gene typing for species identification. *Journal of Forensic Sciences* 37: 396–403.

Roelants K, Bossuyt F. 2005. Archaeobatrachian paraphyly and Pangaean diversification of crown-group frogs. *Systematic Biology* 54: 111–126.

San Mauro D, Vences M, Alcobendas M, Zardoya R, Meyer A. 2005. Initial diversification of living amphibians predated the breakup of Pangaea. *The American Naturalist* 165: 590–599.

Silva DMZA, Utsunomia R, Pansonato-Alves JC, Oliveira C, Foresti F. 2015. Chromosomal mapping of repetitive DNA sequences in five species of *Astyanax* (Characiformes, Characidae) reveals independent location of U1 and U2 snRNA sites and association of U1 snRNA and 5S rDNA. *Cytogenetic and Genome Research* 146: 144–152.

Vences M, Vieites DR, Glaw F, Brinkmann H, Kosuch J, Veith M, Meyer A. 2003. Multiple overseas dispersal in amphibians. *Proceedings of the Royal Society of London B: Biological Sciences* 270: 2435–2442.

Paper 5: **Cytogenetic Analysis of the Fish Genus Carassius Indicates Divergence, Fission, and Segmental Duplication as Drivers of Tandem Repeat and Microchromosome Evolution**

GBE

Cytogenetic Analysis of the Fish Genus *Carassius* Indicates Divergence, Fission, and Segmental Duplication as Drivers of Tandem Repeat and Microchromosome Evolution

Nicola R. Fornaini[1], Halina Černohorská[2], Lívia do Vale Martins[3], and Martin Knytl [1,4,*]

[1]Department of Cell Biology, Faculty of Science, Charles University, Prague 12843, Czech Republic
[2]Genetics and Reproductive Biotechnologies, CEITEC—Veterinary Research Institute, Brno 62100, Czech Republic
[3]Department of Biology, Federal University of Piauí, Floriano, Piauí, Brazil
[4]Department of Biology, McMaster University, Hamilton, Ontario L8S4K1, Canada

*Corresponding author: E-mail: martin.knytl@natur.cuni.cz.

Accepted: February 03, 2024

Abstract

Fishes of the genus *Carassius* are useful experimental vertebrate models for the study of evolutionary biology and cytogenetics. *Carassius* demonstrates diverse biological characteristics, such as variation in ploidy levels and chromosome numbers, and presence of microchromosomes. Those *Carassius* polyploids with ≥150 chromosomes have microchromosomes, but the origin of microchromosomes, especially in European populations, is unknown. We used cytogenetics to study evolution of tandem repeats (U1 and U2 small nuclear DNAs and H3 histone) and microchromosomes in *Carassius* from the Czech Republic. We tested the hypotheses whether the number of tandem repeats was affected by polyploidization or divergence between species and what mechanism drives evolution of microchromosomes. Tandem repeats were found in tetraploid and hexaploid *Carassius gibelio*, and tetraploid *Carassius auratus* and *Carassius carassius* in conserved numbers, with the exception of U1 small nuclear DNA in *C. auratus*. This conservation indicates reduction and/or loss in the number of copies per locus in hexaploids and may have occurred by divergence rather than polyploidization. To study the evolution of microchromosomes, we used the whole microchromosome painting probe from hexaploid *C. gibelio* and hybridized it to tetraploid and hexaploid *C. gibelio*, and tetraploid *C. auratus* and *C. carassius*. Our results revealed variation in the number of microchromosomes in hexaploids and indicated that the evolution of the *Carassius* karyotype is governed by macrochromosome fissions followed by segmental duplication in pericentromeric areas. These are potential mechanisms responsible for the presence of microchromosomes in *Carassius* hexaploids. Differential efficacy of one or both of these mechanisms in different tetraploids could ensure variability in chromosome number in polyploids in general.

Key words: teleost fish, polyploidy, U1 and U2 snDNAs, histone H3, chromosome painting, FISH.

Significance

Fish of the genus *Carassius* (Teleostei: Cyprinidae) are very popular models for studying genome and karyotype evolution, but there is a large gap in knowledge of microchromosome evolution and non-nucleolar tandemly repeated sequences at the level of experimental multispecies comparative studies. Based on cytogenetic investigation of closely related species with different ploidies, we propose three major processes that drive the evolution of microchromosomes and tandem arrays—divergence, fission, and post-polyploidization segmental duplication. All three drivers have a crucial impact on the evolution of *Carassius* and may trigger diversification into a plethora of individual extant species in the world.

Introduction

In the fish family Cyprinidae (Cypriniformes, Teleostei), several independent polyploidization events (multiplications of haploid set of chromosomes) have occurred, giving rise to species with a large diversity of ploidy levels (Cherfas 1966). Ancestral number of chromosomes for the entire group of cyprinids (cyprinids, cyprinid group = the whole family Cyprinidae) is estimated to be 50 (Winfield and Nelson 2012).

Within Cyprinidae, the paleotetraploid clade Cyprinini (sensu Yang et al. 2010) includes the *Carassius* and *Cyprinus* genera, both of which have 100 chromosomes and solely *Carassius* has ~150 and ~200 chromosomes. It is clear that at least three polyploidization events occurred in this genus (since the independent evolution of the clade Cyprinini). The first polyploidization occurred in the common ancestor of Cyprinini and resulted in a chromosome number equal to 100 (Yang et al. 2010). The second polypolyploidization gave rise to the chromosome number ~150 and the third to ~200. Species from the clade Cyprinini that have 100 chromosomes are considered evolutionary tetraploids because of the most recent diploid ancestor did have 50 chromosomes (Ohno et al. 1967). In terms of biological development, these evolutionary tetraploids produce reduced gametes with 50 chromosomes that fuse during fertilization and the offspring continues to develop with recombinant and restored unreduced genetic information. The karyotype formula of a diploid member of Cyprinini shows biological and evolutionary ploidy by means of $2n = 4x$, where n defines the number of chromosomes in a gamete of the extant species (biological ploidy), and x refers to the number of chromosomes in a gamete of the most recent diploid ancestor of the extant species (evolutionary ploidy) (Knytl et al. 2017). In the following text, ploidy levels will be referred to the evolutionary term of ploidy, i.e. tetraploid, hexaploid, and octoploid *Carassius* are those with 100, ~150, and ~200 chromosomes, respectively.

Carassius is the most commonly used Cyprinini model for biological research (e.g. Pang et al. 2017; Ağdamar et al. 2020; Khosravi et al. 2022; Pavlov 2022a, 2022b; Tapkir et al. 2022; Wang et al. 2022a; Fedorčák et al. 2023; Jan et al. 2023; Tapkir et al. 2023). Its exceptional diversity of skills represents possible biological phenomena such as the presence of three ploidy levels—tetraploid, hexaploid, and octoploid (Kalous and Knytl 2011; Xiao et al. 2011; Knytl et al. 2022). The alternation of sexual and asexual (gynogenetic) mode of reproduction (Cherfas 1966; Przybył et al. 2020; Fuad et al. 2021) gives *Carassius* a competitive advantage in the rate of spatial expansion of asexuals. In addition, sexual reproduction should ensure higher resistance to parasites than gynogenesis due to recombination processes (Hakoyama et al. 2001). Another biological phenomena is sex determination, which in *Carassius* is governed by sex determining genes (Wen et al. 2020) and environmental temperature (Li et al. 2018). Variation in the number of chromosomes in *Carassius* polyploids (biologically speaking, individuals who possess ≥150 chromosomes) was revealed as another exceptional trait and may be caused by male genetic contribution into the egg/embryo (i.e. paternal leakage) during gynogenesis, leading to the presence of different numbers of microchromosomes in karyotypes (Yi et al. 2003; Ding et al. 2021). Macrochromosomes are larger than microchromosomes and possess clearly visible centromere, chromatids, and telomeres at both ends (Nanda and Schmid 1994).

Microchromosomes were originally thought to be redundant components of genomes, but have been found to be gene-rich and low in the content of the repetitive fraction (International Chicken Genome Sequencing Consortium 2004). In birds they occur in relatively high numbers (30–40 pairs) and their numbers are extremely conserved across various species (Waters et al. 2021; de Souza et al. 2023). However, this is not the case for *Carassius*. In *Carassius*, the number of microchromosomes ranges between 6 (Zhou and Gui 2002; Knytl et al. 2013b, 2018) and 18 (Zhao et al. 2021). There are only a few studies focusing on microchromosome painting, which usually crossed two strains of *Carassius* and analyzed their artificial offspring (Li et al. 2016, 2018; Zhao et al. 2021). The effect of paternal leakage in artificial *Carassius* progeny was evidenced by inseminating the *Carassius* egg with heterologous (i.e. from a species other than maternal one) sperm. The newly arisen offspring contained microchromosomes in karyotypes unlike the maternal karyotype, which did not contain them (Yi et al. 2003).

In the Czech Republic, *Carassius* is represented by four species. Commonly occurring invasive *Carassius gibelio* consists of tetraploid, hexaploid, and octoploid ploidy levels (Lusk et al. 2010; Knytl et al. 2013b). *Carassius auratus*, very well-known due to its colorful varieties as goldfish. This species also forms tetraploids, hexaploids, and octoploids (Xiao et al. 2011; Rylková et al. 2013). The third species, *Carassius carassius*, native to the Czech Republic, has been considered critically endangered since 2017 (Chobot and Němec 2017) and is strictly tetraploid (Knytl et al. 2013a). The fourth, *Carassius langsdorfii*, was discovered in the Czech Republic in 2007 by Kalous et al. (2007). The discovered female was hexaploid, but no cytogenetic examination other than conventional Giemsa staining has been conducted. Additionally, several *Carassius* hybrids were identified in natural Czech waters (Papoušek et al. 2008; Knytl et al. 2013b, 2018).

Due to the very complex characteristics and possible cryptic hybridization between *Carassius* species, it is difficult to reveal the origin of polyploids in the sense of allopolyploidy (more ancestors) or autopolyploidy (single ancestral species). Nevertheless, mixed allo- and autopolyploid origin was revealed and subgenomes were identified in hexaploid

C. gibelio by whole genome sequencing (Kuhl et al. 2022). Subgenomes are genomic units that originate from lower ploidy ancestors. Genome of hexaploid *C. gibelio* consists of three subgenomes (Kuhl et al. 2022; Wang et al. 2022b). It is clear that hybridization and an allopolyploid event caused changes in the number of chromosomes and microchromosomes, but the origin and function of the microchromosomes in *Carassius* remain obscure, as well as the number and localization of the U1 and U2 loci of small nuclear DNA (snDNA) and/or histone H3, which represent the repetitive fraction of a genome by tandemly repeated arrays and are not associated with nucleolus (Huang and Spector 1992), hereafter referred to as (non-nucleolar) tandem repeats.

We used *Carassius* from natural waters of the Czech Republic to study inter-ploidy relationships within a species and between multiple species, specifically tetraploid and hexaploid *C. gibelio*, and tetraploid *C. auratus* and *C. carassius*. We used fluorescent in situ hybridization (FISH) to map U1 and U2 snDNAs and H3 histone in tetraploids and hexaploids. Moreover, we used painting FISH to map microchromosomes in hexaploids and genomic regions associated with microchromosomes in tetraploids. We addressed to answer the following questions: (i) Do interspecific *Carassius* tetraploids share the same number of non-nucleolar tandem repeats examined? (ii) Do hexaploid females have one and a half times higher proportion of these tandem repeat loci than tetraploids? (iii) Are there any differences in the number and position of FISH signals for microchromosomes in hexaploids? (iv) What are the possible origins of microchromosomes and the evolutionary forces behind their evolution? Here, we consider the distribution of tandem repeats and microchromosomes in *Carassius* tetraploid and hexaploid karyotypes in an evolutionary context.

Results

FISH with Repetitive DNA Probes

We hybridized *C. gibelio* U1, U2, and H3 probes in four different groups: tetraploid ($2n = 4x = 100$) and hexaploid ($3n = 6n = 157$) *C. gibelio*, tetraploid *C. auratus* ($2n = 4x = 100$), and tetraploid *C. carassius* ($2n = 4x = 100$) (Fig. 1). Evolutionary relationships among the *Carassius* species examined are shown in the phylogenetic tree with *Cyprinus carpio* as an outgroup. *Carassius gibelio* and *C. auratus* form a single mitochondrial clade, while *C. carassius* is more distant to the others. FISH using U1 and U2 probes showed two signals (on one homologous pair) for each gene, except for the U1 gene in *C. auratus*, which showed four clear signals, while two signals for the U2 gene are consistent with the other species. FISH using H3 probe showed four signals in each species. The same number of loci did not support the expectation that hexaploid *C. gibelio* should have one and a half as many snDNA loci as tetraploid *C. gibelio*. These results indicate a copy number reduction or loss of the entire U1, U2, and H3 loci in a subgenome (after polyploidization). The variation in the number of FISH signals in individuals with the same ploidy level and the chromosome number may be explained by a variation in the copy numbers of tandem repeats per locus, which is explained in detail in section "snDNA Tandem Repeats".

Intra-ploidy Painting FISH with Whole Microchromosome Painting Probe

Microchromosomes selected for microdissection and subsequent FISH procedure were identified based on the following criteria: they are tiny, have an unclear centromere position and indistinguishable chromatids, and may be unpaired in a karyotype.

The first painting FISH experiment was conspecific (*C. gibelio* probe against *C. gibelio* metaphases) and within individuals with the same ploidy level (hexaploid probe against hexaploid metaphases), referred to as intra-ploidy conspecific painting FISH. We conducted these experiments as a control to see if the whole microchromosome painting probe worked well, and also to see if the number of microchromosomes differed among *Carassius* populations. We used *Carassius* chromosomes from three different river basins in the Czech Republic. Conspecific painting FISH revealed variation in the number of microchromosomes, which ranged from six to nine (Fig. 2).

Five investigated females possessed 150 (Odra River basin, Fig. 2A), 149, 150 (both Elbe River basin, Fig. 2B, C), 150 (Mrlina River basin, Fig. 2D), and 153 (Elbe River basin, Fig. 2E) chromosomes with 6, 6, 7, 8, and 9 microchromosomes, respectively. *Carassius* used to generate the whole chromosome painting probe originated from the Odra River basin. The variation in the number of microchromosomes was consistent with previous studies (Zhou and Gui 2002; Knytl et al. 2013b; Li et al. 2016; Knytl et al. 2018; Li et al. 2018). The FISH signal was consistently spread over the entire surface of the microchromosomes, indicating the high efficacy of the FISH technique conducted. The presence of clearly highlighted chromosomes indicates that the probe and competitor DNA collaborated properly and that nonspecific hybridization of the probe to repetitive regions was inhibited. The *Carassius* microchromosomes did not show a high degree of heterochromatization, as is typical for B chromosomes, which are sometimes considered to be microchromosomes (Bishani et al. 2021; Gvoždík et al. 2023). Our finding is consistent with a high gene content and a low proportion of a repetitive fraction within the microchromosomes.

Inter-ploidy Painting FISH with Whole Microchromosome Painting Probe

The other aim of the study was to trace the origin of microchromosomes using tetraploid *Carassius* relatives and to

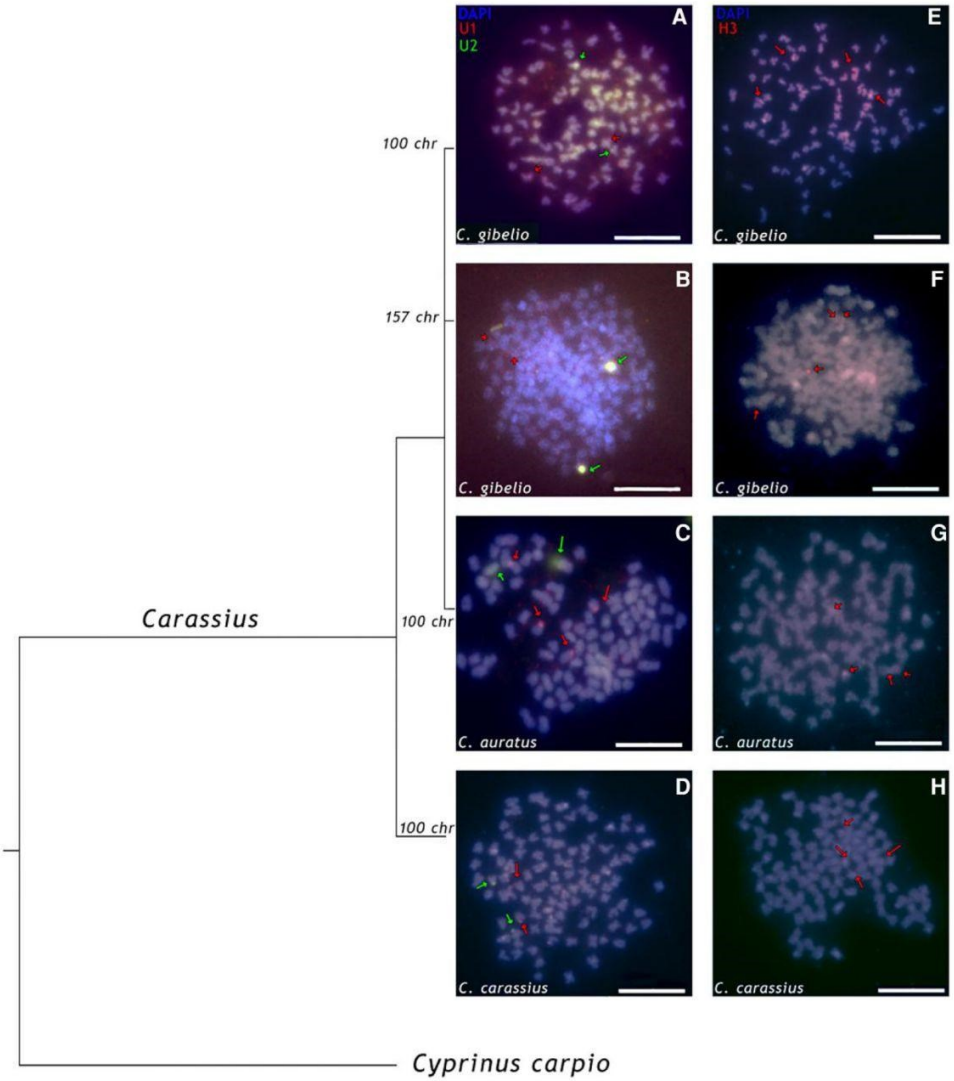

Fig. 1.—Double-color FISH with U1 and U2 snDNA probes (A, B, C, D). The U1 probe reveals one clear signal (= a pair of homologous chromosomes) in tetraploid (A) and hexaploid (B) *C. gibelio*, tetraploid *C. carassius* (D), while the same FISH shows two signals in tetraploid *C. auratus* (C). The U2 probe shows one signal in all species. The green and red arrows correspond to the U2 and U1 repeat loci, respectively. The U1 and U2 signals are located in the telomeric part of chromosomes as well as the H3 signals. Single-color FISH with the H3 snDNA probe (E, F, G, H). The probe shows two clear signals for all species: *C. gibelio* (E, F), *C. auratus* (G), and *C. carassius* (H). Chromosomes were counterstained with 4′, 6-diamidino-2-phenylindole (DAPI) in blue/gray. Some DAPI-intensive spots are also visible at centromere positions or cover entire chromosomes (B, D, E, no arrows). Scale bars represent 10 μm. Each *Carassius* metaphase is anchored in the phylogenetic tree to visualize the phylogenetic distance between specimens. Each branch depicts the number of chromosomes that corresponds to the appropriate individual. *Cyprinus carpio* is used as outgroup at the bottom of the figure.

determine whether some of the genome sequences in tetraploids are similar to those sequences in microchromosomes in hexaploids. We hybridized the whole microchromosome painting probe (the same one as we used for intra-ploidy painting FISH) to metaphase spreads of tetraploid male and female *C. gibelio* (inter-ploidy conspecific painting

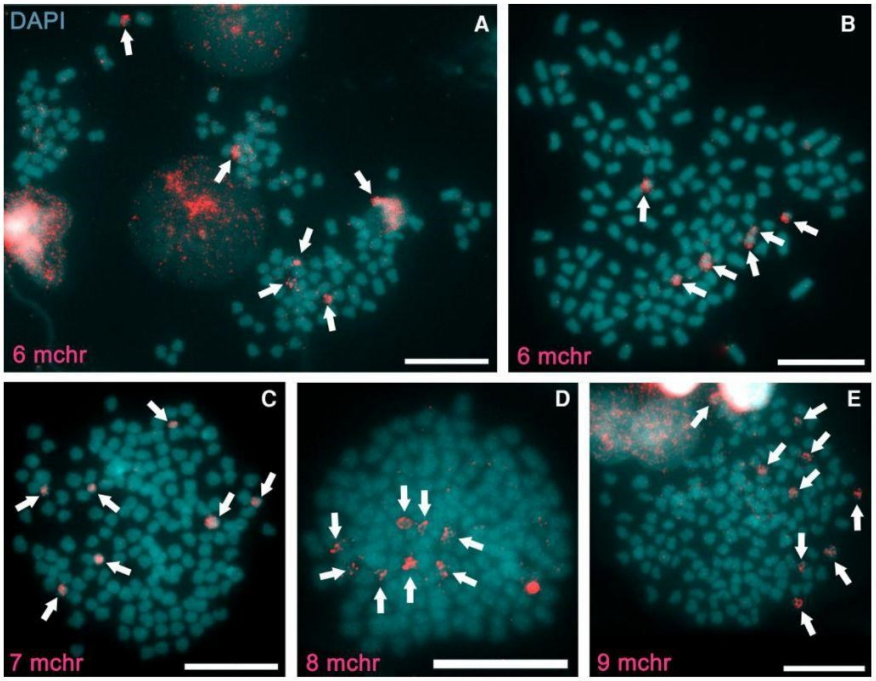

Fig. 2.—Intra-ploidy conspecific painting FISH with the *C. gibelio* whole microchromosome painting probe hybridized to the hexaploid *C. gibelio* females. Each metaphase represents a different individual. The microchromosome probe (red signal, arrows) shows different numbers of microchromosomes in each individual, respectively, six (A, B), seven (C), eight (D), and nine (E). Chromosomes were counterstained with DAPI in blue/gray. Nuclei with unfragmented chromatin are visible (top left, A, E). Scale bars represent 10 μm.

FISH), *C. auratus*, *C. carassius*, and *C. carpio* (inter-ploidy interspecific painting FISH). Inter-ploidy painting FISH showed the similarity of microchromosomes to some genomic regions in tetraploids (microchromosome-associated regions). Fluorescent signals do not cover the entire chromosome lengths and are usually located in pericentromeric regions of mapped chromosomes. The highlighted pericentromeric region indicates that this portion gave rise to the microchromosomes by fission of macrochromosomes, followed by segmental duplication of specific pericentromeric regions (see in "Mechanism of Origin of Carassius Microchromosomes"). The number and intensity of the FISH signals decrease with increasing phylogenetic distance (Fig. 3). As expected, *C. gibelio* (Fig. 3A) showed the highest intensity and the highest number of the FISH signals. On the other hand, *C. carpio* (Fig. 3D), the most distant relative, showed very low intensity of the FISH signals. The number of signals ranges from 8 to 10 in *C. gibelio*, from 6 to 8 in *C. auratus*, and from 4 to 6 in *C. carassius*. The number of signals in *C. carpio* was stable and showed four loci related to the microchromosome-associated regions. No differences between males and females were found.

Considering the mapping of tandem repeats and microchromosomes together, we can exclude co-localization of the investigated tandem repeats with microchromosome-associated regions, and thus we can exclude mutual interactions of U1 or U2 snDNAs or H3 histones with microchromosome-associated regions within a single chromosome. The FISH signals of tandem repeats are situated in pericentromeric regions of telocentric and/or subtelocentric chromosomes with measured centromeric index 0–25. Microchromosome-associated fragments are also located in pericentromeric regions but on submetacentric and metacentric chromosomes (centromeric index 25–50). In each *Carassius* species, a pair of chromosomes carrying the microchromosome-associated locus is one of the largest chromosomes in the karyotype.

Discussion

snDNA Tandem Repeats

Carassius is a widely used experimental model for its extraordinary characteristics, but is rarely used for tandem repeat mapping or microchromosome painting. The consequences of genome duplication and divergence can be studied if we

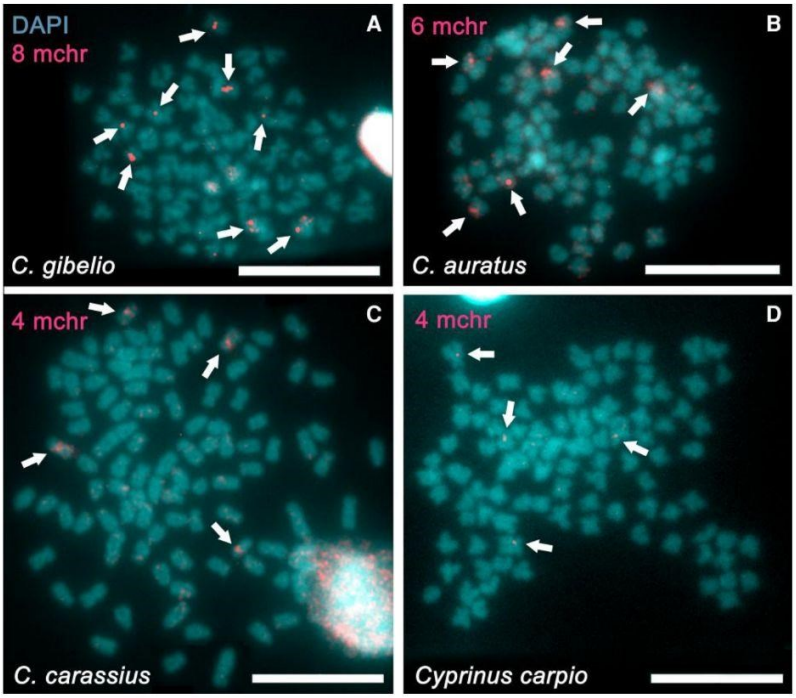

Fig. 3.—Inter-ploidy painting FISH with the *C. gibelio* whole microchromosome painting probe mapped to chromosomes of four tetraploid species, *C. gibelio*, *C. auratus*, *C. carassius*, and *C. carpio*. The microchromosome probe (red) shows signals on portions of the pericentromeric chromosomal regions, indicated by arrows. The number of FISH signals varies by species: eight in *C. gibelio* (A), six in *C. auratus* (B), four in *C. carassius* (C), and four in *C. carpio* (D). Chromosomes were counterstained with DAPI in blue/gray. Scale bars represent 10 μm.

can compare the number of tandem repeat loci between different ploidy levels of closely related species (Fornaini et al. 2023), and this is precisely what can be examined in *Carassius*.

One way to find out these evolutionary consequences is to map tandem repeats on chromosomes using FISH. We compared the number of FISH signals of non-nucleolar tandem repeats (U1 and U2 snDNA and H3 histone) in tetraploid *C. gibelio* with hexaploid *C. gibelio*. Our hypothesis was that hexaploid *C. gibelio* would have one and a half as many signals as tetraploid *C. gibelio*. However, we found equal numbers of all tandem repeat loci in both tetraploids and hexaploids (Fig. 1). The expectations were not met, and we found out that divergence affected the number of tandem repeats more effectively than polyploidization. Since we found the same number of tandem repeats in *C. gibelio* tetraploids and hexaploids, hexaploids may experience a reduction in the number of tandem repeat copies per locus or a complete loss of a tandem repeat locus, likely due to an ongoing evolutionary process of re-diploidization with no need to duplicate and produce more snRNA or H3 histones than in tetraploids (Fornaini et al. 2023). In the other investigated tetraploids, *C. auratus* and *C. carassius*, we found the same number of tandem repeats as in hexaploid *C. gibelio*, except for the U1 locus in *C. auratus* localized on two chromosome pairs. The number of mapped loci is summarized in Table 1.

Mapping of snDNAs is rare throughout Cyprinidae. To our knowledge, this is the first cytogenetic localization of U1 snDNA within the clade Cyprinini. For instance, in the cyprinid genus *Hypophthalmichthys*, which is not paleotetraploid as Cyprinini, a single chromosome pair carries the U1 snDNA locus (Sember et al. 2020). Why the U1 locus was retained duplicated in *C. auratus* and why this locus was reduced in other *Carassius* species is not yet clear, but few other known U1 mapping studies carried out on species other than cyprinids show that the U1 locus is present in a karyotype on single chromosome pair (Cabral-De-Mello et al. 2012; Carvalho et al. 2017; Malimpensa et al. 2020) as well as on six chromosome pairs (Silva et al. 2015). The U2 snDNA locus was previously mapped to *C. carassius* and *C. gibelio* (Bishani et al.

2021). The number of the U2 snDNA signals in *C. carassius* agrees with our results, however, Bishani et al. (2021) identified six U2 signals (two triplets) in the hexaploid *C. gibelio* versus two signals we found in this study. This inconsistency may be due to genetic variation in the copy number of U2 tandem repeats per locus between different *C. gibelio* populations because *C. gibelio* is a complex of individuals with diverse biological skills and different origins (Knytl et al. 2022; Lu et al. 2023).

Another type of tandem repeats is ribosomal RNA which underpins and organizes the nucleolar organizer structure (NOR) and contains 18S, 5.8S, and 28S clusters of ribosomal DNA, rDNA (nucleolar tandem repeats) (Symonová and Howell 2018). The number of nucleolar tandem repeats in tetraploid *Carassius* appears to be more complex. Tetraploid *Carassius* has NORs on two chromosome pairs (Spoz et al. 2014; Knytl et al. 2018; Knytl and Fornaini 2021) which indicates the multiplication of the NOR number due to whole genome duplication and is consistent with paleotetraploid origin (Yang et al. 2010). Cytogenetic mapping of nucleolar tandem repeats in *Carassius* hexaploids indicates a complete/incomplete loss of this locus in one subgenome because their number in hexaploid is equal to the number of NORs in tetraploids (Knytl et al. 2018).

Both nucleolar and non-nucleolar tandem repeats have similar evolutionary destinies leading to loss and/or deletion of redundant copies or reduced copy number per locus—one pair of U1, one pair of U2 snDNAs, and two pairs of H3 histones in tetraploid and hexaploid *C. gibelio* (this study); two pairs of NORs in tetraploid and hexaploid *Carassius* (Knytl et al. 2018).

Table 1
Numbers of U1 and U2 SnDNA, histone H3, and microchromosome-associated (Mchr.) loci in *Carassius* found in this study

Specimen	Ploidy	U1	U2	H3	Mchr.
C. gibelio	$2n = 4x$	2	2	4	8–10
C. gibelio	$3n = 6x$	2	2	4	6–9
C. auratus	$2n = 4x$	4	2	4	6–8
C. carassius	$2n = 4x$	2	2	4	4–6
C. carpio	$2n = 4x$	NA	NA	NA	4

Note. Signals are counted per whole genome (one locus = signal on one chromosome regardless of homologous or non-homologous). NA = information not available from this study.

Evolution of *Carassius* Microchromosomes

The complex of the genus *Carassius* is a group of representatives with different characteristics and in some cases they do not meet the definition of a species (Kalous et al. 2012; Knytl et al. 2022). Therefore, it is important to comprehend the phylogeny of this group. For this reason, we generated a phylogenetic tree from the known mitochondrial sequences of the cytochrome b gene. This analysis confirmed the closest relationship between *C. gibelio* and *C. auratus* and a greater evolutionary distance between the latter two species and *C. carassius* (phylogenetic tree in Fig. 1). Chromosome painting with the whole microchromosome painting probe coincides with the phylogenetic distance and shows the highest intensity and number of signals in the most closely related tetraploid *C. gibelio* and *C. auratus* (Fig. 3A, B and Table 1). Tetraploid and hexaploid *C. gibelio* can form polyphyletic lineage (Kalous et al. 2012), and since there is a diversity of abilities between these ploidy levels, such as origin and modes of reproduction, definition of species is somewhat of controversial (Kalous et al. 2012). When we used the whole microchromosome painting probe on *C. carassius* chromosomes, the intensity and number of fluorescent signals are obviously lower than on *C. gibelio* and *C. auratus* chromosomes, but spatially the signal in *C. carassius* covers at least the same-size or even larger chromosomal region than in *C. gibelio*/*C. auratus* (Fig. 3A–C). In the most distant *C. carpio*, intensity of the signal is the lowest from all specimens tested, and the number of signals is equal to the number of signals in *C. carassius*.

High intensity and strength of the FISH signal may be indicative of repetitive elements, as is the case of tandem repeats in this study or a different type of repetitions in other studies (e.g. Knytl et al. 2018). We tried to avoid a repetitive signal by using autoclaved competitor DNA. This DNA blocking approach inhibits binding of a probe to repetitions. We successfully used the same DNA blocking technique for painting FISH to map unique genomic sequences (Knytl et al. 2013b, 2017, 2023). We also increased stringency washing because signals were not detected using the previously verified FISH protocol. Using the described DNA blocking and protocol modifications,

Table 2
Tandem repeats used for FISH analysis, their GenBank accession numbers, lengths, sequences of primers, and studies in which primers were designed

Gene name	Accession no.	Length (bp)	Primer sequence	Reference
Small nuclear RNA U1	OR366029	112	U1F 5′--GCAGTCGAGATTCCCACATT--3′	Silva et al. (2015)
			U1R 5′--CTTACCTGGCAGGGGAGATA--3′	
Small nuclear RNA U2	OR366030	140	U2F 5′--ATCGCTTCTCGGCCTTAT--3′	Bueno et al. (2013)
			U2R 5′--TCCCGGCGGTACTGCAATA--3′	
Histone H3	OR596332	375	H3F 5′--ATGGCTCGTACCAAGCAGAC (ACG) GC--3′	Colgan et al. (1998)
			H3R 5′--ATATCCTT (AG) GGCAT (AG) AT (AG) GTGAC--3′	

we exclude random nonspecific binding of the probe to chromosomes.

It has been proposed that the number of microchromosomes varies within *Carassius* species (Yi et al. 2003; Li et al. 2016, 2018) and microchromosomes are one of the sources associated with variation in chromosome number in *Carassius*. Yi et al. (2003) carried out a crossbreeding experiment in which *C. gibelio* eggs were fertilized with heterologous sperm of *Megalobrama amblycephala*. The newly produced artificial progeny possessed from 5 to 15 microchromosomes. The microchromosomes were microdissected and used for whole microchromosome painting probe. The probe was hybridized with chromosomes of both parental species. The maternal karyotype did not show any FISH signals, indicating absence of microchromosomes. The paternal karyotype of *M. amblycephala* contained microchromosome-associated regions on four chromosome pairs and the signal was spread over parts of the chromosomes. Two signals were situated on telomeres and the remaining two signals in pericentromeric regions. The study brought evidence of paternal leakage into the allogynogenetic offspring. Similarly, we observed signals in the pericentromeric regions of two to four pairs of chromosomes in *Carassius* tetraploids and *C. carpio*.

Mechanism of Origin of *Carassius* Microchromosomes

If the microchromosomes in the hexaploid females we examined were derived from the paternal leakage, all six to nine microchromosomes would have originated from the father, as suggested by the artificial crosses conducted by Yi et al. (2003). There is no evidence as to what species was the donor of the microchromosomal genome complement in our study. Both maternal genome complement and paternal leakage could have led to the synergistic collaboration and microchromosome formation in hexaploids. The number of microchromosomes can shape/change independently multiple times due to paternal leakage through gynogenesis (Yi et al. 2003; Lamatsch and Stöck 2009; Knytl et al. 2013b). It was found that microchromosomes are building blocks in birds, reptiles, and mammals that undergo the mechanism of macrochromosome fission and/or fusion of two micro- or micro- and macrochromosomes (Kretschmer et al. 2020; Waters et al. 2021). For instance, mammals do not have microchromosomes (Srikulnath et al. 2021) and therefore fusions involving microchromosomes occurred in their common progenitor(s), but after divergence with birds and reptiles that do have microchromosomes (Waters et al. 2021). In *Carassius*, the most likely mechanism for the origin of microchromosome is fission of macrochromosomes. Our results indicate that microchromosomes arose by fission from the pericentromeric regions of the submeta- and metacentric chromosomes of tetraploid *Carassius* species.

The number of microchromosomes in hexaploid females (6–9) corresponds to the number of microchromosome-associated regions in tetraploids (4–10), but the painting signal in tetraploids covers only a portion of the chromosomal area compared to the signal on entire chromosomes in hexaploids, so there should be an additional mechanism besides fission that amplifies microchromosome-like regions. Duplication of an entire block of gene(s) translocated from the macrochromosome to the microchromosome after genome duplication, i.e. segmental duplication (Leister 2004), might be an accompanying mechanism that played an important role in the evolution of *Carassius* microchromosomes. Presumably, tandem duplication, a process in which gene(s) is/are replicated at the original chromosomal locus without subsequent relocation (Blanc et al. 2000), might collaborate with fission after whole genome duplication in *Carassius*. Segmental or tandem duplications can be followed by gene loss at the original locus (Leister 2004) due to divergence (see less widespread FISH signals in tetraploids than in hexaploids; Figs. 2 and 3). Segmental/tandem duplications were evidenced, for example, in plants of the genus *Arabidopsis* (Blanc et al. 2000; Cannon et al. 2004; Leister 2004).

Direct proof of our proposed mechanisms can be provided by sequencing of *Carassius* microchromosomes. This analysis requires microdissection, library preparation, and sequencing of every single microchromosome. While this analysis is time consuming and costly, future evidence is desirable for a better mechanistic understanding of the evolution of *Carassius* microchromosomes. Since *Carassius* genomes have already been sequenced (Li et al. 2021; Kuhl et al. 2022; Wang et al. 2022b), it is possible to map sequences from microdissected microchromosomes and compare them with microchromosome sequences from Chinese *Carassius* populations (Ding et al. 2021).

Back in Time: Microchromosomes in the Most Recent Common Ancestor of Bony Vertebrates

Bony vertebrates (Euteleostomi, sensu lato Osteichthyes) are a clade of vertebrates that formed after divergence from agnathans and chondrichthyians. It is estimated that the ancestral karyotype of bony vertebrates is similar to that of spotted gar (*Lepisosteus oculatus*). The present-day karyotype of this species contains 58 chromosomes, involving macrochromosomes and from 18 to 20 microchromosomes (Braasch et al. 2016; Symonová et al. 2017). *Lepisosteus oculatus* represents a strong conservation of microchromosome structure and synteny over 450 million years, for example, compared to the chicken genome (Braasch et al. 2016). It is assumed that the ancestral karyotype of bony vertebrates contained 12 microchromosomes (Sacerdot et al. 2018), a number similar to that of *Carassius*. It is questionable whether *Carassius* microchromosomes arose independently from macrochromosomes of *Carassius*

tetraploids, or whether these microchromosomes are highly conserved and homologous to the microchromosomes of ancestor of bony vertebrates, eventually to those of chicken and gar. Our results suggest an independent origin of the *Carassius* microchromosomes, as neither *Carassius* tetraploids nor *C. carpio* have any microchromosomes, but this does not exclude the hypothesis that *Carassius* microchromosomes are homologous to microchromosomes of chicken and/or gar. Microchromosomes can arise and disappear spontaneously during evolution due to the fusion–fission model of macro- and microchromosomes (reviewed in Srikulnath et al. 2021). Mapping *Carassius* microchromosomes to genomes that are not only closely related to *Carassius* genomes, but also to genomes related to the most recent common ancestor of bony vertebrates, i.e. the basal lineages of gars, is a challenge for further *Carassius* research.

Conclusion

Both repetitive elements and microchromosomes are integral components of the *Carassius* genome and their evolution can be affected by polyploidization or divergence between species. Analysis of tandem repeat mapping showed evolutionary conservation in the number of these mapped repeats between *Carassius* species with different ploidy levels, except for the U1 snDNA locus in *C. auratus*. This conservation suggests a reduction and loss of copy number per locus (particularly in hexaploids) that may have occurred by divergence after polyploidization. For further examples of reduction, loss, and/or expansion of copy number of tandem repeats per locus, see, e.g. Fornaini et al. (2023). Analysis of the whole microchromosome painting revealed evolution by fission followed by post-polyploidization segmental duplication of pericentromeric macrochromosomal regions as a potential mechanism responsible for the presence of microchromosomes in *Carassius* hexaploids. Other examples of these latter evolutionary mechanisms are Cannon et al. (2004) and Kretschmer et al. (2020). We did not find co-localization of tandem repeats with microchromosome-associated regions, so we ruled out their cooperation within the same chromosome locus. Both structures evolved independently in *Carassius*. All of our findings are consistent with structural genomic changes that follow genome duplication.

Materials and Methods

Fish Sampling and Origin

Carassius auratus was obtained via the aquarium trade (transported to the Czech Republic from Israel). *Carassius carassius* was collected in alluvial ponds and old oxbows of the Elbe River basin close to the city Lysá nad Labem, the Bohemia region. *Carassius gibelio* was captured in the Elbe River basin close to the city Lysá nad Labem, the Bohemia region (hexaploids); in the Mrlina River basin, Global Positioning System: 50 °15 ′35.8 ″N, 15 °08 ′43.4 ″E, the village Zábrdovice, the Bohemia region (hexaploids); in the Odra River basin, the Moravian-Silesian region (tetraploids, hexaploids). All three river basin districts are located in the Czech Republic. Field surveys of ichthyofauna were performed in 2010–2012 and then in the River Mrlina in 2021. More detailed information on morphological analysis, voucher specimens, and location coordinates are given in Knytl et al. (2013b). Sex of individuals was identified based on dissection of gonads. Males and females of *Carassius* tetraploids and females of *Carassius* hexaploids were used in this study. *Cyprinus carpio* gonads were not inspected by dissection and sex of this individual was not identified. Because *C. carpio* was used as an outgroup for our analyses, knowledge of sex and origin is not crucial to our investigation.

Chromosome Preparations

Chromosome spreads were prepared from tetraploid males and females (*C. gibelio*, *C. auratus*, and *C. carassius*) and hexaploid *C. gibelio* females. For all *Carassius* species, we used a method in which chromosome suspension was prepared directly from the cephalic kidney (Bertollo and Cioffi 2015). Mitotic activity was stimulated by intraperitoneal injection of 0.1% $CoCl_2$ per 100 g of weight 24 h before colchicine (Sigma, St. Louis, MO, USA) application (Knytl et al. 2018). Ready-to-use chromosome suspension was stored in fixative solution (methanol:acetic acid, 3: 1, v/v) at −20 °C as described in Knytl and Fornaini (2021). *Cyprinus carpio* chromosomes were obtained from regenerating fin tissues according to Kalous et al. (2010). The methods of colchicine treatment and hypotonization were originally adopted from *Chromaphyosemion* killifishes (Cyprinodontiformes, Nothobranchiidae) (Völker et al. 2006). Tissue fixation was performed and metaphases were spread on slides in the same manner as described in the embryo preparation protocol in Völker and Kullmann (2006). Microscopy and processing of metaphase images were conducted using Leica Microsystem (Wetzlar, Germany) as detailed in Seroussi et al. (2019). At least 20 metaphases were analyzed per each individual and five individuals were investigated per each analysis.

FISH with Repetitive DNA Probes

In order to generate probes for FISH, genomic DNA (gDNA) from hexaploid *C. gibelio* was used as a template for amplification of the U1 and U2 snDNA regions, and H3 histone. DNA was extracted from adult fish tissues using the DNeasy Blood and Tissue Kit (Qiagen, Hilden, Germany) according to the manufacturer's instructions. Primers used for amplification are listed in Table 2. The annealing temperature was 54 °C and the elongation step 30 s for all polymerase

chain reactions (PCR); other conditions for PCR amplification with PPP Master Mix (Top-Bio, Prague, Czech Republic) followed the manufacturer's recommendations. PCR amplification of the U1, U2, and H3 genes consistently resulted in 112, 140, and 375 bp long fragments, respectively. The search using the `blastn` algorithm confirmed the locus- and species-specificity of each amplicon: 98.98% identity with the U1 DNA sequence of *C. gibelio* (accession number XR_008182931.1), 97.10% identity with the U2 DNA sequence of *C. gibelio* (accession number XR_008154662.1), and 97.53% identity with H3 DNA of *C. gibelio* (accession number XM_052561945.1). Labeling PCR was performed as described in Knytl and Fornaini (2021). Digoxigenin-11-deoxyuridine triphosphate (dUTP) (Jena Bioscience, Jena, Germany) was used for U2 and H3 labeling, and biotin-16-dUTP (Jena Bioscience) was used for U1 labeling. *Carassius gibelio* U1 and U2 snDNA and H3 probes were then hybridized to chromosome spreads of *C. carassius* and *C. auratus* and tetraploid and hexaploid *C. gibelio*. The procedures for hybridization mixture preparation, denaturation, and subsequent overnight hybridization were previously described for rDNA FISH (Knytl et al. 2023). Post-hybridization stringency washing and blocking reactions were performed as described for painting FISH in Krylov et al. (2010). Probe signal was visualized following Knytl et al. (2017).

Phylogenetic Tree

We used mitochondrial cytochrome b of *C. carassius* (accession number KR131839), *C. auratus* (accession number KX688781), diploid (tetraploid) *C. gibelio* (accession number KX688784), and triploid (hexaploid) *C. gibelio* (accession number KX601125.1) to construct the phylogenetic tree. The *C. carpio* mitochondrial genome (accession number NC_001606) was used as an outgroup. Sequences were aligned using the multiple sequence comparison by log-expectation (MUSCLE) algorithm (Edgar 2004) through MEGA11 software (Tamura et al. 2021). After alignment, Iq-tree2 software (Minh et al. 2020) was used to predict the nucleotide substitution model using ModelFinder (Kalyaanamoorthy et al. 2017) and to create the tree. The best fitting model was found to be Hasegawa-Kishino-Yano (HKY+F) (Hasegawa et al. 1985). The tree was displayed using FigTree http://tree.bio.ed.ac.uk/software/figtree/.

Painting FISH with Whole Microchromosome Painting Probe

Microchromosomes from a single *C. gibelio* female were isolated individually by laser microdissection as previously described in Kubickova et al. (2002) using a PALM Microlaser system (Carl Zeiss MicroImaging GmbH, Munich, Germany). A total of 10 single microchromosomes were dissected from multiple metaphases (approximately two microchromosomes from each metaphase). These microchromosomes were then pooled and used to paint a whole microchromosome FISH probe, subsequently completed using the GenomePlex Single Cell whole genome amplification Kit (WGA4), Sigma-Aldrich, according to the manufacturer's protocol for whole genome amplification with extracted gDNA. GenomePlex WGA Reamplification (WGA3), Sigma-Aldrich, and labeling with digoxigenin-11-dUTP (Jena Bioscience) were carried out as described in Krylov et al. (2010). Autoclaved *C. gibelio* gDNA (Bi and Bogart 2006) was used as a competitor (blocking DNA). The digoxigenin-labeled probe was detected by anti-digoxigenin-fluorescein (Roche, Basel, Switzerland). Conspecific painting FISH *C. gibelio*–*C. gibelio* was conducted as detailed in painting FISH in Krylov et al. (2010). Inter-ploidy painting FISH was carried out as described in Zoo-FISH in Krylov et al. (2010), with minor changes (Knytl et al. 2017). In addition, the current protocol was modified by increasing the total salt concentration from 2*x*SCC to 4*x*SCC (8*x*SCC with 50% formamide, 1 : 1, v/v) for less effective stringency washing. Chromosomes were counterstained with ProLong™ Diamond Antifade Mountant with the fluorescent 4*ifinmath*,6-diamidino-2-phenylindole (DAPI) stain (Invitrogen by Thermo Fisher Scientific, Waltham, MA, USA).

Acknowledgments

The authors thank Lukáš Kalous, Štěpán Romočuský, and Jiří Knytl for help with sample collection and storage. Authors also thank two anonymous reviewers for their valuable suggestions in early version of the manuscript. This work is supported in part by funds from the P JAC project # CZ.02.01.01/00/22_010/0002902 MSCA Fellowships CZ–UK (M.K.), Grant Agency of Charles University # 54123 (N.R.F., M.K.), and Ministry of Agriculture of the Czech Republic, institutional support # MZE-RO0523 (H.C.). Open access publishing was supported by the National Technical Library in Prague (CzechELib).

Author Contributions

N.R.F., H.C., and M.K. conducted the experiments, received funding; N.R.F. and M.K. analyzed the results, designed graphics, prepared original draft; L.V.M. and M.K. conceptualized the study; M.K. is responsible for resources, visualization, data curation and validation, project administration, and supervision. All authors reviewed, edited, and approved the final version of the manuscript.

Conflict of Interest

No competing interest is declared.

Data Availability

All the data supporting the findings of this study are available within the article. Sanger sequencing data are deposited in the GenBank NCBI database, https://www.ncbi.nlm.nih.gov/genbank/ (see Table 2 for accession numbers).

Statement of Ethics

M.K. is a holder of the certificate of professional competence to design experiments according to § 15d(3) of the Czech Republic Act No. 246/1992 coll. on the Protection of Animals against Cruelty (Registration number CZ 03973), provided by the Ministry of Agriculture of the Czech Republic.

References

Ağdamar S, Baysal Ö, Yıldız A, Tarkan AS. Genetic differentiation of non-native populations of Gibel Carp, *Carassius gibelio* in Western Turkey by ISSR and SRAP markers. Zool Middle East. 2020:66(4):302–310. https://doi.org/10.1080/09397140.2020.1835215.

Bertollo LAC, Cioffi MdB. Direct chromosome preparation from freshwater teleost fishes. In: Ozouf-Costaz C, Pisano E, Foresti F, Foresti LdAT, editors. Fish cytogenet. Tech. Ray-Fin fishes chondrichthyans. Enfield: CRC Press; 2015. p. 21–26.

Bi K, Bogart JP. Identification of intergenomic recombinations in unisexual salamanders of the genus *Ambystoma* by genomic in situ hybridization (GISH). Cytogenet Genome Res. 2006:112(3–4):307–312. https://doi.org/10.1159/000089885.

Bishani A, et al. Evolution of tandemly arranged repetitive DNAs in three species of Cyprinoidei with different ploidy levels. Cytogenet Genome Res. 2021:161(1–2):32–42. https://doi.org/10.1159/000513274.

Blanc G, Barakat A, Guyot R, Cooke R, Delseny M. Extensive duplication and reshuffling in the *Arabidopsis* genome. Plant Cell. 2000:12(7):1093–1101. https://doi.org/10.1105/tpc.12.7.1093.

Braasch I, Gehrke AR, Smith JJ, Kawasaki K, Manousaki T, Pasquier J, Amores A, Desvignes T, Batzel P, Catchen J, et al. The spotted gar genome illuminates vertebrate evolution and facilitates human-teleost comparisons. Nat Genet. 2016:48(4):427–437. https://doi.org/10.1038/ng.3526.

Bueno D, Palacios-Gimenez OM, Cabral-de-Mello DC. Chromosomal mapping of repetitive DNAs in the grasshopper *Abracris flavolineata* reveal possible ancestry of the B chromosome and H3 histone spreading. PLoS One. 2013:8(6):e66532. https://doi.org/10.1371/journal.pone.0066532.

Cabral-De-Mello DC, Valente GT, Nakajima RT, Martins C. Genomic organization and comparative chromosome mapping of the U1 snRNA gene in cichlid fish, with an emphasis in *Oreochromis niloticus*. Chromosome Res. 2012:20(2):279–292. https://doi.org/10.1007/s10577-011-9271-y.

Cannon SB, Mitra A, Baumgarten A, Young ND, May G. The roles of segmental and tandem gene duplication in the evolution of large gene families in *Arabidopsis thaliana*. BMC Plant Biol. 2004:4(1):10. https://doi.org/10.1186/1471-2229-4-10.

Carvalho PC, et al. First chromosomal analysis in Hepsetidae (Actinopterygii, Characiformes): insights into relationship between African and Neotropical fish groups. Front Genet. 2017:8(203):1–12. https://doi.org/10.3389/fgene.2017.00203.

Cherfas NB. Natural triploidy in females of the unisexual form of silver crucian carp (*Carassius auratus* gibelio Bloch). Genetika. 1966:5:16–24.

Chobot K, Němec M. Červený seznam ohrožených druhů České republiky. Obratlovci: red list of threatened species of the Czech Republic. Příroda. 2017:34:1–182.

Colgan DJ, et al. Histone H3 and U2 snRNA DNA sequences and arthropod molecular evolution. Aust J Zool. 1998:46(5):419. https://doi.org/10.1071/ZO98048.

de Souza MS, et al. Highly conserved microchromosomal organization in passeriformes birds revealed via BAC-FISH analysis. Birds. 2023:4(2):236–244. https://doi.org/10.3390/birds4020020.

Ding M, et al. Genomic anatomy of male-specific microchromosomes in a gynogenetic fish. PLoS Genet. 2021:17(9):1–25. https://doi.org/10.1371/journal.pgen.1009760.

Edgar RC. MUSCLE: multiple sequence alignment with high accuracy and high throughput. Nucleic Acids Res. 2004:32(5):1792–1797. https://doi.org/10.1093/nar/gkh340.

Fedorčák J, Križek P, Koščo J. Which factors influence spatio-temporal changes in the distribution of invasive and native species of genus *Carassius*? Aquat Invasions. 2023:18(2):219–230. https://doi.org/10.3391/ai.2023.18.2.105240.

Fornaini NR, et al. Consequences of polyploidy and divergence as revealed by cytogenetic mapping of tandem repeats in African clawed frogs (*Xenopus*, Pipidae). Eur J Wildl Res. 2023:69(4):81. https://doi.org/10.1007/s10344-023-01709-8.

Fuad MMH, Vetenk L, Šimková A. Is gynogenetic reproduction in gibel carp (*Carassius gibelio*) a major trait responsible for invasiveness? J Vertebr Biol. 2021:70(4):21049. https://doi.org/10.25225/jvb.21049.

Gvoždík V, Knytl M, Zassi-Boulou AG, Fornaini NR, Bergelová B. Tetraploidy in the Boettger's dwarf clawed frog (Pipidae: *Hymenochirus boettgeri*) from the Congo indicates non-conspecificity with the captive population. Zool J Linn Soc. 2023:1–14. https://doi.org/10.1093/zoolinnean/zlad119

Hakoyama H, Nishimura T, Matsubara N, Iguchi K. Difference in parasite load and nonspecific immune reaction between sexual and gynogenetic forms of *Carassius auratus*. Biol J Linn Soc. 2001:72(3):401–407. https://doi.org/10.1006/bijl.2000.0507.

Hasegawa M, Kishino H, Yano T. Dating of the human-ape splitting by a molecular clock of mitochondrial DNA. J Mol Evol. 1985:22(2):160–174. https://doi.org/10.1007/BF02101694.

Huang S, Spector DL. U1 and U2 small nuclear RNAs are present in nuclear speckles. Proc Natl Acad Sci USA. 1992:89(1):305–308. https://doi.org/10.1073/pnas.89.1.305.

International Chicken Genome Sequencing Consortium. Sequence and comparative analysis of the chicken genome provide unique perspectives on vertebrate evolution. Nature. 2004:432(7018):695–716. https://doi.org/10.1038/nature03154.

Jan G, et al. Karyotypic analysis of crucian carp, *Carassius Carassius* (Linnaeus, 1758) from cold waters of Kashmir Himalayas. Caryologia. 2023:76(2):23–30. https://doi.org/10.36253/caryologia-2112.

Kalous L, Bohlen J, Rylková K, Petrtýl M. Hidden diversity within the Prussian carp and designation of a neotype for *Carassius gibelio* (Teleostei: Cyprinidae). Ichthyol Explor Freshwaters. 2012:23(1):11–18.

Kalous L, Knytl M. Karyotype diversity of the offspring resulting from reproduction experiment between diploid male and triploid female of silver Prussian carp, *Carassius gibelio* (Cyprinidae, Actinopterygii). Folia Zool. 2011:60(2):115–121. https://doi.org/10.25225/fozo.v60.i2.a5.2011.

Kalous L, Knytl M, Krajáková L. Usage of non-destructive method of chromosome preparation applied on silver Prussian carp

(*Carassius gibelio*). In: Kubík Š, Barták M, editors. Work. Anim. biodiversity. Jevany: Czech University of Life Sciences in Prague; 2010. p. 57–60.
Kalous L, Šlechtová V, Bohlen J, Petrtýl M, Švátora M. First European record of *Carassius langsdorfii* from the Elbe basin. J Fish Biol. 2007:70(sa):132–138. https://doi.org/10.1111/j.1095-8649.2006.01290.x.
Kalyaanamoorthy S, Minh BQ, Wong TKF, von Haeseler A, Jermiin LS. ModelFinder: fast model selection for accurate phylogenetic estimates. Nat Methods. 2017:14(6):587–589. https://doi.org/10.1038/nmeth.4285.
Khosravi M, Abdoli A, Tajbakhsh F, Ahmadzadeh F, Nemati H. An effort toward species delimitation in the genus *Carassius* (Cyprinidae) using morphology and the related challenges: a case study from Inland waters of Iran. J Ichthyol. 2022:62(2):185–194. https://doi.org/10.1134/S0032945222020096.
Knytl M, Fornaini N. Measurement of chromosomal arms and fish reveal complex genome architecture and standardized karyotype of model fish, genus *Carassius*. Cells. 2021:10(9):2343. https://doi.org/10.3390/cells10092343.
Knytl M, et al. Divergent subgenome evolution in the allotetraploid frog *Xenopus calcaratus*. Gene. 2023:851:146974. https://doi.org/10.1016/j.gene.2022.146974.
Knytl M, Forsythe A, Kalous L. A fish of multiple faces, which show us enigmatic and incredible phenomena in nature: biology and cytogenetics of the genus *Carassius*. Int J Mol Sci. 2022:23(15):8095. https://doi.org/10.3390/ijms23158095.
Knytl M, Kalous L, Rab P. Karyotype and chromosome banding of endangered Crucian carp, *Carassius Carassius* (Linnaeus, 1758) (Teleostei, Cyprinidae). Comp Cytogenet. 2013a:7(3):205–213. https://doi.org/10.3897/compcytogen.v7i3.5411.
Knytl M, et al. Morphologically indistinguishable hybrid *Carassius* female with 156 chromosomes: a threat for the threatened Crucian carp, *C. carassius*, L. PLoS One. 2018:13(1):e0190924. https://doi.org/10.1371/journal.pone.0190924.
Knytl M, Kalous L, Symonová R, Rylková K, Ráb P. Chromosome studies of European cyprinid fishes: cross-species painting reveals natural allotetraploid origin of a *Carassius* female with 206 chromosomes. Cytogenet Genome Res. 2013b:139(4):276–283. https://doi.org/10.1159/000350689.
Knytl M, et al. Chromosome divergence during evolution of the tetraploid clawed frogs, *Xenopus mellotropicalis* and *Xenopus epitropicalis* as revealed by Zoo-FISH. PLoS One. 2017:12(5):e0177087. https://doi.org/10.1371/journal.pone.0177087.
Kretschmer R, et al. Novel insights into chromosome evolution of charadriiformes: extensive genomic reshuffling in the wattled jacana (*Jacana jacana*, Charadriiformes, Jacanidae). Genet Mol Biol. 2020:43(1):1–8. https://doi.org/10.1590/1678-4685-GMB-2019-0236.
Krylov V, et al. Preparation of *Xenopus tropicalis* whole chromosome painting probes using laser microdissection and reconstruction of *X. laevis* tetraploid karyotype by Zoo-FISH. Chromosome Res. 2010:18(4):431–439. https://doi.org/10.1007/s10577-010-9127-x.
Kubickova S, Cernohorska H, Musilova P, Rubes J. The use of laser microdissection for the preparation of chromosome-specific painting probes in farm animals. Chromosome Res. 2002:10(7):571–577. https://doi.org/10.1023/A:1020914702767.
Kuhl H, et al. Equilibrated evolution of the mixed auto-/allopolyploid haplotype-resolved genome of the invasive hexaploid Prussian carp. Nat Commun. 2022:13(1):1–11. https://doi.org/10.1038/s41467-022-31515-w.
Lamatsch D, Stöck M. Sperm-dependent parthenogenesis and hybridogenesis in teleost fishes. In: Schöne I, Martens K, van Dijk P, editors. Lost sex evol. biol. parthenogenes. Dordrecht: Springer; 2009. p. 399–432.
Leister D. Tandem and segmental gene duplication and recombination in the evolution of plant disease resistance genes. Trends Genet. 2004:20(3):116–122. https://doi.org/10.1016/j.tig.2004.01.007.
Li XY, et al. Origin and transition of sex determination mechanisms in a gynogenetic hexaploid fish. Heredity (Edinb). 2018:121(1):64–74. https://doi.org/10.1038/s41437-017-0049-7.
Li JT, et al. Parallel subgenome structure and divergent expression evolution of allo-tetraploid common carp and goldfish. Nat Genet. 2021:53(10):1493–1503. https://doi.org/10.1038/s41588-021-00933-9.
Li XY, et al. Extra microchromosomes play male determination role in polyploid gibel carp. Genetics. 2016:203(3):1415–1424. https://doi.org/10.1534/genetics.115.185843.
Lu M, Zhou L, Gui J. Evolutionary mechanisms and practical significance of reproductive success and clonal diversity in unisexual vertebrate polyploids. Sci China Life Sci. 2023. https://doi.org/10.1007/s11427-023-2486-2.
Lusk S, Lusková V, Hanel L. Alien fish species in the Czech Republic and their impact on the native fish fauna. Folia Zool. 2010:59(1):57–72. https://doi.org/10.25225/fozo.v59.i1.a9.2010.
Malimpensa GDC, et al. Chromosomal diversification in two species of *Pimelodus* (Siluriformes: Pimelodidae): comparative cytogenetic mapping of multigene families. Zebrafish. 2020:17(4):278–286. https://doi.org/10.1089/zeb.2020.1892.
Minh BQ, et al. IQ-TREE 2: new models and efficient methods for phylogenetic inference in the genomic era. Mol Biol Evol. 2020:37(5):1530–1534. https://doi.org/10.1093/molbev/msaa015.
Nanda I, Schmid M. Localization of the telomeric (TTAGGG)n sequence in chicken (*Gallus domesticus*) chromosomes. Cytogenet Cell Genet. 1994:65(3):190–193. https://doi.org/10.1159/000133630.
Ohno S, Muramoto J, Christian L, Atkin NB. Diploid–tetraploid relationship among old-world members of the fish family Cyprinidae. Chromosoma. 1967:23(1):1–9. https://doi.org/10.1007/BF00293307.
Pang M, et al. Quantitative trait loci mapping for feed conversion efficiency in crucian carp (*Carassius auratus*). Sci Rep. 2017:7(1):1–11. https://doi.org/10.1038/s41598-017-17269-2.
Papoušek I, et al. Identification of natural hybrids of gibel carp *Carassius auratus gibelio* (Bloch) and crucian carp *Carassius carassius* (L.) from lower Dyje river floodplain (Czech Republic). J Fish Biol. 2008:72(5):1230–1235. https://doi.org/10.1111/j.1095-8649.2007.01783.x.
Pavlov DA. Features of inner ear morphology of gibel carp *Carassius gibelio* (Cyprinidae). J Ichthyol. 2022a:62(2):195–204. https://doi.org/10.1134/S0032945222020138.
Pavlov DA. Life history of two *Carassius* (Cyprinidae) species in the conditions of sympatry. J Ichthyol. 2022b:62(6):1100–1115. https://doi.org/10.1134/S0032945222060212.
Przybył A, et al. Sex, size and ploidy ratios of *Carassius gibelio* from Poland. Aquat Invasions. 2020:15(1):1–20. https://doi.org/10.3391/ai.2020.15.2.08.
Rylková K, Kalous L, Bohlen J, Lamatsch DK, Petrtl M. Phylogeny and biogeographic history of the cyprinid fish genus *Carassius* (Teleostei: Cyprinidae) with focus on natural and anthropogenic arrivals in Europe. Aquaculture. 2013:380–383:13–20. https://doi.org/10.1016/j.aquaculture.2012.11.027.
Sacerdot C, Louis A, Bon C, Berthelot C, Roest Crollius H. Chromosome evolution at the origin of the ancestral vertebrate genome. Genome Biol. 2018:19(1):166. https://doi.org/10.1186/s13059-018-1559-1.
Sember A, et al. Taxonomic diversity not associated with gross karyotype differentiation: the case of bighead carps, genus *hypophthalmichthys* (Teleostei, Cypriniformes, Xenocyprididae). Genes (Basel). 2020:11(5):479. https://doi.org/10.3390/genes11050479.

Seroussi E, et al. Avian expression patterns and genomic mapping implicate leptin in digestion and TNF immunity, suggesting that their interacting adipokine role has been acquired only in mammals. Int J Mol Sci. 2019:20(18):4489. https://doi.org/10.3390/ijms20184489.

Silva DM, Utsunomia R, Pansonato-Alves JC, Oliveira C, Foresti F. Chromosomal mapping of repetitive DNA sequences in five species of *astyanax* (Characiformes, Characidae) reveals independent location of U1 and U2 snRNA sites and association of U1 snRNA and 5S rDNA. Cytogenet Genome Res. 2015:146(2):144–152. https://doi.org/10.1159/000438813.

Spoz A, et al. Molecular cytogenetic analysis of the crucian carp, *Carassius carassius* (Linnaeus, 1758) (Teleostei, Cyprinidae), using chromosome staining and fluorescence in situ hybridisation with rDNA probes. Comp Cytogenet. 2014:8(3):233–248. https://doi.org/10.3897/compcytogen.v8i3.7718.

Srikulnath K, Ahmad SF, Singchat W, Panthum T. Why do some vertebrates have microchromosomes? Cells. 2021:10(9):1–33. https://doi.org/10.3390/cells10092182.

Symonová R, Howell WM. Vertebrate genome evolution in the light of fish cytogenomics and rDNAomics. Genes (Basel). 2018:9(2):1–27. https://doi.org/10.3390/genes9020096.

Symonová R, et al. Genome compositional organization in gars shows more similarities to mammals than to other ray-finned fish. J Exp Zool Part B Mol Dev Evol. 2017:328(7):607–619. https://doi.org/10.1002/jez.b.22719.

Tamura K, Stecher G, Kumar S. MEGA11: molecular evolutionary genetics analysis version 11. Mol Biol Evol. 2021:38(7):3022–3027. https://doi.org/10.1093/molbev/msab120.

Tapkir S, et al. Invasive gibel carp (*Carassius gibelio*) outperforms threatened native crucian carp (*Carassius carassius*) in growth rate and effectiveness of resource use: field and experimental evidence. Aquat Conserv Mar Freshw Ecosyst. 2022:32(12):1901–1912. https://doi.org/10.1002/aqc.3894.

Tapkir S, et al. Invasive gibel carp use vacant space and occupy lower trophic niche compared to endangered native crucian carp. Biol Invasions. 2023:25(9):2917–2928. https://doi.org/10.1007/s10530-023-03081-9.

Völker M, Kullmann H. Sequential chromosome banding from single acetic acid fixed embryos of *Chromaphyosemion* killifishes (Cyprinodontiformes, Nothobranchiidae). Cybium. 2006:30(2):171–176.

Völker M, Sonnenberg R, Ráb P, Kullmann H. Karyotype differentiation in *Chromaphyosemion* killifishes (Cyprinodontiformes, Nothobranchiidae) II: cytogenetic and mitochondrial DNA analyses demonstrate karyotype differentiation and its evolutionary direction in *C. riggenbachi*. Cytogenet Genome Res. 2006:115(1):70–83. https://doi.org/10.1159/000094803.

Wang J, et al. A novel allotriploid hybrid derived from female goldfish × male Bleeker's yellow tail. Front Genet. 2022a:13(880591):1–12. https://doi.org/10.3389/fgene.2022.880591.

Wang Y, et al. Comparative genome anatomy reveals evolutionary insights into a unique amphitriploid fish. Nat Ecol Evol. 2022b:6(9):1354–1366. https://doi.org/10.1038/s41559-022-01813-z.

Waters PD, et al. Microchromosomes are building blocks of bird, reptile, and mammal chromosomes. Proc Natl Acad Sci USA. 2021:118(45):1–11. https://doi.org/10.1073/pnas.2112494118.

Wen M, et al. Sex chromosome and sex locus characterization in goldfish, *Carassius auratus* (Linnaeus, 1758). BMC Genomics. 2020:21(1):1–12. https://doi.org/10.1186/s12864-020-06959-3.

Winfield IJ, Nelson JS. 2012. Cyprinid fishes: systematics, biology and exploitation. Dordrecht: Springer Science & Business Media. https://doi.org/10.1007/978-94-011-3092-9.

Xiao J, et al. Coexistence of diploid, triploid and tetraploid crucian carp (*Carassius auratus*) in natural waters. BMC Genet. 2011:12(1):20. https://doi.org/10.1186/1471-2156-12-20.

Yang L, et al. Molecular phylogeny of the fishes traditionally referred to Cyprinini sensu stricto (Teleostei: Cypriniformes). Zool Scr. 2010:39(6):527–550. https://doi.org/10.1111/j.1463-6409.2010.00443.x.

Yi MS, et al. Molecular cytogenetic detection of paternal chromosome fragments in allogynogenetic gibel carp, *Carassius auratus gibelio* Bloch. Chromosome Res. 2003:11(7):665–71. https://doi.org/10.1023/a:1025985625706.

Zhao X, et al. Genotypic males play an important role in the creation of genetic diversity in gynogenetic gibel carp. Front Genet. 2021:12(691923):1–9. https://doi.org/10.3389/fgene.2021.691923.

Zhou L, Gui JF. Karyotypic diversity in polyploid gibel carp, *Carassius auratus gibelio* Bloch. Genetica. 2002:115(2):223–232. https://doi.org/10.1023/A:1020102409270.

Associate editor: Federico Hoffmann